جامعة الشيخ الشهيد العربي التبسي
SHEIKH ECHAHID LARBI TEBESSI UNIVERSITY
كلية العلوم و التكنولوجيا
FACULTY OF SCIENCES AND TECHNOLOGY
قسم الهندسة الكهربائية
DEPARTMENT OF ELECTRICAL ENGINEERING

Final Year Project

For the award of the degree

MASTER THESIS

Specialty: Industrial Electrotechnics

On the theme:

Study and Sizing of an Electrical Supply System for a Site Isolated by a Hydrogen Source

---

Presented by:
Mr. OTMANI Zakaria
Mrs. MAALEM Bouchra

18/06/2025

Presented and defended on 10/06/2025 in front the jury composed of:

Prof. BOUKADOUM Aziz	- President
Prof. DIB Jalel	- Supervisor
Dr. DJEDDI Abdelghani	- Co-supervisor
Dr. NEHAL Ouassila	- Examiner

Academic Year 2024-2025


بسم الله الرحمن الرحيم

Acknowledgments

First and foremost, we express our gratitude to Allah, who granted us the strength, courage, and determination to carry out this work.

We would like to extend my heartfelt thanks to Professors Dib Djalel and Djeddi Abdelghani from the University of Tébessa for their kind and diligent supervision of this thesis. we are deeply grateful for his valuable guidance, scientific expertise, and human qualities, all of which played a significant role in the successful completion of this research.

We also wish to express our sincere appreciation to all the professors and doctors of the Electrical Engineering Department, especially Dr. Lemita Abdallah and Dr. Saadi Moufida, for their valuable contributions to our academic journey through their dedication and guidance throughout our university studies.

DEDICATION

To the one who has been my pillar of strength and support at every step With her prayers and sacrifices to offer me a dignified life, to my heart and soul my beloved mother May God bless her with a long and healthy life, to the one who taught me that life is a struggle and that its weapon is knowledge and learning.

To the one who was with me at the beginning of the road and waited with me to see its end But God's plan comes first, to the one I lost the one who lives forever in my heart my father.

To my dear cousins Dikra, Nesrine, Asma, Selma, Norhane, Hanin.

To my best friends Ouissal, Nihal, Rayane, Ouiem, Sirine, Hadil, Rima, and Aya.

To all my other friends.

And all that helps and guides me to finish this modest work.

Bouchra

DEDICATION

I dedicate this work to my beloved family, whose unwavering support, encouragement, and sacrifices have been the foundation of my academic journey.To my parents, who instilled in me the values of education and perseverance.To all my professors and friends who supported me throughout this journey.And to everyone who believed in me and inspired me to never give up.

Zakaria Bourhaneeddine

الملخص

تتناول هذه الأطروحة نظام توليد الكهرباء القائم على الهيدروجين. تبدأ بدراسة الأثر البيئي للوقود الأحفوري وتعزيز استخدام مصادر الطاقة المتجددة مثل الطاقة الشمسية. ثم تنتقل الدراسة إلى المبادئ الأساسية للهيدروجين كمصدر للطاقة ومفاهيم عمل خلايا الوقود. يتم استخدام النمذجة الرياضية وتقنيات المحاكاة لتصميم وتقييم نظام يعمل بخلايا وقود الهيدروجين، حيث تُستخدم هذه النماذج لتحسين أداء النظام وتوجيه مراحل تطويره. وأخيرًا، تتطرق الأطروحة إلى الجانب العملي من خلال بناء نموذج أولي يهدف إلى تقييم كفاءة وجدوى استخدام الهيدروجين كمصدر نظيف لتوليد الكهرباء، بالإضافة إلى حساب التكلفة الإجمالية للنظام المقترح.

Abstract

This thesis studies a hydrogen-based electricity generation system. It begins by examining the environmental impact of fossil fuels and the promotion of renewable energies such as solar energy. The study then delves into the fundamental principles of hydrogen as an energy carrier and the operational concepts of fuel cells. Mathematical modeling and simulation techniques are employed to design and evaluate a hydrogen-powered fuel cell system. These models are used to optimize system performance and guide further development. Finally, the thesis addresses the practical implementation by constructing a prototype, which serves to assess the efficiency and viability of hydrogen as a clean energy source for electricity generation and the total cost of the proposed system.

Résumé

Ce mémoire étudie un système de production d'électricité basé sur l'hydrogène. Il commence par examiner l'impact environnemental des combustibles fossiles et la promotion des énergies renouvelables telles que l'énergie solaire. L'étude explore ensuite les principes fondamentaux de l'hydrogène en tant que vecteur énergétique ainsi que les concepts de fonctionnement des piles à combustible. Des techniques de modélisation mathématique et de simulation sont utilisées pour concevoir et évaluer un système à pile à hydrogène. Ces modèles permettent d'optimiser les performances du système et d'orienter son développement futur. Enfin, le mémoire aborde la mise en œuvre pratique à travers la construction d'un prototype, qui permet d'évaluer l'efficacité et la viabilité de l'hydrogène comme source d'énergie propre pour la production d'électricité, ainsi que le coût total du système proposé.

List of Figures

1.1 Total energy supply world wide, 2022 . . . 18
1.2 Schematic diagram of a typical solar PV system. . . . 21
1.3 How hydrogen is stored . . . 26
1.4 Fuel cell operation diagram . . . 27

2.1 Photovoltaic (PV) system under a Maximum Power Point Tracking (MPPT) controller . . . 30
2.2 Equivalent circuit of a PV cell . . . 31
2.3 Curves of the PV panel under different irradiance levels and a constant temperature of 25°C . . . 33
2.4 Outline of the method Perturb and observe . . . 33
2.5 Flowchart of Perturb and Observe algorithm . . . 34
2.6 Boost converter circuit . . . 34
2.7 Battery behavior in 24-hours cycle . . . 36
2.8 The Voltage in function of the current density . . . 41
2.9 The Voltage in function of the current density with different temperature values 41
2.10 The current density in function of the water content . . . 42
2.11 Hydrogen Production rate and faradiac efficiency . . . 43
2.12 Pressure vs. Hydrogen Mass for 500L Tank at 25°C . . . 44
2.13 The equivalent circuit of PEMFC . . . 47
2.14 Curve of Cell Voltage in function of The Current Density . . . 48
2.15 Membrane Resistance in function of water content . . . 48
2.16 Voltage in function of current With variable values of Temperature . . . 49
2.17 Current density in function of channel coordinate x . . . 50
2.18 The power of the PEMFC . . . 50
2.19 Water distribution in function of channel coordinate x and membrane coordinate y 51
2.20 The voltage of the equivalent circuit . . . 52
2.21 The current of the equivalent circuit . . . 52
2.22 The response of the equivalent circuit in Open loop . . . 53
2.23 The response of the equivalent circuit in feedback loop . . . 53
2.24 Full bridge single-phase inverter . . . 54

3.1 The full model of the simulation using MATLAB, Simulink . . . 57

3.2 Simulink Circuit for the PV system . . . 58
3.3 The chosen solar panel in different sun irradiance . . . 59
3.4 The solar panels power in different sun power using MPPT . . . 60
3.5 Sun irradiance applied to the PV array . . . 61
3.6 Curves of the current and voltage using MPPT . . . 61
3.7 Curves of the current and voltage after the boost converter . . . 62
3.8 The power delivered by the PV array using boost regulation . . . 62
3.9 The battery charging dischargin circuit PI regulated . . . 63
3.10 Battery state of charge under different sun irradiances . . . 64
3.11 Curves of the current and voltage of the battery . . . 64
3.12 Simulink/Simscape schematic of the PEM electrolyzer model . . . 65
3.13 Hydrogen flow rate response . . . 65
3.14 Electrolyzer power consumption . . . 66
3.15 Electrolyzer cell voltage transient . . . 66
3.16 The Temperature PI controlled with its response . . . 67
3.17 The Pressure PI controlled with its response . . . 68
3.18 Hydrogen storage model and dynamic response . . . 69
3.19 Fuel cell V-I and P-I curves . . . 70
3.20 Stack Parameters . . . 70
3.21 Simulink circuit used for fuel cell part . . . 71
3.22 Hydrogen flow rate . . . 72
3.23 Fuel cell stack hydrogen consumption . . . 72
3.24 The fuel cell efficiency . . . 73
3.25 The fuel cell voltage . . . 74
3.26 The fuel cell current . . . 74
3.27 The power output of the fuel cell stack . . . 75
3.28 Hydrogen flow rate PI regulated . . . 76
3.29 Stack consumption of hydrogen and oxygen PI regulated . . . 76
3.30 Stack Efficiency PI regulated . . . 76
3.31 Stack Voltage PI regulated . . . 77
3.32 Stack current PI regulated . . . 77
3.33 The Voltage output of boost converter . . . 78
3.34 The current output of the boost converter . . . 78
3.35 The Power output of the boost converter . . . 79
3.36 Single Phase inverter with PWM command . . . 80
3.37 The voltage output of the inverter . . . 80
3.38 The current of the inverter . . . 81
3.39 The inverter output power . . . 81

4.1 The PV array of the hydrogen house . . . 85
4.2 The battery pack . . . 85

4.3 The 5.5 kWh PEM electrolyzer . . . 86
4.4 Hydrogen storage . . . 87
4.5 The Compressor . . . 87
4.6 PEM fuel cell . . . 88
4.7 The Arduino UNO . . . 89
4.8 Arduino pin diagram . . . 90
4.9 Enter Caption . . . 90
4.10 PEM water electrolyzer . . . 91
4.11 The PEM fuel cell . . . 92
4.12 Battery pack . . . 93
4.13 Breadboard contain photoresistor (LDR) and LED . . . 93
4.14 The Command that drives the system . . . 94
4.15 Tinker cad circuit of the proposed system . . . 94
4.16 The prototype realization . . . 95
4.17 Measurement the voltage of batteries . . . 95
4.18 PEM electrolyzer in action . . . 96
4.19 Measure the output voltage of the fuel cell . . . 97
4.20 Small Dc motor as load for the fuel cell . . . 97

List of Tables

1.1 Renewable energy capacity in Algeria ,2023 22

4.1 The cost of each component of the system. 98
4.2 Comparison with Other Energy Systems 99

List of Symbols

PV	Photovoltaic
MPPT	Maximum Power Point Tracking
PEMFC	Polymer Electrolyte Membrane Fuel Cell
CCS	Carbon Capture and Storage Technologies
DOE	Department of Energy
SOFC	Solid Oxide Fuel Cell
DMFC	Direct Methanol Fuel Cell
PAFC	Phosphoric Acid Fuel Cell
AFC	Alkaline Fuel Cell
SOC	State Of Charge
P&O	Perturb and Observe
I_{ph}	Current generated by light or photo current (A)
I_P	Current flowing through the parallel resistor (A)
I_0	The current of the diode, proportional to the saturation current
I_s	Reverse saturation current (A)
q	Electron charge (1.6×10^{-19} C)
K	Boltzmann constant (1.38×10^{-23} J/K)
A	Ideality factor
T_c	Cell temperature in Kelvin (K)
R_s	Series resistor (Ω)
I_{sc}	Short-circuit current at 25°C and 1000 W/m^2
K_i	Temperature coefficient of the cell's short-circuit current
T_{ref}	Reference temperature of the cell (K) (= 25°C + 273)
G	Solar irradiance (W/m^2)
G ref	Reference irradiance (= 1000 W/m^2)
E_g	Band gap energy of the semiconductor (eV)
I_{sc}	Short-circuit current (A)
N_s	Number of cells in series of a PV module
τ	Transmission coefficient of the PV panel cover
α	Absorption coefficient of the PV panel
H_T	Total solar irradiation at PV panel level
U_L	Thermal transfer coefficient of PV panel covers

$\boldsymbol{T_c}$	PV cell temperature
$\boldsymbol{T_A}$	Ambient temperature
$\boldsymbol{E}$	Actual cell potential
$\boldsymbol{E_0}$	Reversible potential
$\boldsymbol{R}$	Universal gas constant (8.314 J/mol·K)
$\boldsymbol{F}$	Faraday constant (96485 C/mol)
$\boldsymbol{P_{H_2O}}$	Partial pressure of water vapor
$\boldsymbol{P_{H_2}}$	Partial pressure of hydrogen
$\boldsymbol{P_{O_2}}$	Partial pressure of oxygen
$\boldsymbol{\eta}$	Overpotential
$\boldsymbol{f_1}, \boldsymbol{f_2}$	Faradic yield calculation parameters ($\mathrm{mA}^2 \cdot \mathrm{cm}^{-4}$)
X_{act}	Reversible voltage (V)
V_{act}	Activation overpotential
$\boldsymbol{P_b}$	Pressure of the tank (gas)
$\boldsymbol{P_{bi}}$	Initial pressure of the storage tank
D_i	Water diffusion coefficient

Contents

Acknowledgments 3

Dedication 5

Abstract 6

List of Figures 8

List of Tables 9

List of Symbols 12

General Introduction 15

1 Overview of the electricity production system based on hydrogen 17

1.1 Introduction . . . 18

1.2 Fossil fuels energy . . . 18

1.2.1 Coal . . . 19

1.2.2 The oil . . . 19

1.2.3 Natural gas . . . 19

1.3 Renewable energy . . . 20

1.3.1 Wind energy . . . 20

1.3.2 Hydropower . . . 20

1.3.3 Solar energy . . . 20

1.3.4 Biomass energy . . . 21

1.3.5 Geothermal energy . . . 22

1.3.6 Renewable energy in Algeria . . . 22

1.4 Hydrogen as energy source . . . 23

1.4.1 General Information about Hydrogen . . . 23

1.4.2 Hydrogen production . . . 23

1.4.3 Hydrogen Storage . . . 25

1.5 Fuel cell . . . 26

1.5.1 Types of fuel cell . . . 26

1.5.2 Principles of fuel cell . . . 26

1.5.3 Advantages of the fuel cell . . . 27
1.5.4 Disdvantages of the fuel cell . . . 28
1.6 Conclusion . . . 28

2 PV-Hydrogen Modeling **29**
2.1 Introduction . . . 30
2.2 Photovoltaic system . . . 30
2.2.1 Equivalent circuit of a PV photovoltaic cell . . . 30
2.2.2 MPPT control of the PV . . . 33
2.2.3 Boost converter . . . 34
2.2.4 Battery . . . 36
2.3 Modeling PEM Electrolyte Cell . . . 37
2.3.1 Mathematical modeling . . . 37
2.3.2 Results . . . 40
2.4 Hydrogen Production rate . . . 42
2.5 Hydrogen tank modeling . . . 43
2.6 Modeling of PEM Fuel cell . . . 44
2.6.1 Mathematical modeling . . . 44
2.6.2 Results . . . 48
2.7 Single phase inverter . . . 54
2.8 Conclusion . . . 55

3 PV-Hydrogen Simulation **56**
3.1 Introduction . . . 57
3.2 The full model . . . 57
3.3 The PV system . . . 58
3.4 Battery . . . 63
3.5 Electrolyzer . . . 65
3.6 Hydrogen Storage . . . 68
3.7 Fuel Cell . . . 69
3.8 Inverter . . . 79
3.9 Conclusion . . . 82

4 From Concept to Practice, Prototype and Cost Analysis **83**
4.1 Introduction . . . 84
4.2 The hydrogen House . . . 84
4.2.1 PV Array . . . 84
4.2.2 battery pack . . . 85
4.2.3 The electrolyzer . . . 86
4.2.4 The storage system . . . 87
4.2.5 The Compressor . . . 87
4.2.6 The fuel cell . . . 88

4.3 Prototype . . . 88
4.3.1 Components . . . 88
4.4 Tinker the Hydrogen prototype . . . 94
4.5 Realization . . . 95
4.5.1 The full prototype . . . 95
4.5.2 Electrolyzer Functionality . . . 96
4.5.3 Fuel cell functionality . . . 97
4.6 Implementation Cost . . . 98
4.7 Comparison with the others energy systems . . . 99
4.8 Conclusion . . . 99

General Conclusion **101**

General Introduction

In the face of climate change and growing concerns over fossil fuel depletion, hydrogen has emerged as a key player in the global transition toward cleaner and more sustainable energy systems. As a versatile energy carrier, hydrogen holds significant potential in transforming electricity production worldwide and reducing reliance on non-renewable energy sources such as coal, oil, and natural gas [1][2].

Hydrogen can be produced using various methods, including water electrolysis powered by renewable energy sources like solar, wind, or hydropower. This form of green hydrogen is entirely clean, emitting no greenhouse gases during its production or use[3][4].

When integrated into electricity production, particularly through hydrogen fuel cells, it enables electricity generation with water as the only byproduct, offering a zero-emission alternative to traditional combustion-based methods[5][6].

Countries worldwide are increasingly investing in hydrogen technologies to decarbonize their power grids, especially in sectors where direct electrification is challenging, such as heavy industry, long-haul transportation, and backup energy storage[7]. Hydrogen also plays a strategic role in grid balancing, storing excess electricity produced during peak renewable energy generation periods and releasing it when demand is high [8].

The adoption of hydrogen in electricity production contributes significantly to reducing the global carbon footprint and advancing energy security. By integrating hydrogen into the global energy mix, nations are not only diversifying their energy sources but also paving the way toward a more resilient and environmentally friendly energy future where non-renewable sources are gradually phased out [8][7].

Solar energy is one of the most abundant and cleanest sources of energy available. However, its intermittent nature (limited to daylight hours and weather conditions) presents challenges for consistent power supply. This is where hydrogen plays a key role [9].

The photovoltaic conversion of solar radiation into electricity is one of the means of exploiting the solar deposit. It is carried out by solar cells. A system coupling a photovoltaic field and an electrolyzer makes it possible to store electricity through storage in the form of gas (hydrogen) [9][10].

Our thesis aims to contribute to a better understanding of a new technology for the production and storage of clean energy. This study is designed to stimulate future work in this field. In this study, we present a simulation study of a photovoltaic system to produce hydrogen through water electrolysis. Electrical energy production is provided by the photovoltaic pan-

els. The system components were modeled, and a flowchart for system performance simulation was executed in MATLAB to determine the most favorable conditions for optimal hydrogen production.

This thesis consists of four coherent and complementary chapters, where the first presents a general overview of an electricity production system based on hydrogen. We are conducting a bibliographic study about the effect of fossil fuels in energy production and going through more safety and renewable sources like solar energy than general and fundamental concepts about hydrogen more specifically.

The second chapter represents the modeling of the PV-hydrogen system from the mathematical equations to the general condition simulation.

The third chapter applies the theories and models developed in the sconed chapter for the optimization of the PV-hydrogen system, by simulating the dynamic interaction between the photovoltaic (PV) array, the electrolyzer, hydrogen storage, and the fuel cell.

The final chapter is dedicated to the system's practical realization with a simple prototype which is presented to experimentally evaluate the efficiency of hydrogen as an energy source, specifically when the photovoltaic (PV) array is substituted by a stack of five 9V batteries. We concluded with a techno-economic analysis.

Chapter 1

Overview of the electricity production system based on hydrogen

1.1 Introduction

Hydrogen, represented by the chemical symbol H_2, is a universal energy carrier that can be produced from various sources, including fossil fuels such as oil, gas, and coal, as well as from water using renewable energies like hydropower, solar, or wind energy, or even through nuclear power. Additionally, biomass can also be used to produce hydrogen. These diverse production methods offer the significant advantage of enabling hydrogen production anywhere in the world, depending on the locally available energy sources. This flexibility could allow many countries to achieve a certain degree of energy independence.

However, it should be noted that hydrogen alone, as an energy carrier, cannot fully resolve the impending energy shortages from fossil fuels. Hydrogen has a broad range of applications, including transportation, electricity generation, and heating for homes, as well as providing backup power.

1.2 Fossil fuels energy

A non-renewable energy source refers to a type of energy whose regeneration occurs either extremely slowly or not at all on a human timescale. These sources are depleted far more quickly than they can be naturally replenished, making them finite and ultimately unsustainable. The most prominent non-renewable energy sources are fossil fuels including coal, oil, and natural gas which are formed over millions of years from the remains of ancient organisms [11]. Unlike renewable sources such as solar and wind, fossil fuels are limited in supply and pose significant challenges for long-term energy security. In 2022, fossil fuels alone accounted for approximately 80.9% of the total global energy consumption, according to the International Energy Agency (see figure 1.1) [12]. This heavy dependence on fossil fuels has been a major contributor to carbon emissions, global warming, and air pollution, making them a central driver of the current environmental crisis. The environmental damage caused by their extraction, transportation, and combustion underscores the urgent need to shift toward cleaner and more sustainable energy alternatives [12].

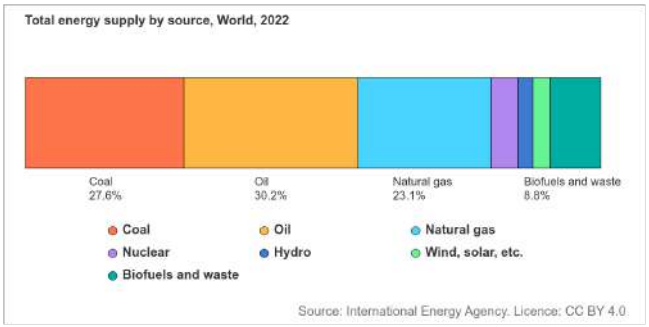


Figure 1.1: Total energy supply world wide, 2022

1.2.1 Coal

Coal is the oldest fossil fuel still in use, having played a pivotal role in powering the First Industrial Revolution in late 18th-century England. Throughout the 19th century, it remained a primary global energy source. Despite the gradual rise of natural gas, coal continues to be the second most consumed fossil fuel worldwide surpassed only by oil and ahead of natural gas [13]. However, coal is also one of the most polluting energy sources, emitting large quantities of carbon dioxide (CO_2), sulfur dioxide (SO_2), nitrogen oxides (NO_x), and particulate matter. These pollutants are major contributors to climate change, acid rain, and poor air quality, posing serious environmental and public health risks [13].

In addition to its use in electricity generation, coal is a source of by-products employed in the pharmaceutical, dye, plastics, and synthetic textile industries, as well as in fertilizer production. In some developing countries, it is still used for domestic purposes such as heating and cooking [13].

Given its significant environmental footprint, coal is increasingly being challenged by cleaner energy alternatives. Among them, hydrogen stands out as a promising solution. When produced from renewable sources and used in fuel cells, hydrogen emits only water vapor, offering a pathway to drastically reduce emissions in sectors currently reliant on coal and other fossil fuels [12].

1.2.2 The oil

Oil, a thick and viscous liquid whose name comes from the Latin "petra-oleum" ("rock oil"), has long been valued for its versatility and energy content. Because of its dark color and economic importance, it is often referred to as "black gold." Known since ancient times initially used for sealing boats and later as a lubricant and lighting fuel -petroleum became a major energy source during the industrial era. Systematic exploration began around the 1860s, particularly in Germany and the United States, leading to rapid growth in its extraction and use. By the early 20th century, petroleum accounted for roughly 40% of global energy consumption [14].

However, oil's dominant role in the global energy mix has come at a significant environmental and geopolitical cost. Its extraction, refining, and combustion are major contributors to greenhouse gas emissions, oil spills, air pollution, and ecosystem disruption [12]. Moreover, the concentration of oil reserves in politically unstable regions often leads to energy insecurity, price volatility, and conflict [12].

1.2.3 Natural gas

Natural gas is a fossil fuel primarily composed of methane (CH_4), formed over millions of years from the decomposition of organic matter [15]. It is widely used for electricity generation, residential heating, and industrial processes due to its high efficiency and relatively lower carbon dioxide emissions compared to coal and oil [12]. It is extracted through conventional drilling

and more recently through hydraulic fracturing (fracking), and is distributed via pipelines or in liquefied form (LNG) for international trade [16].

Despite its lower CO_2 emissions, natural gas presents serious environmental concerns. Methane, its main component, is a highly potent greenhouse gas over 80 times more effective at trapping heat in the atmosphere than CO_2 over a 20-year period [16][17]. Leaks from extraction, transportation, and storage infrastructure (known as fugitive emissions) significantly undermine the climate benefits often attributed to natural gas [15]. Furthermore, fracking has been linked to groundwater contamination, increased seismic activity, and negative public health impacts due to chemical exposure and air pollution [18, 19].

1.3 Renewable energy

Renewable energy refers to energy derived from natural sources that are continuously replenished, such as the sun, wind, water, and biomass. Unlike fossil fuels, which are finite and contribute to environmental pollution, renewable energy sources provide a cleaner, more sustainable way to meet global energy needs.

1.3.1 Wind energy

Wind energy is generated by converting the kinetic energy of wind into electricity using wind turbines. It is a clean, renewable source of power with low operating costs once the turbines are installed. Wind energy is abundant and can be harnessed onshore and offshore. However, its main drawback is the intermittent nature of wind, meaning it is not always available when needed. Wind energy also raises concerns regarding noise and visual impact, and the turbines can pose a threat to birds and bats, although technological improvements are addressing this issue[20].

1.3.2 Hydropower

Hydropower is the dominant renewable source of electricity, accounting for approximately 2.51% of global electrical power in 2022, with an installed capacity of 4476 TWh[12]. Hydropower is a renewable energy source that generates electricity by using flowing or falling water to spin turbines. It is reliable, produces no direct emissions, and is used worldwide. While large dams can impact ecosystems, hydropower remains a key component in sustainable energy systems due to its efficiency and ability to provide consistent power [21].

1.3.3 Solar energy

Solar energy production involves capturing sunlight using photovoltaic (PV) panels or solar thermal systems to generate electricity. PV panels convert sunlight directly into electricity using semiconductor materials, making them ideal for homes, businesses, and large-scale solar

farms. Solar energy is renewable, clean, and increasingly cost-effective, contributing to a reduction in greenhouse gas emissions and dependence on fossil fuels. As technology improves and installation costs drop, solar power continues to grow as a major source of sustainable energy worldwide[22].

The amount of electricity produced depends on several factors

- Solar irradiance (W/m^2) this varies according to the time of day, season, and weather,
- Temperature Excessively high temperatures can reduce the panel's efficiency,
- The orientation and tilt of the panel,
- The cleanliness of the surface (dust, shade, etc.).

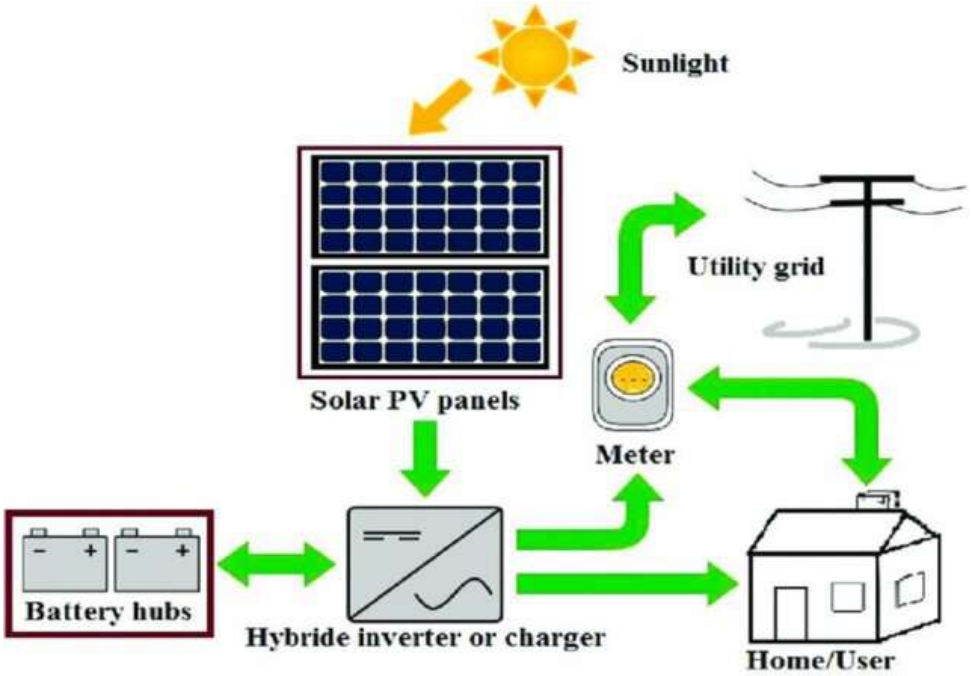


Figure 1.2: Schematic diagram of a typical solar PV system.

To be usable by most electrical devices, direct current is converted into alternating current (AC) using an inverter. In stand alone systems, the energy can also be stored in batteries (figure 1.2)[23]. Thanks to this technology, solar energy can power homes, industries, or isolated systems, offering a clean, renewable energy solution with no greenhouse gas emissions.

1.3.4 Biomass energy

Biomass energy involves the combustion or conversion of organic materials like wood, agricultural waste, and biofuels into energy. This energy source is renewable and widely available, often utilizing waste materials that would otherwise end up in landfills. Biomass can be carbon-neutral if managed sustainably, as the CO_2 released during combustion is absorbed by plants during their growth. It is a versatile energy source used for heating, electricity, and biofuels.

However, burning biomass still releases pollutants such as CO_2 and particulate matter, contributing to air pollution. In some cases, the use of wood and other biomass materials can lead to deforestation and habitat loss, especially when harvested unsustainably. Additionally, biomass tends to have lower energy efficiency compared to fossil fuels and other renewable sources like wind or solar[24][25].

1.3.5 Geothermal energy

Geothermal energy utilizes the Earth's internal heat to generate electricity or provide direct heating. It is a highly reliable and consistent energy source, producing power 24/7 without relying on weather conditions. Geothermal energy has very low carbon emissions, making it a clean alternative to fossil fuels. It also requires less land space compared to other renewables such as wind or solar farms. However, the initial costs of geothermal power plants are high due to the need for deep drilling into the Earth's crust. Furthermore, geothermal energy is location-specific, making it only viable in regions with significant geothermal activity, such as volcanic areas. There is also a risk of induced seismic activity, where drilling can cause minor earthquakes[26].

1.3.6 Renewable energy in Algeria

The rising costs of conventional energy and the depletion of fossil fuel resources are driving a growing shift toward renewable energy, which offers advantages such as abundance, environmental sustainability, and availability worldwide. Solar energy, in particular, has gained renewed interest, especially for applications in remote areas. Algeria, with its vast solar potential, is well-positioned to harness renewable energy. By the end of 2023, Algeria had 437 MW of solar generation capacity installed, but the government has set a goal of reaching a production capacity of 4 GW by the end of 2025. building on the Solar 2000MW and Solar 1000MW launched by Algeria's state-owned company Sonelgaz.The government aims to diversify its revenue streams and reduce reliance on natural gas, which is currently primarily used for power generation in the country[27].

Table 1.1: Renewable energy capacity in Algeria ,2023

Energy Source	**Installed Capacity (MW)**	**Share of Total Renewable Capacity**
Solar PV	436.8	72.6%
Hydropower	164.1	27.3%
Total	**600.9**	**100%**

Table 1.1 shows that Algeria is actively developing renewable energy[28][29], primarily solar photovoltaic, which represents approximately 73% of installed capacity. In 2023, the country had 600.9 MW of renewable capacity, including 436.8 MW of solar (Around 388.95 MW of the PV of the PV totals is connected to the grid, and the rest is off-grid)[29], and 164.1 MW

of hydroelectricity. The national objective is to reach 4,000 MW by 2025 and 15,000 MW by 2035, representing 27% of electricity production. Thanks to strong sunshine and international partnerships, Algeria seeks to become a major player in the energy transition[28].

1.4 Hydrogen as energy source

In the field of renewable energy, particularly in photovoltaic electricity generation, one major challenge is the intermittency of production, especially at night or during cloudy days. To address this issue, energy storage solutions are necessary to ensure a continuous power supply. Among the various storage methods, batteries and hydrogen stand out as an effective solution for the lack of power in the world today[30]. Hydrogen plays a crucial role as an intermediate energy carrier by allowing excess electricity generated from solar panels to be stored in the form of hydrogen through electrolysis. This hydrogen can then be converted back into electricity using fuel cells when needed, ensuring a stable and reliable energy supply[31]. The use of hydrogen storage enhances the efficiency and feasibility of renewable energy integration into the power grid, making it a promising solution for sustainable energy systems[32].

1.4.1 General Information about Hydrogen

Hydrogen was first identified as a distinct element in 1776 by Henry Cavendish, a British physicist and chemist. Later, in 1783, the French scientist Antoine Lavoisier named it "hydrogen," derived from the Greek words "hydro" (water) and "gene" (generate). Represented by the symbol H, hydrogen has an atomic number of 1 and is colorless, odorless, non-toxic, and highly flammable [7]. Hydrogen does not naturally exist in its free state and is typically found in combination with other elements

- With oxygen forming water (H_2O)
- With carbon present in hydrocarbons (oil, gas)
- With carbon and oxygen found in plant biomass, carbohydrates, and organic compounds.

1.4.2 Hydrogen production

Hydrogen production is a key process in the transition to sustainable energy, as hydrogen serves as a versatile and clean energy carrier. Since hydrogen does not exist freely in nature, it must be extracted from various sources through different methods. The most common hydrogen production techniques include steam methane reforming (SMR) from natural gas, electrolysis of water using electricity, and biomass gasification. Among these, green hydrogen, produced through electrolysis powered by renewable energy, is gaining attention as an environmentally friendly alternative. The development of efficient and cost-effective hydrogen production methods is essential for integrating hydrogen into energy systems, reducing carbon emissions, and advancing clean energy solutions [32][2].

Hydrogen Production from Fossil Fuels (Hydrocarbons)

Hydrogen can be extracted from various fossil fuels, including natural gas, coal, and oil. However, the production process is complex due to the release of carbon dioxide (CO_2) as a by-product. While this method can have economic advantages, it poses environmental challenges, as CO_2 emissions contribute to climate change. Developing carbon capture and storage (CCS) technologies can help mitigate the environmental impact of hydrogen production from fossil fuels [1][33].

Natural Gas Steam Reforming

Steam reforming is a key process for hydrogen production using methane (CH_4) from natural gas. Before the reaction, natural gas undergoes desulfurization to remove impurities. The process involves two main reactions synthesis gas formation and carbon monoxide conversion. However, since these reactions are thermodynamically balanced, some methane and carbon monoxide remain unreacted in the final output[34][10].

Hydrogen Production from Coal

Hydrogen production from coal is mainly done through a process called coal gasification. In this process, coal is heated in the presence of steam and oxygen to produce a mixture called syngas (hydrogen, carbon monoxide, and CO_2). The hydrogen is then separated for use, while CO_2 can be captured and stored (with CCS – Carbon Capture and Storage)[33].

Electrolysis of Water

Electrolysis is an electrochemical process that uses electrical energy to split water (H_2O) into hydrogen (H_2) and oxygen (O_2). This method offers a clean and sustainable way to produce hydrogen when powered by renewable or low-carbon electricity sources, thus generating what is known as green hydrogen [35][12]. Electrolysis occurs within an electrolyzer, which typically consists of two electrodes an anode and a cathode separated by an electrolyte that facilitates ion transport [35]. electrolyzers consist of an anode and a cathode separated by an electrolyte. Different electrolyzers function in different ways, mainly due to the different type of electrolyte material involved and the ionic species it conducts[35]. There are three main types of electrolyzers distinguished by their electrolyte and operating conditions

- Alkaline electrolyzers (A-E) use a liquid alkaline solution as the electrolyte and have been widely used due to their durability and lower costs, but they generally operate at lower current densities [35].
- Proton exchange membrane electrolyzers (PEM-E) use a solid polymer electrolyte membrane, allowing for higher current densities, faster response times, and greater flexibility with variable renewable power sources, though at higher capital costs [12].

- Solid oxide electrolyzers (SO-E) operate at high temperatures (600–900°C) and use a ceramic electrolyte, enabling higher electrical efficiency and the potential to use waste heat from industrial processes, but they are less mature commercially [35][12].

The production of green hydrogen through electrolysis is rapidly gaining attention as a key enabler for decarbonizing sectors that are otherwise difficult to electrify, such as heavy industry, long-haul transport, and seasonal energy storage [36][12]. Unlike hydrogen produced from fossil fuels (grey hydrogen) or hydrogen with carbon capture (blue hydrogen), green hydrogen offers a truly zero-carbon pathway, supporting global climate goals and reducing dependence on non-renewable energy sources [36].

In this thesis, the focus on electrolysis underlines its potential to replace fossil fuel-based hydrogen production, thereby advancing sustainable energy systems and contributing to the global transition toward a low-carbon future [12].

1.4.3 Hydrogen Storage

Hydrogen storage is a key technological barrier to the development and widespread use of fuel cell power technologies in transportation, stationary, and portable applications. DOE's efforts focus primarily on the early-stage research and development (R and D) of on-board vehicular hydrogen storage systems that will allow for a driving range of greater than 300 miles while meeting packaging, cost, safety, and performance requirements to be competitive with current vehicles. While hydrogen fuel cell electric vehicles traveling more than 300 miles on a single fill are now commercially available in selected regions in the United States, this driving range must be achievable across different vehicle models and without compromising space, performance, or cost[37].

Methods of Hydrogen Storage (see figure 1.3)[37]

- Compressed hydrogen gas storage is the most common method, where hydrogen is stored in high-pressure tanks at 350–700 bar (5,000–10,000 psi).
- liquid hydrogen storage involves cooling hydrogen to cryogenic temperatures of -253°C (-423°F) to convert it into a liquid
- Solid hydrogen storage involves trapping hydrogen inside solid materials like metal hydrides, chemical compounds, or nanostructured materials

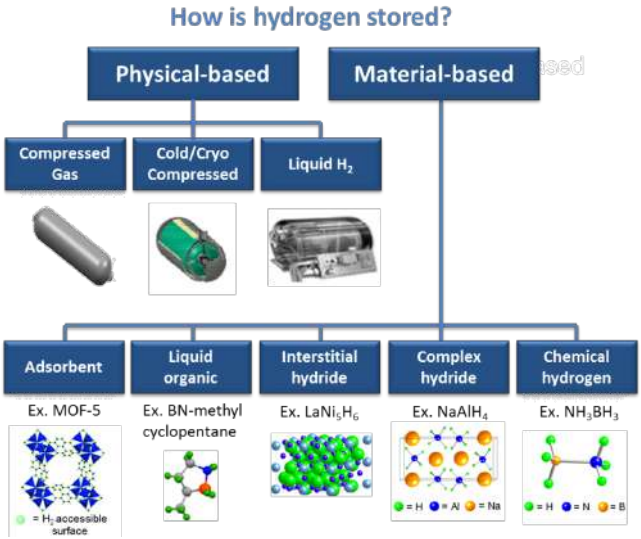


Figure 1.3: How hydrogen is stored

1.5 Fuel cell

Fuel cells are devices that generate electricity through electrochemical redox reactions, not combustion. In short, they convert the chemical energy of fuels, such as hydrogen or methane, directly into electrical energy by combining them with oxygen. Because the chemical energy does not need to be converted into thermal energy and mechanical energy first, fuel cells are extremely efficient. Besides minimizing energy losses, fuel cells are also less polluting than classic combustion carbon emissions are much lower. If green hydrogen – hydrogen created using renewable energy sources - is fueling the cell, they only emit vapor and warm air[38].

1.5.1 Types of fuel cell

There are several types of fuel cells, differentiated by the type of electrolyte separating the fuel from the oxygen. This classification determines the kind of electro-chemical reactions that take place in the cell, the required catalysts, the operating temperature, the required fuel, and other factors [38]. These are 4 common categories of fuel cells

- Proton Exchange Membrane (PEM) fuel cells
- Alkaline fuel cells
- Solid oxide fuel cells
- Phosphoric acid fuel cells

1.5.2 Principles of fuel cell

There are various types of FC systems. However, the principle of their function is similar. For a fuel cell system, three pillars are required an anode, a cathode, and an electrolyte. FCs

are categorized by the type of electrolyte material used. An FC can be composed of hundreds of individual cells, but each has the three same fundamental components. The electrolyte is located between the cathode and the anode. Figure 1.4 depicts a schematic of a polymer electrolyte FC (PEMFC) operation diagram [39]. This FC type is also known as a proton exchange membrane FC.

The PEMFC is what is most commonly used in mobile power applications, such as vehicles. While the electrolyte material used varies depending on the type of FC, the general function of the FC is as follows fuel (pure hydrogen) is fed into the anode compartment of the fuel cell while air or pure oxygen is fed into the cathode side of the FC. On the anode side of the cell, electrons are separated as the gas tries to make its way through the electrolyte membrane. The membrane acts as a filter to separate the electrons and the hydrogen ions while only allowing the hydrogen ions to pass through. In the cathode compartment, the hydrogen ions that passed through the membrane combine with the oxygen atoms from the air supply to produce H2O as a by-product; heat is also produced as a by-product [32]. Unlike internal combustion engines, where the fuel is mixed with air and fuel, there is separation of the fuel and the oxidant with no combustion of the fuel in an FC. Therefore, FCs do not produce the harmful emissions that internal combustion engines produce.

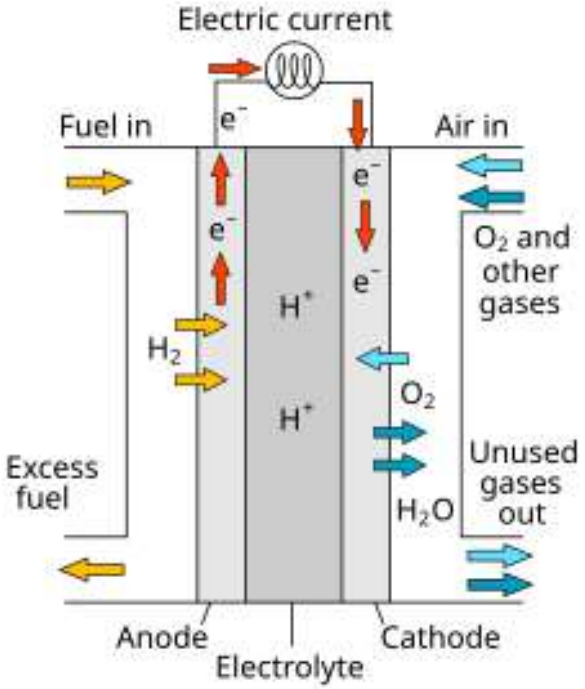


Figure 1.4: Fuel cell operation diagram

1.5.3 Advantages of the fuel cell

- High Efficiency Fuel cells can achieve higher efficiencies compared to traditional combustion-based power sources. For instance, hydrogen fuel cells can potentially generate electricity at approximately 65% efficiency, whereas conventional power stations operate at about 33-35% efficiency[32].

- Environmental Benefits When using hydrogen as a fuel, the primary byproduct is water vapor, resulting in zero harmful emissions. This makes fuel cells an environmentally friendly alternative to fossil fuels[32].
- Quiet Operation Fuel cells operate quietly, making them suitable for applications where noise reduction is important, such as in residential areas or for portable power sources[40].
- Scalability and Versatility Fuel cells can be scaled to various sizes and used in a wide range of applications, from small portable devices to large power plants and vehicles[41].

1.5.4 Disdvantages of the fuel cell

- High Production Costs The manufacturing of fuel cells is expensive, primarily due to the high cost of catalysts like platinum. This makes them less economically competitive compared to traditional energy sources[42].
- Hydrogen Production and Storage Challenges Producing hydrogen, the most common fuel for fuel cells, is energy-intensive and can be costly. Additionally, hydrogen storage and distribution infrastructure is currently limited, posing challenges for widespread adoption[3].
- Durability and Longevity Issues Fuel cells can be sensitive to temperature changes and impurities in the fuel, which can affect their durability and lifespan. Ongoing research aims to improve these aspects [43].

1.6 Conclusion

Hydrogen possesses significant advantages that position it as a promising intermediate energy carrier for the future. Its versatile applications span transportation, stationary power, and portable devices, all benefiting from hydrogen's high energy efficiency. Moreover, when produced using clean, renewable sources such as solar energy, hydrogen becomes a truly sustainable and environmentally friendly fuel. This aspect is particularly important given the growing global concern over greenhouse gas emissions and climate change.

The upcoming chapter provides a comprehensive overview of the components involved in photovoltaic-hydrogen (PV-H_2) systems. It begins by detailing the sources of electrical energy, with a focus on solar photovoltaic (PV) generation, and proceeds to discuss methods of energy storage. The chapter then explores hydrogen production and storage techniques, followed by an examination of fuel cells. The theoretical framework is supported by relevant equations and models, providing a general outlook on the integration of electrolyzers and hydrogen storage within PV-hydrogen systems.

Chapter 2

PV-Hydrogen Modeling

2.1 Introduction

The production of green hydrogen, obtained from renewable energy sources, is a promising avenue for a sustainable energy future. Among these sources, solar photovoltaic (PV) energy stands out for its abundance and technological maturity. Modeling an integrated PV-powered hydrogen production system is a crucial step in understanding, optimizing, and effectively sizing such systems.

This modeling involves the mathematical representation of the system, starting with the PV panel, the MPPT method (Perturb and Observe), the storage element, and the boost converter, followed by the study of the electrolyzer and the hydrogen tank, the PEMFC and finally the DC/AC inverter to transform the energy produced for the user.

To visualize the equations in this chapter there is graph had been created using MATLAB graphing tool and go through careful analysis to better understand PEMFC and PEMEC in their general state.

2.2 Photovoltaic system

Photovoltaic system consists of four blocks, the first block represents the energy source (photovoltaic panel) whose role is to convert the illuminance into direct current, the second block is a DC-DC static converter that allows an impedance adaptation to be made so that the panel delivers the maximum energy., the third block represents the MPPT control system based on an algorithm that allows to act on the duty cycle to extract in maximum power.The photovoltaic system is controlled by the MPPT control as shown in figure 2.1. The fourth block represents the load[44].

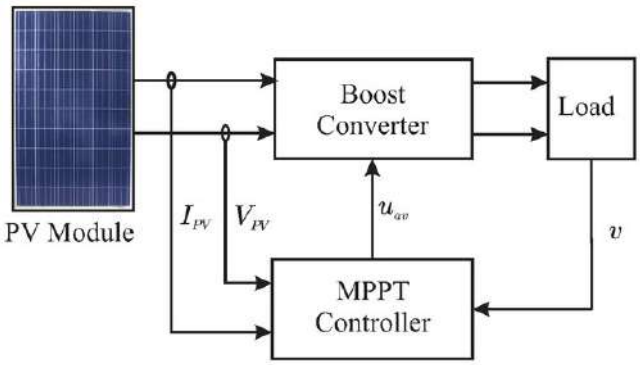


Figure 2.1: Photovoltaic (PV) system under a Maximum Power Point Tracking (MPPT) controller

2.2.1 Equivalent circuit of a PV photovoltaic cell

A PV module consists of a number of solar cells connected in series and parallel to achieve the desired voltage and current levels. A solar panel cell is essentially a p-n semiconductor junction. When exposed to light, a direct current is generated. For simplicity, the single-diode

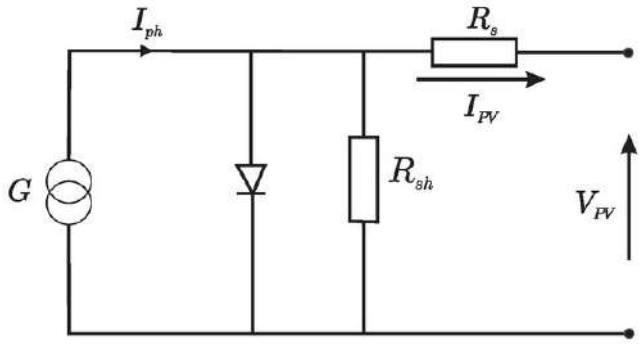


Figure 2.2: Equivalent circuit of a PV cell

model in Figure 2.2 [44]. This model offers a good compromise between simplicity and precision with the basic structure. The equivalent circuit of the general model consists of a photocurrent (Iph), a diode, a parallel resistor (Rp) expressing a leakage current and a series resistor (Rs) due to the contacts between the semiconductors and the metal parts.

In Figure 2.2. Applying Kirchhoff's law, the current will be obtained by the following equation 2.1 :

$$I_{PV} = I_{ph} - I_0 - I_p \tag{2.1}$$

$\mathbf{I_{PH}}$ – is a current generated by light or photo current;

$\mathbf{I_P}$ – current flowing through the parallel resistor is given in the following equation 2.2

$$\mathrm{I_p} = \frac{\mathrm{V} + \mathrm{IR_s}}{\mathrm{R_p}} \tag{2.2}$$

$\mathbf{I_0}$ the current of the diode which is proportional to the saturation current, it is given in equation 2.3

$$\mathrm{I_0} = \mathrm{I_s}\left[\exp\left(\frac{\mathrm{q.(V + IR_s)}}{\mathrm{K.T_cA}}\right) - 1\right] \tag{2.3}$$

$\mathbf{I_s}$ – is the reverse saturation current in ampere (A);

$\mathbf{q}$ – electron charge (1.6 × 10-19 C);

$\mathbf{K}$ – Boltzmann constant (1.38 × 10-23 J/K);

$\mathbf{T_c}$ – is a cell temperature in Kelvin (K);

$\mathbf{A}$ – is an ideal factor;

$\mathbf{R_s}$ – is a series resistor.

We substitute in equation 2.1, the characteristic voltage-current equation of a solar cell is given as follows:

$$\mathrm{I_{PV}} = \mathrm{I_{ph}} - \mathrm{I_s}\left[\exp\left(\frac{\mathrm{q.(V + IR_s)}}{\mathrm{K.T_cA}}\right) - 1\right] - \frac{\mathrm{V + IR_s}}{\mathrm{R_p}} \tag{2.4}$$

The current photo depends mainly on the sunlight and the operating temperature of the cell, which is described by the following equation 2.5 :

$$I_{ph} = [I_{sc} + K_i.(T_c - T_{ref})].\frac{G}{G_{ref}} \tag{2.5}$$

$\mathbf{I_{sc}}$ – is the short-circuit current of the cell at 25°C and 1000 W/m2;

$\mathbf{K}_i$ – the temperature coefficient of the cell's short-circuit current;

$\mathbf{T}_{ref}$ – is the reference temperature of the cell, in Kelvin (K) (= 25°C + 273.15);

G – is the amount of sunshine in watts/square meter (W/m2).

On the other hand, the saturation current of the cell varies with the temperature of the cell, which is described as follows :

$$I_s = I_{rs}(\frac{T_c}{T_{ref}}).\exp\left(\frac{q.E_g(\frac{T_c - T_{ref}}{T_{ref}.T_c})}{K.A}\right) - 1 \tag{2.6}$$

$\mathbf{I_{rs}}$ – The reverse saturation current of the cell at a reference temperature and solar radiation;

$\mathbf{E}_g$ – is the gap energy of the semiconductor used in the electron volt (eV) cell;

A – is the deal factor that depends on the PV technology.

The reverse saturation current is given by the following equation 2.7 :

$$I_{rs} = \frac{I_{sc}}{\exp\left(\frac{q.V_{oc}}{N_s T_c K A}\right) - 1} \tag{2.7}$$

$\mathbf{I}_{sc}$ – is the short-circuit current (Amps);

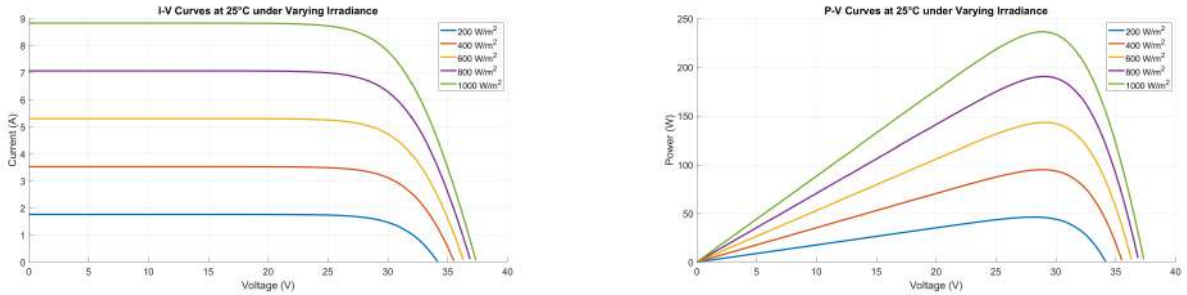
$\mathbf{V}_{oc}$ – is the open-circuit voltage (Volts);

$\mathbf{N}_s$ – Number of cells in series of a PV module.

The power generated by the photovoltaic cell is obtained by multiplying the previous expression by the output voltage (V) and is written as :

$$P = V.I_{ph} - VI_s\left[\exp\left(\frac{q.V_{oc}}{N_s T_c K A}\right) - 1\right] - V.I_p \tag{2.8}$$

The results of the PV modeling are illustrated in Figure 2.3. Figure 2.3 2.3a shows the I-V curves for different values of solar irradiance at a constant temperature of 25°C, while Figure 2.3 2.3b presents the corresponding P-V curves under the same conditions. As shown in these figures, solar irradiance primarily affects the current output, with higher irradiance levels leading to increased current. In contrast, the output voltage remains relatively stable. This behavior highlights how irradiance directly impacts the power output of a PV panel, as observed through the upward shift of the maximum power point in the P-V curves.



(a) I-V curves (b) P-V curves

Figure 2.3: Curves of the PV panel under different irradiance levels and a constant temperature of 25°C

2.2.2 MPPT control of the PV

Maximum Power Point Tracking (MPPT) is a key technique in photovoltaic systems to maximize solar energy extraction. Solar panels have a nonlinear current-voltage characteristic, and their maximum power point (MPP) varies depending on sunlight and temperature conditions. MPPT dynamically adjusts the system's operating point so that the product of voltage and current ($P = V \times I$) is always optimal. This control is typically implemented using a DC-DC converter (such as a buck, boost, or buck-boost) controlled by a tracking algorithm[45]. Popular methods include the Perturb and Observe technique, which gently perturbs the voltage or current and observes the power variation to decide the direction of the next step, and the more accurate Incremental Conductance algorithm, which is based on the derivative of power with respect to voltage. Other advanced techniques, such as fuzzy logic, neural networks, or bio-inspired algorithms (e.g., PSO), allow for even more precise adaptation to varying environmental conditions. Thus, MPPT significantly improves the overall efficiency of a solar system by making the most of the available energy[46].

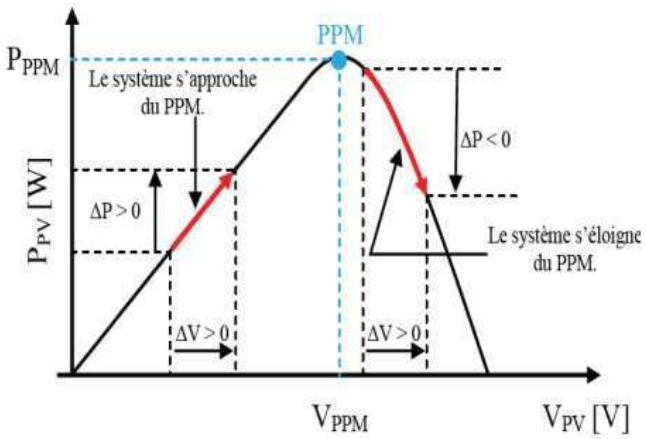


Figure 2.4: Outline of the method Perturb and observe

The figure 2.4 represents the principle of the perturb and pbserve type MPPT controls consists in disturbing the Vpv voltage by a small amplitude around its initial value and analyzing the behavior of the Vpv power variation.

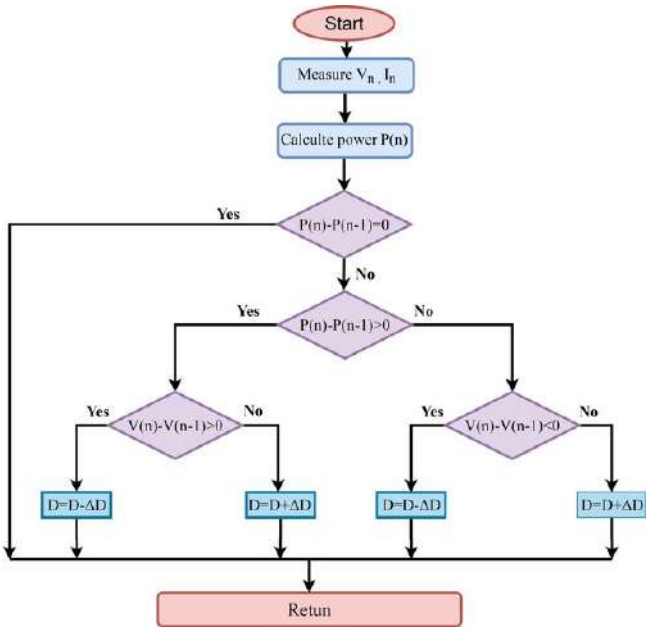


Figure 2.5: Flowchart of Perturb and Observe algorithm

Figure 2.5 illustrates the algorithm implementing a Perturb and Observe type MPPT control, where the evolution of the photovoltaic power is evaluated after each voltage perturbation. In this control strategy, two sensors are essential one measuring the current and the other measuring the voltage of the PV panels in order to accurately determine the instantaneous power output. By analyzing the change in power following each disturbance, the algorithm adjusts the operating point to converge toward the maximum power point[46].

2.2.3 Boost converter

A photovoltaic generator (PVG) has a maximum power point (MPP) that varies depending on illumination and temperature. In direct connection, the power transferred to the load can be much lower than this maximum power[45]. To address this, an adaptation stage, such as a DC-DC converter with MPPT control, is used to adjust the operating point and maximize the energy transferred to the load.

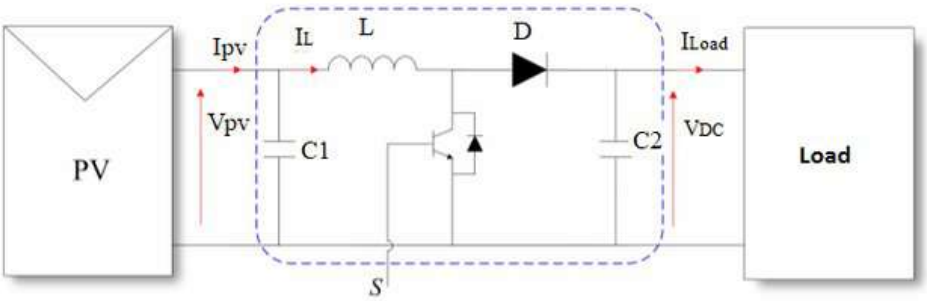


Figure 2.6: Boost converter circuit

Consider the example in the figure 2.6 of a boost DC-DC converter. This type of converter

can be used as a load source adapter when the load needs a voltage higher than that of the PV array. At the first time (αT), the transistor (S) is closed, the current in the inductor gradually increases, and as it goes along, it stores energy, until the end of the first interval. Then, the transistor (S) opens and the inductor (L) opposing the current decrease (IL), generates a voltage that is added to the source voltage, which is applied to the load through the diode (D).

Equivalent mathematical model

Given a DC-DC boost converter connected to a photovoltaic (PV) source, the following equations describe its ideal behavior:

1. Output Voltage

The relationship between the output voltage V_{DC} and the PV input voltage V_{pv} is:

$$V_{\text{DC}} = \frac{V_{pv}}{1-\alpha} \tag{2.9}$$

where:

- α is the duty cycle ($0 < \alpha < 1$)
- V_{pv} is the voltage of the PV module

2. Output Current

Assuming an ideal converter, the output current I_{Load} is related to the inductor current I_L by:

$$I_{\text{Load}} = I_L(1-\alpha) \tag{2.10}$$

3. Inductor Behavior

When the switch is ON (S closed):

$$V_L = V_{pv} \tag{2.11}$$

When the switch is OFF (S open):

$$V_L = V_{pv} - V_{\text{DC}} \tag{2.12}$$

4. Power Balance (Ideal)

In steady-state and assuming 100% efficiency:

$$P_{pv} = V_{pv} \cdot I_{pv} = V_{\text{DC}} \cdot I_{\text{Load}} \tag{2.13}$$

2.2.4 Battery

In a photovoltaic system, energy storage is essential for conserving energy produced by the PV generator during periods of insufficient production (e.g., nighttime or bad weather), thereby ensuring continuous power supply [47]. Batteries serve as fundamental electrochemical storage devices characterized by key parameters including nominal voltage, ampere-hour (Ah) capacity, watt-hour (Wh) energy rating [48], state of charge (SOC), depth of discharge (DOD) [49], cycle life dependent on charge/discharge patterns, and C-rate defining operational current limits [50]. Additional critical characteristics encompass energy efficiency, internal resistance (affecting voltage stability and thermal behavior), and self-discharge rate [51]. These parameters collectively determine battery performance and longevity in renewable energy applications.

The state of charge (SOC), representing the available energy reservoir, evolves dynamically according to [52] :

$$\mathrm{SOC}(t) = \mathrm{SOC}_0 + \frac{1}{Q_{\mathrm{nom}}} \int_0^t I_{\mathrm{batt}}(\tau) d\tau \tag{2.14}$$

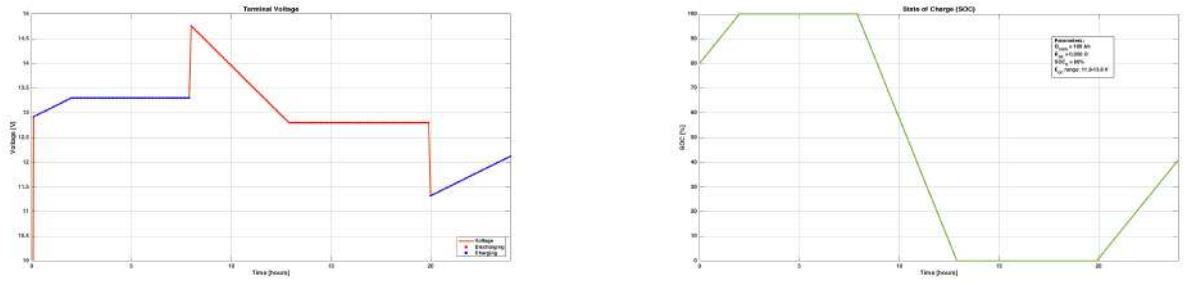
Where SOC_0 denotes initial charge state (%); Q_{nom} is nominal capacity (Ah); and I_{batt} represents battery current (A), with negative values indicating charging.

Terminal voltage behavior, critical for power delivery stability, according to [53] :

$$V_{\mathrm{batt}} = E_{\mathrm{oc}}(SOC) - I_{\mathrm{batt}} R_{\mathrm{int}}(SOC, T) \tag{2.15}$$

Where E_{oc} is open-circuit voltage (V) - a function of SOC; and R_{int} signifies internal resistance (Ω) dependent on both SOC and temperature T.

Results



(a) Battery voltage (b) battery soc

Figure 2.7: Battery behavior in 24-hours cycle

Figure 2.7b shows the battery starting at 80% charge, increasing to 100% by hour 2.5, and staying full until hour 8. It then discharges steadily to 0% by hour 13, remains empty until hour 20, and begins charging again until the end of the 24-hour period. Correspondingly, Figure 2.7a indicates a steady rise during charging, stabilizing around 13.3 V during full charge. During discharge, voltage initially peaks around 14.8 V, then drops gradually. From hours 13 to 20,

voltage remains at about 12.8 V despite 0% SOC, and it rises again when charging resumes after hour 20.

2.3 Modeling PEM Electrolyte Cell

2.3.1 Mathematical modeling

The anode (positive) and cathode (negative) are connected by an external power source to form a circuit, when enough potential difference is applied across the water, the positive ions move through the anode and the positive ions move to the cathode, resulting in the formation of oxygen and hydrogen gas at the anode and the cathode respectively. The half-reaction at the anode is called Oxygen Evolution Reaction (OER) and the half-reaction at the cathode is called (HER) and are represented by Eq. 2.16 and Eq 2.17 :

Anode:

$$\mathrm{H_2O}(l) \rightarrow \frac{1}{2}\mathrm{O_2}(g) + 2\mathrm{H^+}(aq) + 2e^- \tag{2.16}$$

Cathode:

$$2\mathrm{H^+}(aq) + 2e^- \rightarrow \mathrm{H_2}(g) \tag{2.17}$$

Overall :

$$2\mathrm{H_2O}(l) \rightarrow 2\mathrm{H_2}(g) + \mathrm{O_2}(g) \tag{2.18}$$

At the anode, water molecules find a strong electric field that has been applied by the electrical supply that is enough to destabilize water molecules and force electrons out (which are then carried away by the external circuit) as electrons are pulled out, the bonds in the water molecules break leaving as with oxygen gas and hydrogen protons this process wouldn't happen if there is no enough voltage (about 1.23 V) to overcome the energy barrier. At the Cathode the generated protons (H+) migrate through the membrane (which lets them through but blocks electrons) toward the cathode which provides the electrons that these protons need to form hydrogen gas, the notable thing here is the advantage that the membrane is providing by separating and keeping everything where it needs to be for the reaction to take place. To better understand how the pressure of the reactants affects the cell potential the following equation which is a form of the Nernst equation comes in handy [54] :

$$E = E_0 - \frac{RT}{nF} \ln\left(\frac{P_{\mathrm{H_2}O}}{P_{\mathrm{H_2}} P_{\mathrm{O_2}}}\right) \tag{2.19}$$

E Actual cell potential This is the voltage required to drive water electrolysis under non-standard conditions (the temperature is above 298.15K or lower so as the pressure for 1 atm) in real conditions there are so many things affecting the PEMEC from gas pressures to the temperature to the water activity and E here tells you the exact amount of voltage you need to apply to make the reaction successful.

E0 Reversible Potential The cell potential under standard conditions (as mentioned before 298.15K and 1 atm) which does have a known value Erev = 1.23V is the lowest value you can

give to the reaction of water electrolysis to happen.

$\frac{RT}{nF}$ Nernst Factor Components

R Universal gas constant (8.314 J/mol K),

T Operating temperature (in Kelvin),

n Number of electrons transferred per reaction (in our case it 4),

F Faraday constant (96485 C/mol) Value of this factor at T = 298.15K (standard value).

$$\frac{RT}{nF} = \frac{(8.314)(298.15)}{(4)(96485)} = 0.0064V$$

This factor scales how much the voltage changes with gas pressures and temperature.

$\ln\left(\frac{P_{H_2O}}{P_{H_2}P_{O_2}}\right)$ Reaction Quotient

PH2O Partial pressure of water vapor (water is a common liquid in PEMEC so activity is used where it equals 1).

PH2 and PO2 Partial pressures of hydrogen and oxygen gases if one of them increases the denominator gets bigger making as a result the whole fraction smaller. The ln term becomes negative increasing E.

The current density is a crucial parameter to better understand the oxygen and hydrogen production rate and here is the equation 2.20 that describes :

$$i = i_0 \left[e^{\frac{\alpha n F \eta}{RT}} - e^{\frac{-(1-\alpha) n F \eta}{RT}} \right] \tag{2.20}$$

i Current density is the net current density (A / m^2) generated during electrolysis. It represents the rate of charge transfer per unit area of the electrode, as I get higher the faster H_2/O_2 production,

i_0 Exchange Current density the equilibrium current density (A/m^2) at zero overpotential a bigger i_0 reduces the overpotential needed to achieve a given current density, improving efficiency,

η Overpotential the extra voltage (volts) applied beyond the reversible potential Erev to drive the reaction at a desired rate higher η increases current density but reduces energy efficiency due to losses,

α Charge transfer coefficient a dimensionless parameter (0¡¡1) that determines the symmetry of the energy barrier for the reaction usually 0.5 for H_2 and 0.2 – 0.5 for O_2 ,

$e^{\frac{\alpha n F \eta}{RT}}$ Represents the forward push to split water or the anodic current,

$e^{\frac{-(1-\alpha) n F \eta}{RT}}$ Represents the backward push or the cathodic current.

Example of calculation : $i_0 = 10^{-3}$ (A / cm^2) — $\alpha = 0.5$ — n = 2 — T = 353 K — $\eta = 0.1$ V

$$i = 10^{-3} \left[e^{\frac{(0.5 \times 2 \times 96485 \times 0.1)}{(8.314 \times 353)}} - e^{\frac{-(1-0.5) \times 2 \times 96485 \times 0.1}{(8.314 \times 353)}} \right]$$

$$i = 0.0265\,\mathrm{A/cm^2}$$

In Eq 2.21 the losses were neglected to simplify things a bit but for the sake of accuracy the actual Nernst equation is as follows including thermodynamic, kinetic, and resistive losses

[55] :

$$E = V_{\text{oc}} + V_{\text{act}} + V_{\text{ohm}} + V_{\text{con}} \tag{2.21}$$

E the operating voltage of the electrolyzer. It's the actual voltage you must apply so that water splits into hydrogen and oxygen.

Voc Reversible voltage represents the minimum thermodynamic voltage required when no current flows.

V_{act} the activation overpotential. This is the extra voltage needed to overcome the inherent kinetic barriers of the electrochemical reactions at the electrodes. In other words, even if thermodynamics would allow the reaction at V_{oc}, you need extra "push" for the electrons to transfer across the interface.

V_{ohm} is the ohmic overpotential. It accounts for voltage drops due to resistive elements in the cell most notably, the ionic resistance in the membrane and any contact resistances between layers.

V_{conc} is the concentration overpotential. It arises when the concentrations of reactants (or products) near the electrode surfaces differ from their bulk values; this mismatch creates additional voltage losses because the reaction is slowed down by limited mass transfer.

The reversible voltage is given by :

$$V_{\text{oc}} = E_0 + \frac{RT}{2F} \ln \left(\frac{P_{\text{H}_2} P_{\text{O}_2}^{0.5}}{\alpha_{\text{H}_2O}} \right) \tag{2.22}$$

This equation shows that if you change the operating temperature or gas pressure, the reversible voltage will shift accordingly.

E_0 is the standard reversible voltage. It's derived from the change in Gibbs free energy (ΔG°) for water splitting under standard conditions. For water electrolysis, E_0 is typically around 1.23 V.

α_{H_2O} is the activity of water. In many practical cases (especially with liquid water feeding the cell) α_{H_2O} is taken as 1.

The activation overpotential is given by the following equation 2.23 (the Butler-Volmer equation) :

$$V_{\text{act}} = \frac{RT}{F\alpha_c} \sinh^{-1} \left(\frac{i}{2i_{0,c}} \right) + \frac{RT}{F\alpha_a} \sinh^{-1} \left(\frac{i}{2i_{0,a}s_0} \right) \tag{2.23}$$

i_{0c} and i_{0a} are the exchange current densities for the cathode and anode reactions, respectively. These parameters indicate how readily the reactions proceed when the system is at equilibrium (no net reaction). A higher i_0 means the electrode reaction is faster and requires less extra voltage (i.e. lower activation losses).

α_c and α_a are the charge transfer (or symmetry) coefficients for the cathode and anode. They reflect the distribution of the energy barrier that must be overcome during the electron transfer process. The function asinh (the inverse hyperbolic sine) appears when the Butler–Volmer equation is rearranged for cases of high overpotential. Its use here indicates that the relationship

between overpotential and current density is exponential.

s_0 represents the liquid water saturation at the anode catalyst layer. Including s_0 accounts for the fact that the local availability of water can affect the reaction kinetics at the anode.

In physical terms, this equation 2.23 quantifies the extra voltage you need to "drive" the electrochemical reactions faster than they would occur at equilibrium. A low exchange current density or poor water saturation will force the cell to operate at a higher overpotential. The ohmic overpotential is given by Ohm's law as :

$$V_{\text{ohm}} = \frac{\delta_{\text{mem}}}{\sigma_{\text{mem}}} i \tag{2.24}$$

δ_{mem} is the thickness of the membrane (in meters). A thicker membrane has a longer path for ion conduction and therefore higher resistance. σ_{mem} is the ionic conductivity of the membrane (in S/m). This parameter depends strongly on the water content (hydration level) of the membrane and the operating temperature. For example, a common empirical model for Nafion is :

$$\sigma_{\text{mem}} = (0.005139\lambda - 0.00326) e^{1268\left(\frac{1}{303} - \frac{1}{T}\right)} \tag{2.25}$$

According to Ohm's law, the voltage drops across a resistive element equals the product of the current and the resistance (here, resistance = δmem/σmem). This term represents the voltage lost because ions have to travel through a medium that isn't perfectly conductive. The concentration overpotential is given by :

$$V_{\text{con}} = \frac{RT}{4F} \ln\left(\frac{C_{\text{O}_2}^{\text{mem}}}{C_{\text{O}_2,\text{mem}}^{0}}\right) + \frac{RT}{2F} \ln\left(\frac{C_{\text{H}_2}^{\text{mem}}}{C_{\text{H}_2,\text{mem}}^{0}}\right) \tag{2.26}$$

$C_{\text{O}_2}^{\text{mem}}$ and $C_{\text{H}_2}^{\text{mem}}$ Represent the concentrations of oxygen and hydrogen, respectively, at the membrane.

$C_{\text{O}_2,mem}^{0}$ and $C_{\text{H}_2}^{\text{mem}}$ Are standard concentrations for oxygen and hydrogen. The logarithmic functions here come from the Nernst-type relationships and indicate that even small deviations in concentration can lead to noticeable voltage penalties. Physically, V_{con} quantifies the extra voltage required when the local concentration of reactants deviates from their ideal values.

2.3.2 Results

First of all, the polarization curve

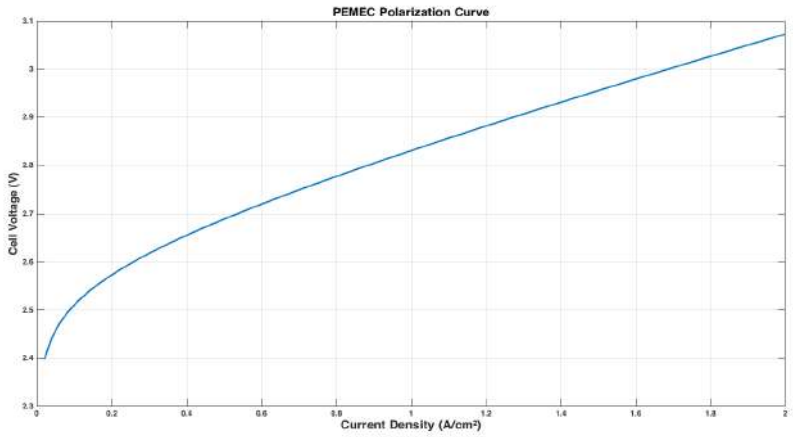


Figure 2.8: The Voltage in function of the current density

Figure 2.8 Illustrates how the cell voltage drops with increasing current density, revealing key losses like activation, ohmic, and mass transport overpotentials. This information is critical for optimizing the performance and efficiency of electrical systems such as fuel cells and electrolyzers, ensuring they operate reliably under various load conditions.

The Nernst equation has so many voltages so those voltages in function of the current density are crucial because it gives clear visualization of how the different voltage losses activation, ohmic, and concentration overpotentials evolve with increasing current density.

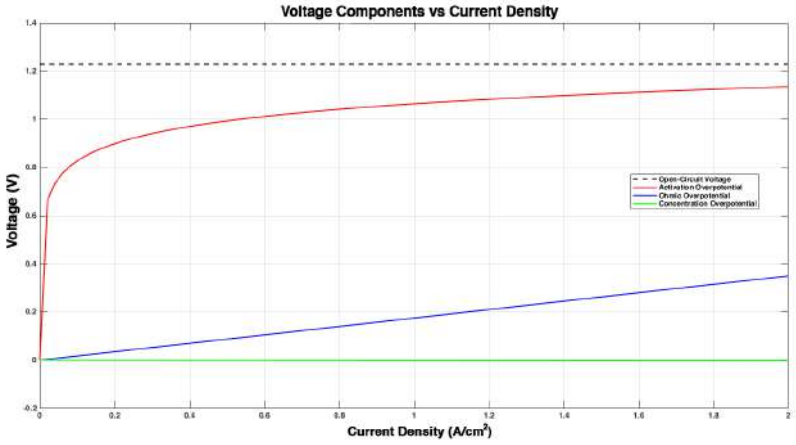


Figure 2.9: The Voltage in function of the current density with different temperature values

The plotted curves in figure 2.9 illustrate how different voltage components vary with increasing current density in a PEM electrolysis cell. The open-circuit voltage (V_{oc}) remains constant. The activation overpotential (V_{act}) is high at low current densities due to reaction kinetics but gradually levels up as the current increases. The ohmic overpotential (V_{ohm}) increases linearly with current density, reflecting resistive losses in the membrane and cell components. The concentration overpotential (V_{con}) initially remains low but rises at higher currents due to mass transport limitations, where reactants struggle to reach the reaction sites efficiently. Water saturation has also a major impact on the PEMEC.

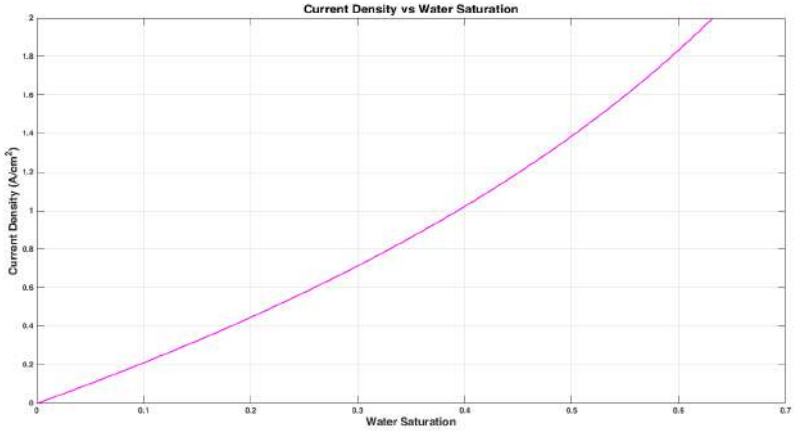


Figure 2.10: The current density in function of the water content

Direct correlation because as water saturation increases the current density also increases, this current has a direct relationship with the hydrogen and oxygen production rate.

2.4 Hydrogen Production rate

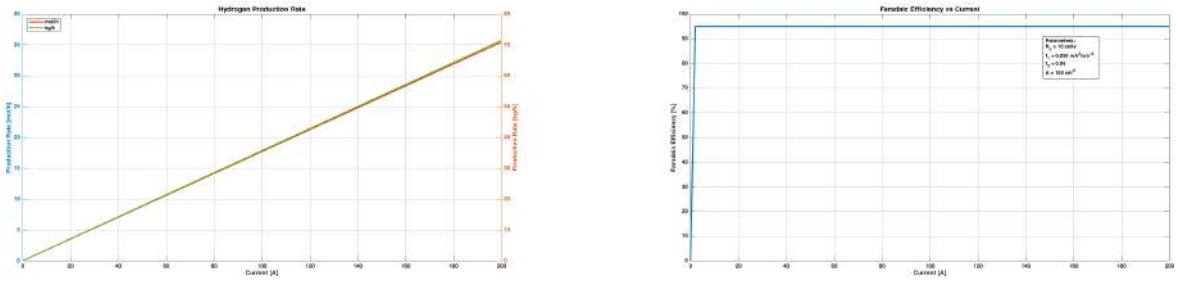
Faraday's law indeed establishes a fundamental relationship between the amount of matter produced or consumed during an electrochemical reaction and the amount of electricity that passes through the circuit. More specifically, Faraday's law states that the amount of matter produced or consumed is directly proportional to the amount of electric charge that has passed through the circuit. In the case of water electrolysis to produce hydrogen, Faraday's law can be applied to determine the rate of hydrogen production based on the rate of electron transfer to the electrodes of the electrolyzer[44].

$$\dot{n}_{H_2\,prod} = \eta_F \frac{N_c I}{2F} \tag{2.27}$$

With: $\dot{n}_{H_2\,prod}$ Hydrogen production rate (mole / sec) $\dot{n}_F$ Faradaic efficiency

$$\eta_F = \frac{\left(\frac{1}{A}\right)^2}{f_1 + \left(\frac{1}{A}\right)^2} f_2 \tag{2.28}$$

with : f1,f2 ($mA^2\ cm^-4$), faradic yield calculation parameters, Objective of the electrolyzer ventilation to maintain a constant system temperature.



(a) Hydrogen Production (b) Faradaic Efficiency vs Current

Figure 2.11: Hydrogen Production rate and faradiac efficiency

Figure 2.11a illustrate the relationship between current and hydrogen production, showing a strong linear correlation consistent with Faraday's Law. As current increases, hydrogen production rises proportionally in both mol/h and kg/h, indicating predictable and scalable system behavior. The Faradaic efficiency Figure 2.11b confirms this, with efficiency rapidly increasing at low currents and stabilizing around 95%. This suggests that nearly all input current contributes to hydrogen generation, with minimal losses. Together, the results demonstrate that the electrolyzer operates efficiently and reliably across a wide current range.

2.5 Hydrogen tank modeling

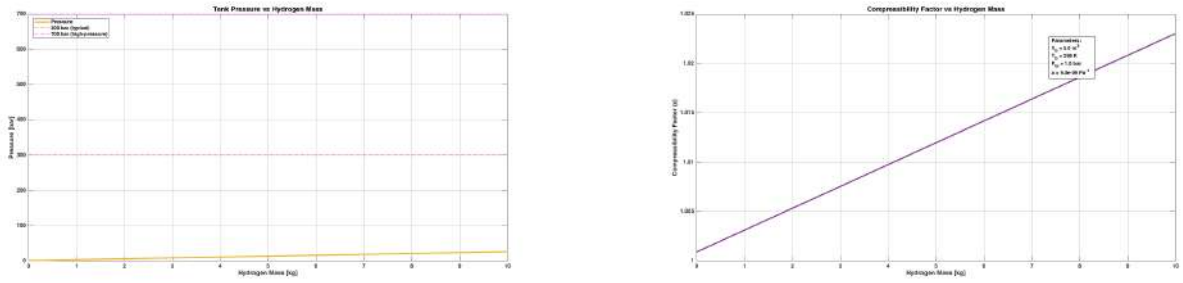
Compressed hydrogen gas or liquid hydrogen can be stored in tanks by using different techniques like physical hydrogen storage. In order to store the hydrogen gas that is produced by the electrolyzer, a dynamic module for the tank is created in MATLAB/Simulink, and can be expressed as follows:

$$P_b - P_{bi} = z \cdot \frac{N_{H_2} R T_b}{M_{H_2} V_b} \tag{2.29}$$

where P_b is the pressure of the tank that is measured in (Pascal), P_{bi} is the initial pressure of the storage tank in (Pascal), R is the universal gas constant (J/kmol.K), T_b is the operating temperature (K), V_b is the volume of the tank (m3), T is the temperature, and Z is the compressibility factor as a function of the pressure as shown in this equation :

$$Z = \frac{PV_m}{RT} \tag{2.30}$$

where, P and V_m are the pressure and molar volume, respectively. It has been noticed that this model determines the tank pressure using the ratio of hydrogen flow rate to the tank. Eq 2.29 is implemented in Simulink in order to get the hydrogen stored and delivered to the fuel cell.[56].



(a) the build up pressure inside the tank (b) the compressibility Factor vs hydrogen mass

Figure 2.12: Pressure vs. Hydrogen Mass for 500L Tank at 25°C

Figure 2.12a shows that tank pressure increases gradually with hydrogen mass, remaining well below the 300 bar typical tank pressure and far from the 700 bar high-pressure limit, indicating a conservative operating range. Figure 2.12b shows a nearly linear increase in the compressibility factor with hydrogen mass, starting slightly above 1 and reaching about 1.023 at 10 kg, suggesting that h_2 gas behavior is only slightly deviating from ideal conditions under the given parameters. Together, these plots confirm that within the specified mass range, the hydrogen behaves nearly ideally and the pressure rise remains modest, ensuring safe and efficient storage conditions.

2.6 Modeling of PEM Fuel cell

2.6.1 Mathematical modeling

To model the PEMFC, the paper by K. Dannenberg, P. Ekdunge, and G. Lindbergh had been used, which explains the internal reactions of the fuel cell, its ability to generate electrical energy from H_2O, H_2, and O_2, and the transport of gases within the membrane, as well as between the anode and cathode. The Stefan-Maxwell equation[57] :

$$\frac{dx_i}{dy} = RT \sum \frac{x_i N_j - x_j N_i}{P D_{ij}} \tag{2.31}$$

The equation 2.31 describes the diffusion of a specific species in a gaseous mixture, where R is the universal gas constant, T is the temperature, P is the pressure, N is the molar flux, and D is the diffusion coefficient. It is used to define the diffusion mechanisms of species within the porous gas medium, as the mole fraction x of each species is influenced by the fluxes of other species in the mixture.

Another crucial coefficient to discuss is the water net flux per molar flux. These key parameters give us a clearer understanding of water transport between the anode and cathode in both directions, which directly impacts the fuel cell's humidity. For the PEMFC to operate efficiently, it must maintain a specific humidity range. Therefore, having a solid grasp of water diffusion and drag is essential, it's given with the following relationship :

$$\alpha = 2n_d - \frac{2F\rho_m}{I(x)M_m} D_\lambda \frac{d\lambda}{dy} \tag{2.32}$$

Where nd is the electroosmotic drag coefficient and Dλ is the water diffusion coefficient in the membrane where λ is the water content and F is the faradaic constant, ρm and Mm are the density and equivalent weight of the membrane, respectively. I(x) the current density.

An important characteristic to note is that membranes absorb significantly more water when in direct contact with liquid water than when exposed to water vapor. In this model, water is considered to be in vapor form (or as negligibly small droplets), even under supersaturated conditions where water activity exceeds 1. To account for increased water uptake beyond saturation, the water content curves for all temperatures were algebraically extended to a water activity of 2.5. At this threshold and beyond, the water content remains constant at 20. Another crucial concept to consider is the resistance to H+ flow. To determine this, we first need to examine conductivity, as resistance is simply its inverse. The following equation 2.33 expresses conductivity as a function of water content[58] :

$$\begin{aligned}\sigma = -0.0051638 + 0.00020217\lambda + 0.0022154\lambda^2 - 0.0002772\lambda^3 + \\ 1.4657 \times 10^{-5}\lambda^4 - 2.7746 \times 10^{-7}\lambda^5\end{aligned} \tag{2.33}$$

For each value of x, the resistance of the membrane is calculated by integrating the reciprocal of the conductivity :

$$R_m(x) = \int_0^{t_m} \frac{1}{\sigma(\lambda)}\, dy \tag{2.34}$$

The cell voltage is calculated from the membrane resistance, current density and electrode overpotential, as follows :

$$E_{\text{cell}} = E_{\text{oc}} - \eta(x) - I(x)R_m(x) \tag{2.35}$$

The equation 2.35 calculates the cell voltage Ecell as a function of the open-circuit voltage Eoc, electrode overpotential η(x), and ohmic losses due to membrane resistance Rm(x) Variations of temperature along the gas channels are calculated according to the following energy balance equation :

$$dM_i \Delta H_i(T) = \sum [M_i(x)c_{p_i}(T)dT + E_{\text{cell}} I(x)h\, dx + q(T - T_{\text{coolant}})h\, dx] \tag{2.36}$$

This energy balance equation accounts for the heat generated by the fuel cell reaction, the heat capacity of the gases, the electrical work provided by the cell, and the heat transfer to the cooling system.

As we will see in the simulation part the pressure of the H_2 and O_2 gases are very important factors to determine the way our PEMFC function and generate electricity so we define them by the following equations[58] First, we write the equation 2.37 that describes the pressure of

O_2 :

$$p^*_{O_2} = p^{\text{sat}}_{\text{H}_2O}\left[\frac{(1 - x^*_{N_2} - x^*_{\text{CO}_2})}{x^*_{\text{H}_2O}} - 1\right] \tag{2.37}$$

Second the pressure of H2 :

$$p^*_{H_2} = 0.5\, p^{\text{sat}}_{\text{H}_2O}\left[\frac{1}{x^{\text{channel}}_{\text{H}_2O}\exp\left(\frac{RTI_{\text{den}}\iota a}{2FP_aD_{\text{H}_2O,H_2}}\right)} - 1\right] \tag{2.38}$$

As we can see, water significantly affects the pressure of both hydrogen and oxygen. Here, R represents the ideal gas constant, T is the temperature, and x is the mole fraction of a species, which indicates its proportion within the mixture relative to the total amount of all species. The mole fraction ranges from 0 to 1, where 0 means the species is entirely absent, and 1 means it is the only component in the mixture.

The average current density for a given cell voltage is calculated by integrating along the whole channel length [x][57] :

$$I_{\text{avg}} = \frac{1}{L}\int_0^L I(x)\, dx \tag{2.39}$$

I(x) is a local geometric current density at each point along the channel, and L is the length of the channel x. The molar flux of the hydrogen can be determined by Faraday's Law :

$$N_{H_2} = \frac{I}{2F} \tag{2.40}$$

This law become very handy in our later study and simulation process where it makes it easy for us to know the moles of hydrogen produced or consumed with just knowing the current and dividing it by the Faraday constant. (more on this in the simulation part).

The molar flux in the cathode and the anode of water is defined with these equations respectively :

$$N_{\text{H}_2O,c}(x) = \frac{\alpha I(x)}{2F} \tag{2.41}$$

$$N_{\text{H}_2O,c}(x) = \frac{(1+\alpha) I(x)}{2F} \tag{2.42}$$

It's obviously having a relationship with the water net flux α that we discussed earlier, with the use of faraday's law we get the molar flux of water the electrical output power is computed as :

$$\dot{q}_{\text{elec}} = V_{\text{out}} \cdot I \tag{2.43}$$

As for any other DC circuit the output is really straight forward the current multiplied by the voltage give us the output power. The equivalent electrical circuit of PEMFC figure 2.13,

that is considering the effect of the accumulation of charges along the electrochemical double layers and the obstruction that the fuel cell is creating for ions to move freely is also represented by a couple of resistances[57] .

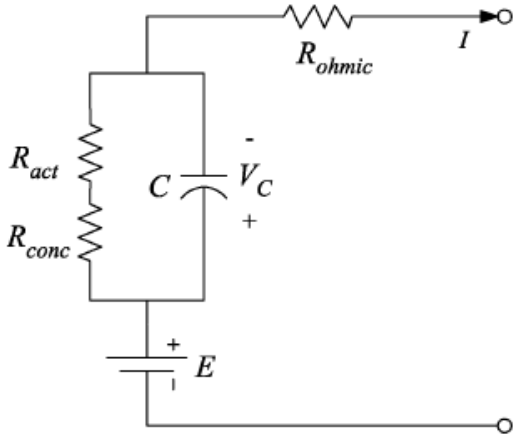


Figure 2.13: The equivalent circuit of PEMFC

The electrical analysis of this circuit gave the following equation :

$$E - V_c - IR_{\text{ohmic}} = 0 \tag{2.44}$$

$$V_c - (R_{\text{act}} + R_{\text{conc}})I_R = 0 \tag{2.45}$$

$$I_R = \frac{V_C}{R_{\text{act}} + R_{\text{conc}}} \tag{2.46}$$

$$I = I_c + I_R \tag{2.47}$$

$$I_c = C\frac{dV_c}{dx} \tag{2.48}$$

$$E - V_c - C\frac{dV_c}{dx}R_{\text{ohmic}} - \frac{R_{\text{ohmic}}}{R_{\text{act}} + R_{\text{conc}}}V_c = 0 \tag{2.49}$$

After applying Laplace Transfer the TF will be as follows :

$$H(p) = \frac{R_{\text{act}} + R_{\text{conc}}}{(R_{\text{act}} + R_{\text{conc}})(pCR_{\text{ohmic}} + R_{\text{ohmic}} + 1)} \tag{2.50}$$

2.6.2 Results

PEMFC Polarization curve

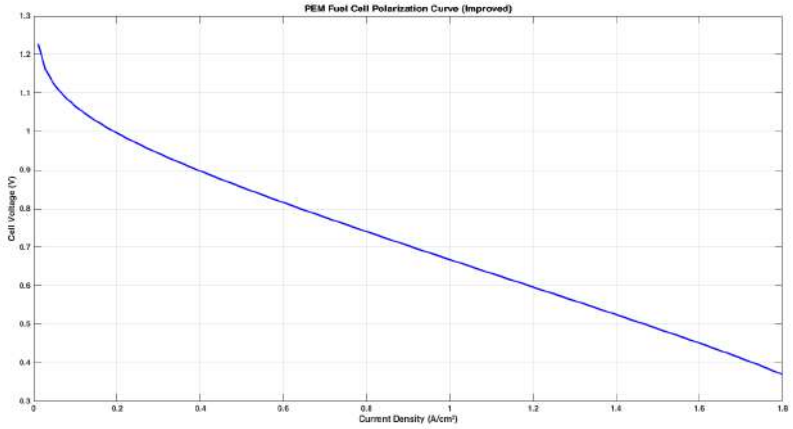


Figure 2.14: Curve of Cell Voltage in function of The Current Density

The graph in Figure 2.14 illustrates the relationship between cell voltage (V) and current density (A/cm^2), showing that voltage decreases as current density increases due to activation, ohmic, and concentration losses. Initially, there is a sharp voltage drop caused by activation losses, followed by a slower decline attributed to ohmic resistance. At higher current densities, concentration losses become predominant, resulting in a greater voltage drop [57].

Resistance of the membrane in the presence of water

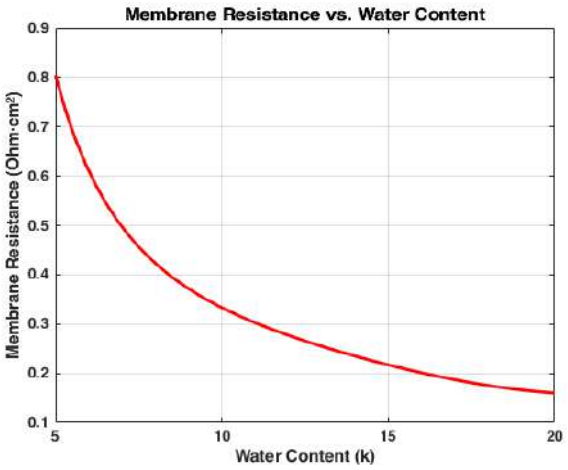


Figure 2.15: Membrane Resistance in function of water content

The humidity is a vital factor for better understanding the PEMFC inner functionality as Figure 2.15 represents the when water content increases the resistance drops gradually this happens because the cell membrane (usually made of Nafion) depends on water to ease out protons H+ transportation from Anode to Cathode.

Temperature effect on the output voltage

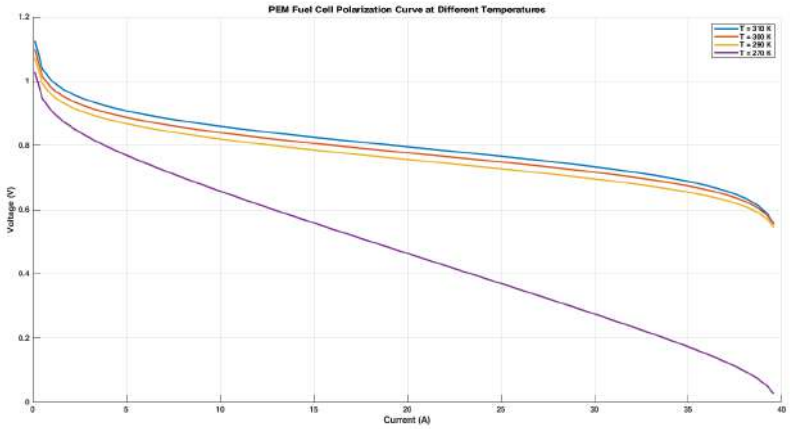


Figure 2.16: Voltage in function of current With variable values of Temperature

Figure 2.16 shows The polarization curve of the PEM fuel cell illustrates the connection among voltage and current at exclusive running temperatures. As the current increases, the voltage decreases because of 3 primary forms of losses. At low current levels, activation losses dominate, as a result of the sluggish kinetics of the electrochemical reactions, specifically at decrease temperatures. As the current increases, ohmic losses come to be extra significant, because of the inner resistance of the membrane and different mobileular components. At very excessive currents, attention losses cause a pointy voltage drop because of the depletion of reactants on the catalyst sites. Higher temperatures, which include 310K, beautify response kinetics and enhance membrane conductivity, main to higher overall performance and better voltage for the identical current. Conversely, at decrease temperatures, which include 265K, accelerated resistance and slower reactions lessen efficiency, inflicting the voltage to drop extra significantly. This explains the downward shift of the curves as temperature decreases, highlighting the significance of temperature manage in optimizing PEM fuel cell overall performance.

Current density alongside the channel length

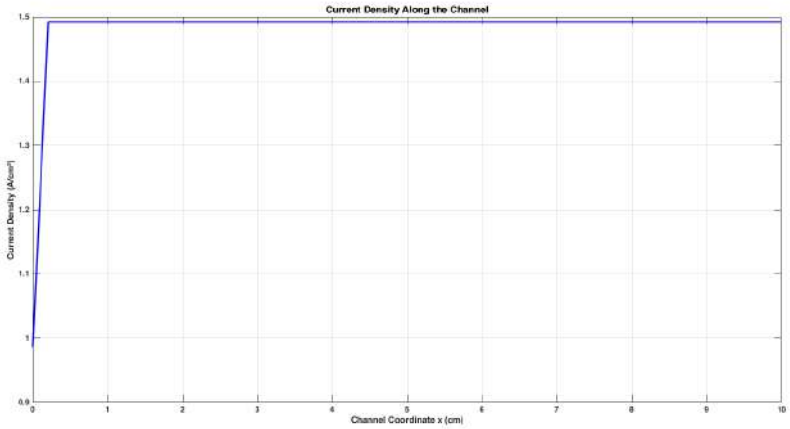


Figure 2.17: Current density in function of channel coordinate x

Figure 2.17 represents the current density in function of the channel length in a PEM Fuel Cell. The x-axis is the channel coordinate (x) in centimeters, while the y-axis represents the current density in A/cm^2. The curve indicates that the current density rapidly increases at the start of the channel after which stabilizes at an almost steady value. This behaviour shows that most of the electrochemical reactions happens near the inlet (where reactant H2 and O2 first enter the cell).

Power output of the PEMFC

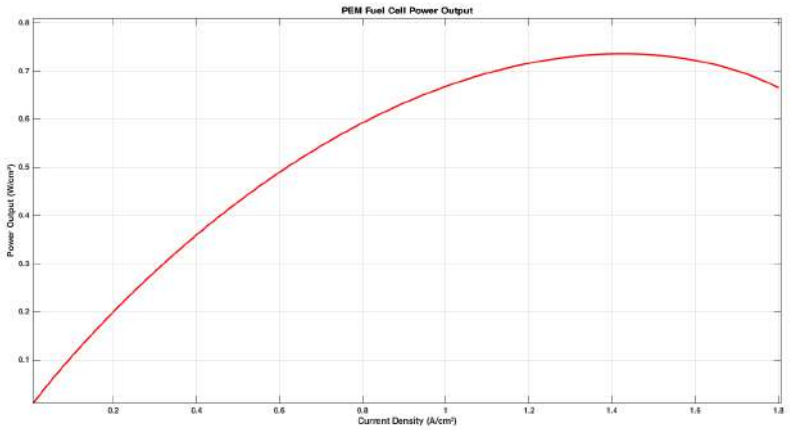


Figure 2.18: The power of the PEMFC

The figure 2.18 shows the graph of power in (W/cm2) in function of the current density (A/cm2) (it could be the voltage as they have the same effect on the power) which is very straight forward graph as current increment the power output also increment.

Water distribution in the fuel cell

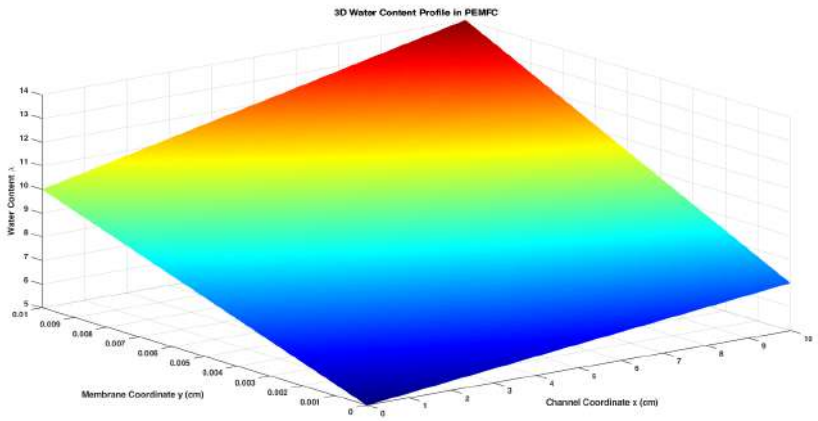


Figure 2.19: Water distribution in function of channel coordinate x and membrane coordinate y

Figure 2.19 is a 3D graph that shows the distribution of water inside the fuel cell channel, at the first glance the red area is the most obvious it represents where the water is mostly accumulating which is the most humid, at the bottom where the blue area that's the driest place in the channel, the variables of this 3D graph are the channel coordinate x (cm) and the membrane channel y (cm) and the z is the water content λ (moles) this graph tell us how the water is distributed in the channel (the channel in shown if figure X) which helps us to determine the conductivity of the channel and the resistance to protons and other ions that might be in the channel.

The equivalent circuit voltage

As we determined earlier the output voltage of this circuit is Vc and the input voltage is E in figure 2.20 we see that that voltage is increasing over time just like a normal exponential function that describes the charging phase of a capacitor which is very accurate in describing what happening inside with the layers as charges positive and negative accumulate around them from both sides the act like real supercapacitor.

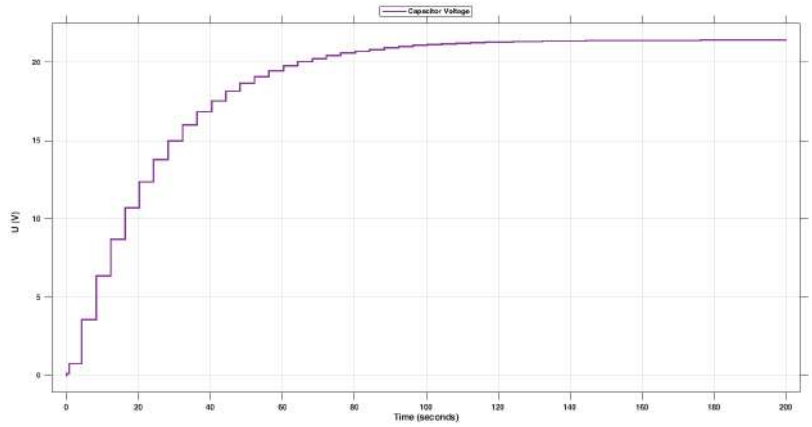


Figure 2.20: The voltage of the equivalent circuit

The equivalent circuit current

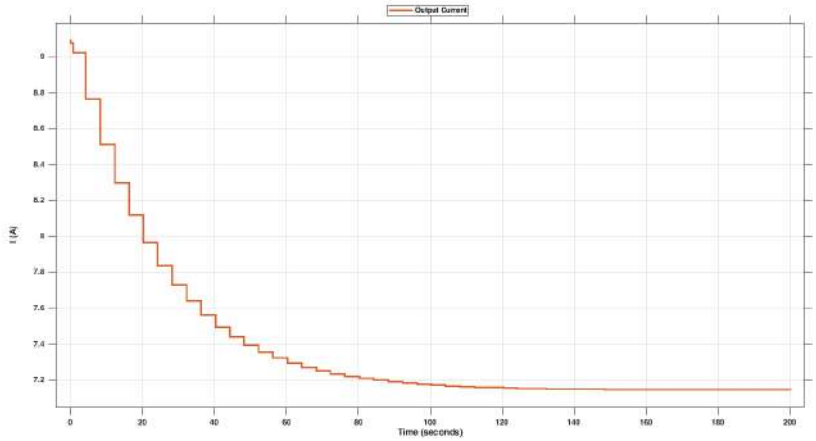


Figure 2.21: The current of the equivalent circuit

The figure 2.21 shows a decreasing graph that stabilizes in the end. This drop down is because, the presence of double-layer capacitance at the electrode-electrolyte interface causes an initially high current, which gradually decreases as the capacitor charges. Activation and concentration polarization losses play a significant role; activation losses dominate at the start, while concentration losses become clearer over time as reactant diffusion slows down., ohmic losses due to the internal resistance Rohmic of the fuel cell result in voltage drops, further decreasing the current. Eventually, the current stabilizes, indicating that the capacitor is fully charged and the fuel cell has reached a steady-state operating condition.

Response of the equivalent circuit result

As figures 2.22, 2.23 are showing us this transfer function is stable for both the open loop and the closed loop configuration Which is a big score of the circuit because the change of the circuit parameters leads to an oscillating step response or a response that goes to infinity.

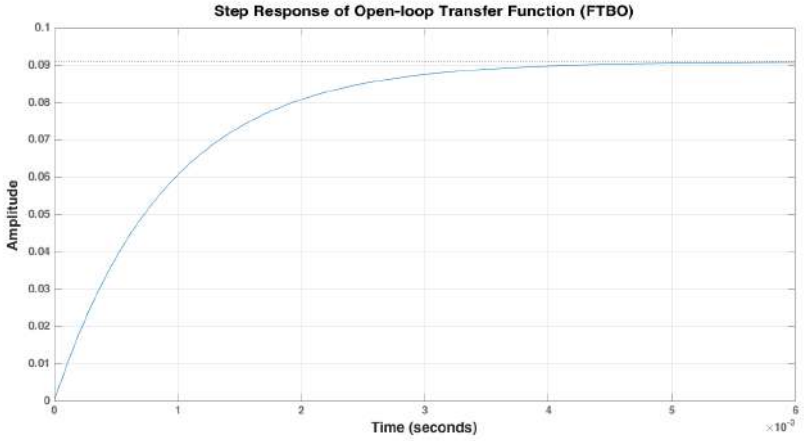


Figure 2.22: The response of the equivalent circuit in Open loop

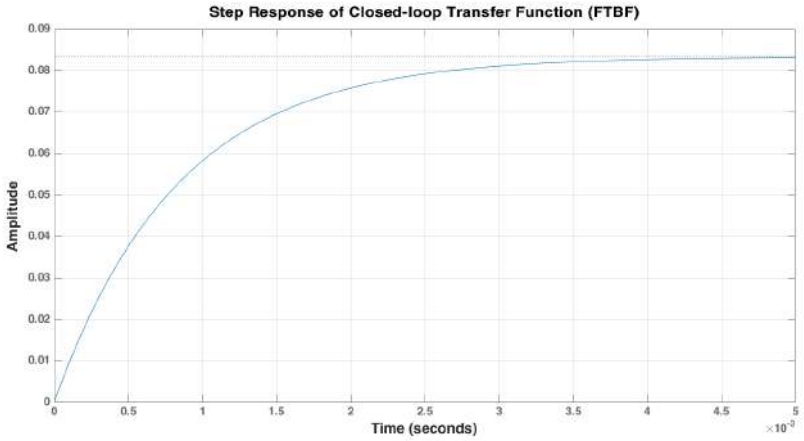


Figure 2.23: The response of the equivalent circuit in feedback loop

2.7 Single phase inverter

In a hydrogen production system powered by a PV panels, the inverter's main function is to convert the direct current (DC) electricity generated by the solar panels into alternating current (AC). This AC power can then be used to supply AC loads or, in grid-tied systems, be fed into the electrical grid. Crucially, inverters often integrate Maximum Power Point Tracking (MPPT) to optimize the energy harvested from the PV array, maximizing the DC power available for the entire system, including the electrolyser (which typically requires DC power, often managed by DC-DC converters). The specific role and configuration of the inverter depend on the system architecture, allowing for flexible energy management strategies like prioritizing loads, grid injection, and integration with battery storage[59]. The conversion principle of an inverter is illustrated in the following figure 2.24

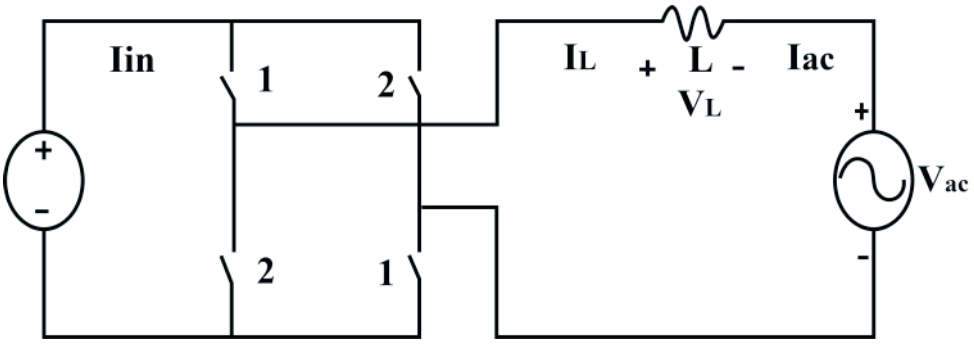


Figure 2.24: Full bridge single-phase inverter

For the first case position (1) :

$$V_L = V_{dc} - V_{ac} \tag{2.51}$$

$$I_L = I_{ac} \tag{2.52}$$

$$I_{in} = I_L \tag{2.53}$$

In the second case the position (2) :

$$V_L = -V_{dc} - V_{ac} \tag{2.54}$$

$$I_L = I_{ac} \tag{2.55}$$

$$I_{in} = -I_L \tag{2.56}$$

$$v_L = \begin{cases} +V_{dc} - V_{ac}, & 0 \leq t \leq \alpha T_s \\ -V_{dc} - V_{ac}, & \alpha T_s \leq t \leq T_s \end{cases} \tag{2.57}$$

$$V_L + V_{ac} = (2\alpha - 1)V_{dc} \tag{2.58}$$

2.8 Conclusion

The described modeling approach involves mathematically representing a complete PV-to-user hydrogen energy system. It starts with the PV panel's energy capture, followed by MPPT optimization, energy storage (likely battery), and a boost converter to power an electrolyzer for hydrogen production and storage. The stored hydrogen is then converted back to electricity using a PEM fuel cell, and finally, a DC/AC inverter transforms this energy for the end-user. This comprehensive model allows for simulation, optimization, and control strategy development for the entire energy conversion chain and which allows us to evaluate the system in different regions.

Chapter 3

PV-Hydrogen Simulation

3.1 Introduction

The transition from theoretical modeling to simulation marks a critical phase in the development of the hybrid PV-hydrogen system. This chapter presents the extreme of efforts to model, simulate, and analyse a hybrid energy system cantered around a proton exchange membrane fuel cell (PEMFC), energized with a photovoltaic (PV) array, hydrogen production/storage infrastructure, and power electronics interfaces. The PV system, governed by a Perturbation and Observation maximum power point tracking (MPPT) algorithm, ensures optimal energy gathering under dynamic irradiance conditions. A boost converter steps up the PV output to smooth out the ripples of the voltage during sun power and match the voltage requirements of the electrolyser, which produces hydrogen for storage in a dedicated tank. The stored hydrogen afterwards feeds the PEMFC, where electrochemical conversion generates electricity, regulated by a boost converter and inverted to AC power for the isolated site/house to be consumed.

Simulation results are presented to validate the efficacity of each subsystem and their collective integration. The PV MPPT algorithm's responsiveness to irradiance fluctuations, the transient behaviour of the boost converter during voltage elevation, and the electrolyser's hydrogen production efficiency is carefully examined. Equally critical is the PEMFC's dynamic performance, particularly its voltage, current and power produced, and the boost converter's role in stabilizing the output. The inverter's ability to maintain sinusoidal output fidelity and harmonic compliance is also assessed.

PID controllers are widely used to regulate various types of equipment, such as battery charging and discharging circuits, as well as temperature and pressure control systems. Due to the intermittent nature of renewable energy sources, they cannot consistently provide a stable power output even when the energy source (in our case, hydrogen) is available. Therefore, continuous monitoring and regulation of the fuel cell is essential to ensure clean and stable power delivery to the isolated system it supplies.

3.2 The full model

The developed model aims at determining how it can just start from small amount of power and getting to double that power using newly developed technologies.

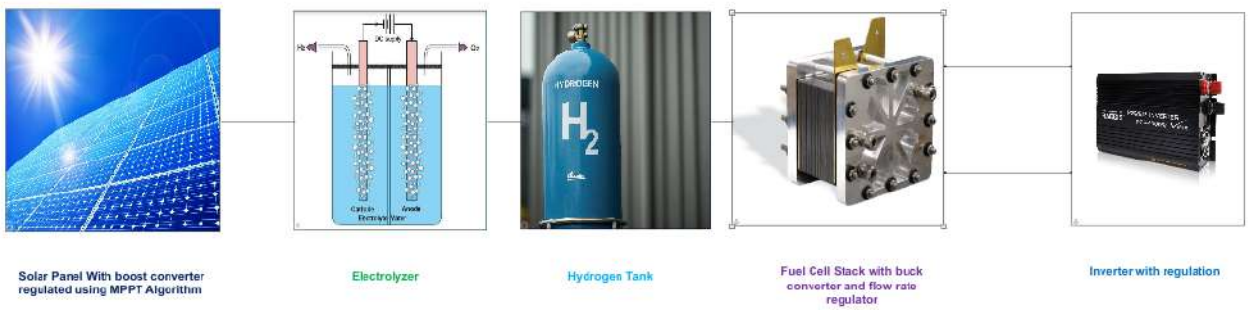


Figure 3.1: The full model of the simulation using MATLAB, Simulink

This system represented in figure 3.1 is a complete solar-to-hydrogen energy conversion and utilization chain. Solar panels, regulated by a boost converter with an MPPT algorithm, optimize the extraction of solar energy, the PV Array is backed up with battery pack that respond when there is no solar energy. This energy is then used to power an electrolyzer, which splits water into hydrogen and oxygen. The produced hydrogen is stored in a hydrogen tank for later use. When energy is needed, the stored hydrogen feeds into a fuel cell stack, which converts the chemical energy back into electricity. A boost converter and flow rate regulator manage the fuel cell's output, while an inverter with regulation converts the DC output into usable AC power for electrical loads.

3.3 The PV system

Firstly, the reason for choosing this energy source is due to the need for clean power source so the hydrogen used to generate power is green hydrogen, which has no negative effects whatsoever on the environment. By choosing solar energy to energize the system, this will have a great impact on the system's durability and scalability, and it can be installed everywhere. The schematic used in Simulink figure 3.2.

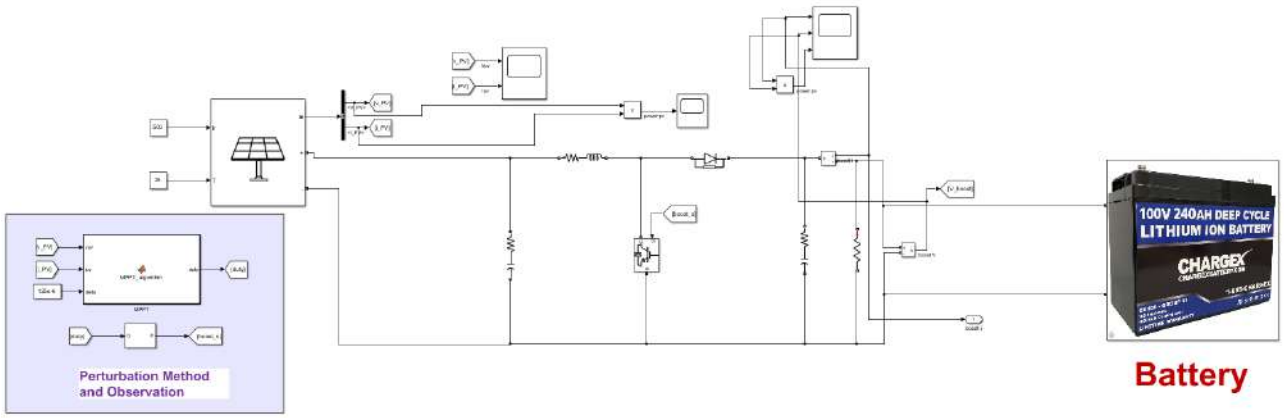


Figure 3.2: Simulink Circuit for the PV system

The solar panel model used in this system is the Advanced Power API-P215, with 2 panels connected in parallel, 2 panels connected in series. Capable of producing up to 800 W under full sun brightness and nominal temperature. It can generate 34.8 volts in an open circuit and deliver up to 16 amps of current. The shunt resistance is 49.25 ohms, which can be considered somewhat moderate not extremely low, but not very high either allowing some current leakage during power generation. Here is a graph that explains the chosen model in more depth.

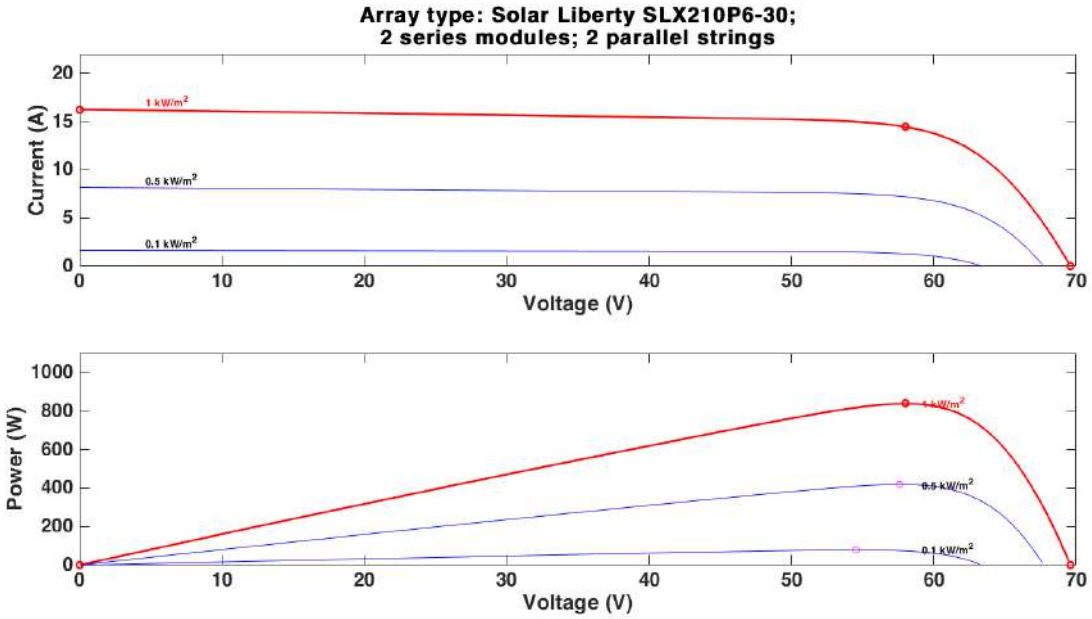


Figure 3.3: The chosen solar panel in different sun irradiance

The figure 3.3 shows the I-V (current vs. voltage) and P-V (power vs. voltage) characteristics of the Advanced Power API-P215 solar array under different irradiance levels 0.1 kW/m², 0.5 kW/m², and 1 kW/m². The configuration used here is two module in series and two modules in parallel.

I-V Curve Analysis

In the top plot, we can clearly see how the current output increases with higher irradiance. At 1 kW/m² (full sunlight), the panel delivers around 16 A, while at lower irradiance levels (0.5 kW/m² and 0.1 kW/m²), the current drops significantly. The voltage, however, does not change drastically with irradiance. It remains close to the open-circuit voltage (around 36 V), which is typical behavior for solar panels. This shows that irradiance mainly affects the current output, not the voltage.

P-V Curve Analysis

In the bottom plot, we observe at full irradiance (1 kW/m²), the system reaches a peak power of just over 800 W, which matches expectations for four panels (each rated 215 W). As irradiance decreases, the peak power drops for instance, around 600 W at 0.5 kW/m² and much lower at 0.1 kW/m².

The most common behavior of renewable like in the case of solar energy is that the power produced is not very stable and cannot be relied on alone to power the system. This is because it highly depends on solar irradiance. This means we cannot depend solely on the energy produced by the solar panel to fully power the system. Therefore, adding a battery pack is needed along with boost converter along with an MPPT controller is obligatory to make the system fully safe and usable.

Boost converter is used to level up the voltage value and keep things run smoothly with the MPPT controller with the method of Perturbation and Observation, this algorithm works by slightly perturbing (increasing or decreasing) the duty cycle of the converter, then observing the change in output power. Which worked great for different values of sun irradiance.

As shown in figure 3.2 current and voltage are fed into the MPPT Algorithm, the idea behind it is to track the maximum power point by adjusting the duty cycle of the converter. It starts with an initial duty cycle and uses persistent variables to store the previous voltage, power, and duty cycle values so it can calculate the difference between old and new readings. At every step, it calculates the power from the product of panel voltage and current. Then, by comparing the change in power and voltage, it decides whether to increase or decrease the duty cycle. The direction of the adjustment depends on whether the change brought an increase or decrease in power. Finally, the duty cycle is clamped between a minimum and maximum limit to keep the system safe and operating within its allowed range. This logic allows the system to continuously follow the maximum power point under changing sunlight conditions.

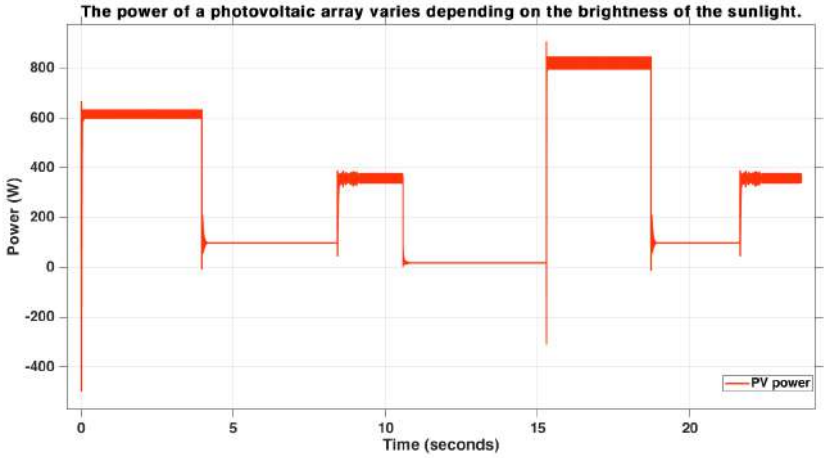


Figure 3.4: The solar panels power in different sun power using MPPT

Figure 3.4 shows the power produced by the solar panel, where the MPPT helps keep it under control so it doesn't fluctuate too much. As seen in the figure 3.4 above the MPPT is doing good job keeping the power in balance, it's clear when the sun irradiance changes the power also dose change but in more predictable way that can be managed and controlled.

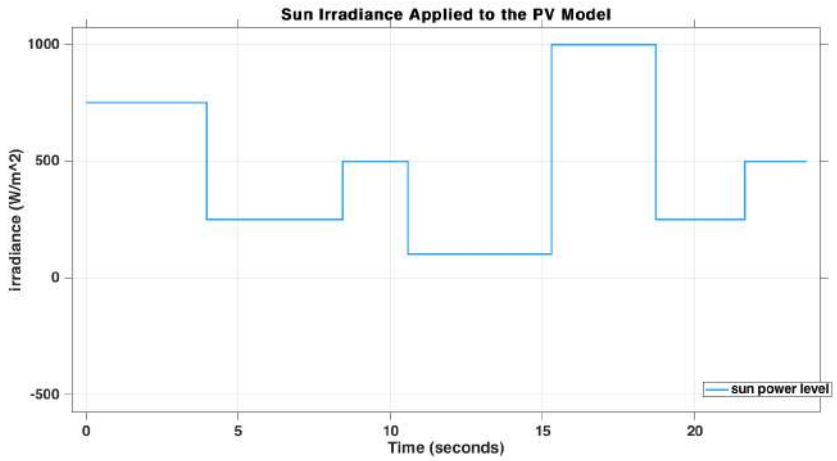
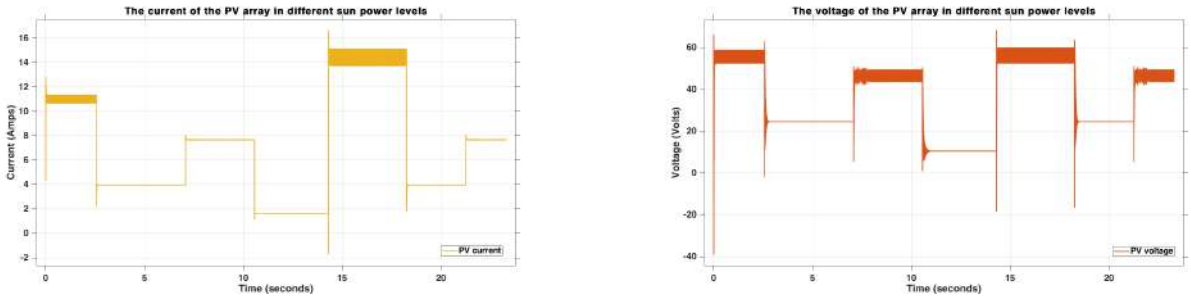


Figure 3.5: Sun irradiance applied to the PV array

Both Figures 3.5 and 3.4 have the same structure as the sun irradiance changes this affects directly the power, its clear for 1000W/m2 (full sunlight brightness) the full power is been delivered by PV array which is about 800 watts.

Both current and voltage have the same form as for power, and they are visible in Figure 3.6 below

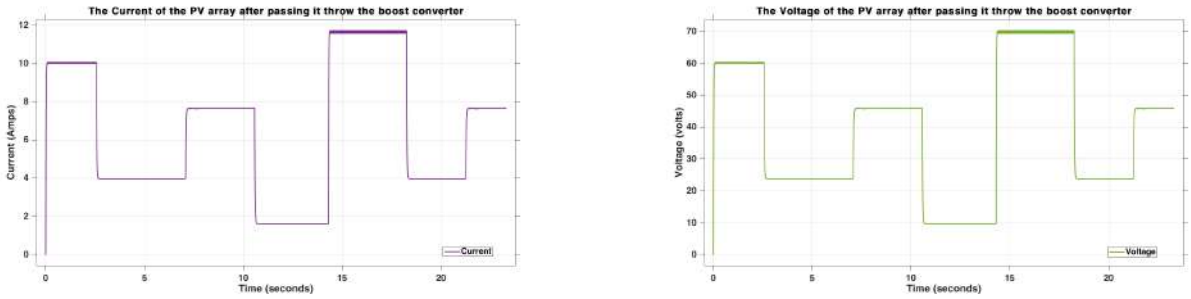


(a) The current (b) The voltage

Figure 3.6: Curves of the current and voltage using MPPT

Both voltage and current reached the intended values for the given sun irradiance. MPPT helps track the best working point and keep these parameters in reasonable values. The small spikes and dips happen due to the dynamic adjustment of the converter, and it's nothing that affects the devices seriously. As long as the voltage and current stays near the desired value most of the time, the system is safe and working fine.

The static converter been used in this part of the system is a boost converter, it is a type of DC-DC converter used to increase (or "boost") the voltage from a lower level to a higher one. In a solar system, it plays a key role in keeping the output voltage stable even when the input from the PV panel changes due to sunlight variations. When combined with MPPT, the boost converter helps smooth out sudden dips or spikes in voltage and current by adjusting the duty cycle. This ensures that the power delivered to the load remains steady and within safe limits.



(a) The current (b) The voltage

Figure 3.7: Curves of the current and voltage after the boost converter

It is clear that the fluctuations are rare and almost gone thanks to the boost converter and its ability to eliminate them from the circuit. Now, this output can be safely fed to the components without any risk. In the case of the electrolyser, which is used to produce hydrogen, voltage drops and spikes can cause serious issues, so it's necessary that the voltage stays within reasonable limits under all sun power conditions. The voltage values appear to increase by a scale of around 10, at 1000 W/m^2, it was 60 V before the boost and 70 V after which confirms that the boost converter is working properly figure 3.7 (b).

All of this applies to the current too, except that the current stays almost the same before and after the boost. This is because the boost converter does not increase current, it only increases the voltage. On the other hand, the current is now more stable and much better than before the boost, as clearly shown in the figure 3.7 (a).

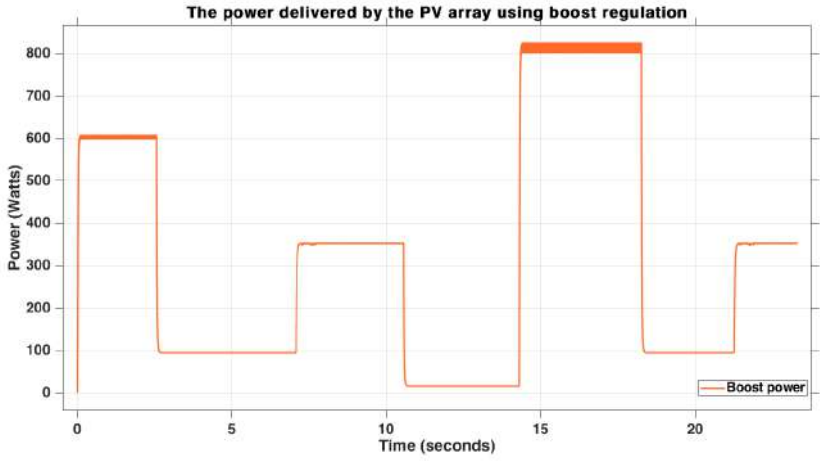


Figure 3.8: The power delivered by the PV array using boost regulation

The output power from the boost converter is stable and smooth, with no noticeable imperfections or sudden drops (figure 3.8). This shows that the converter is doing its job properly by maintaining a steady flow of energy, even when the input from the solar panel changes. Since the power is now clean and consistent, it can be safely fed into the electrolyzer without any risk of damage.

To sum up, the PV array in this system performs well when combined with MPPT and a boost converter. The voltage remains steady across different sunlight levels, and the current

responds smoothly to irradiance changes without causing instability. Together, they produce a stable and reliable power output that can be used directly without issues. The combination of MPPT tracking and voltage boosting ensures that the system operates efficiently, delivering clean energy that meets the requirements of sensitive components like the electrolyzer.

3.4 Battery

Every PV system includes a battery pack to store excess energy, so the system doesn't shut down and the consumer still has energy available. By adding a charging and discharging system for the battery, the setup now fully supports the hydrogen production phase. Even if the hydrogen tank reaches its limit during the night, the battery can continue supporting this phase by powering the electrolyser to produce the needed hydrogen. Figure 3.9 shows the Simulink circuit used for the battery pack. As for regulation, a discrete PID controller is used with a specified range to keep everything under control for example, the IGBT duty cycle is limited between [0, 0.95] to avoid abnormal values in the system.

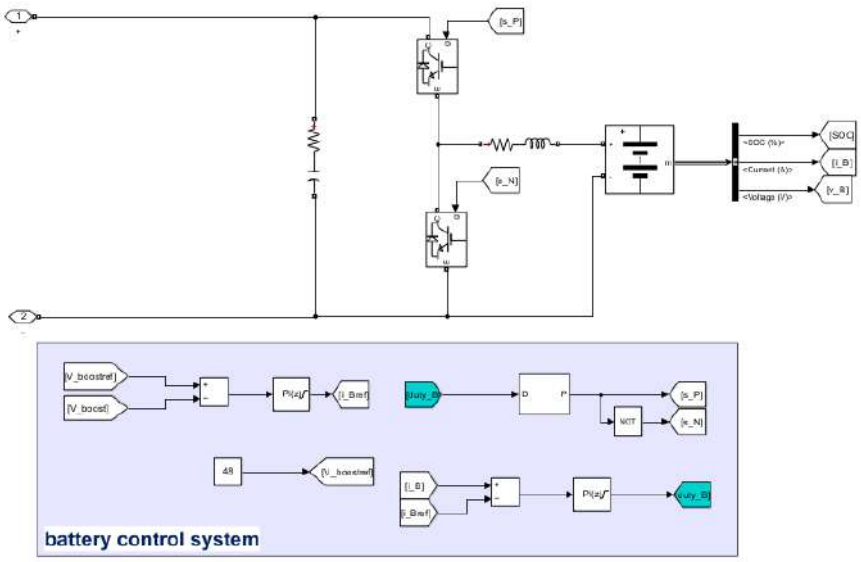


Figure 3.9: The battery charging dischargin circuit PI regulated

This system works as follows it charges the battery during the day when there is sunlight and discharges it during the night when there is no solar input. This ensures continuous operation without interruptions. Below are the results obtained for the battery's state of charge, current, and voltage, which clearly show how the battery responds throughout the day-night cycle.

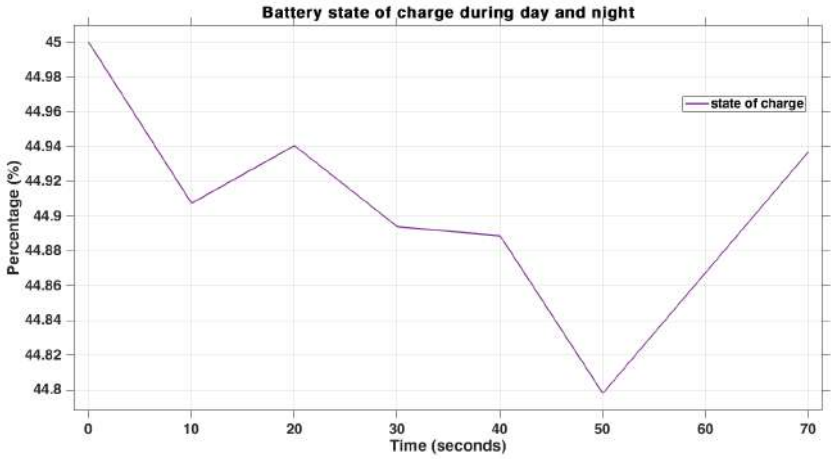
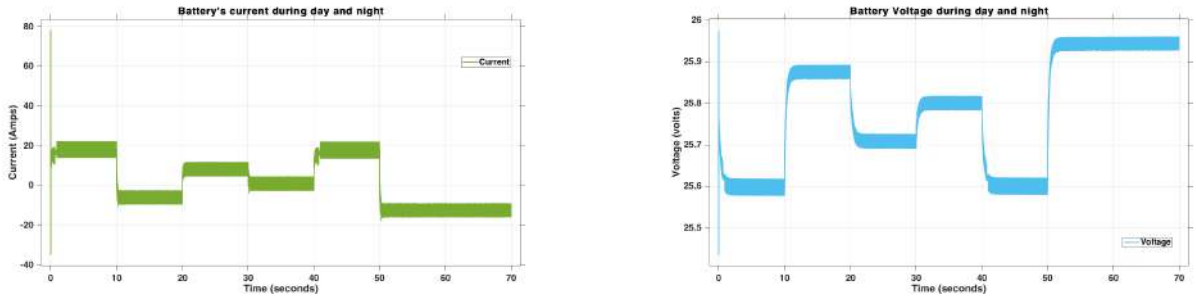


Figure 3.10: Battery state of charge under different sun irradiances

Figure 3.10 illustrates how the battery's state of charge (SOC) responds to variations in solar irradiance. When solar power is unavailable, the SOC decreases as the battery discharges to ensure continuous power supply, preventing system shutdown. Conversely, when solar energy becomes available, the battery begins to charge, and its SOC increases accordingly. This charging and discharging cycle allow the system to maintain a stable power flow to the load.



(a) The current (b) The voltage

Figure 3.11: Curves of the current and voltage of the battery

The battery current is positive during the discharging phase, indicating that the battery is acting as a current source and supplying power to the system. In contrast, during the charging phase, the current becomes negative because the battery is receiving power from the PV array. This change in current direction clearly reflects the battery's dual role in storing and delivering energy based on system needs (figure 3.11) (a).

As for the voltage, it behaves in the opposite way to the current. As shown in Figure 3.11 (b), under low solar irradiance, the battery voltage is relatively low because the battery is supplying power to the system on its own. However, when solar power becomes available, the battery begins to charge, and its voltage rises as it receives energy from the PV array. This behavior reflects the natural response of the battery under different operating conditions.

3.5 Electrolyzer

This section develops and validates a PEM electrolyzer model to assess how current, temperature, and pressure affect hydrogen production and electrical consumption.

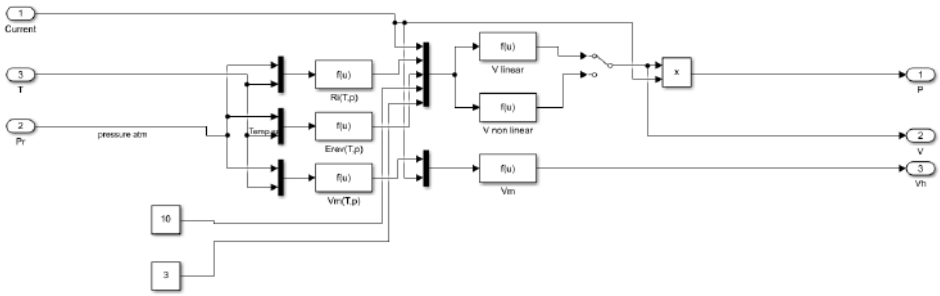


Figure 3.12: Simulink/Simscape schematic of the PEM electrolyzer model

By Faraday's First Law, the hydrogen mass flow rate $\dot{m}_{\mathrm{H_2}}$ is given by

$$\dot{m}_{\mathrm{H_2}} = \frac{I\, M_{\mathrm{H_2}}}{2\, F},$$

where I is the electrolyzer current, $M_{\mathrm{H_2}} = 2.016$ g/mol is the molar mass of hydrogen, and $F = 96485$ C/mol is Faraday's constant (see Eq. 2.19).

Operating conditions and control loops.

- **Current set-point** $I = 40$ A, maintained by the PV–battery power regulator.
- **Temperature** controlled at 65 °C via a PI loop.
- **Pressure** regulated at 5 bar by a cascaded control system.

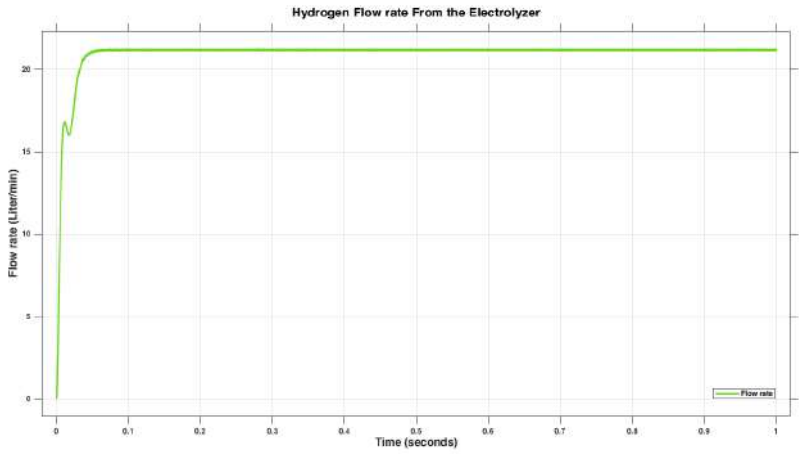


Figure 3.13: Hydrogen flow rate response

Figure 3.13 shows the H_2 production stabilizing at 20 L/min after a 5 s ramp-up, with a standard deviation below 0.2 L/min, confirming tight current and thermal control.

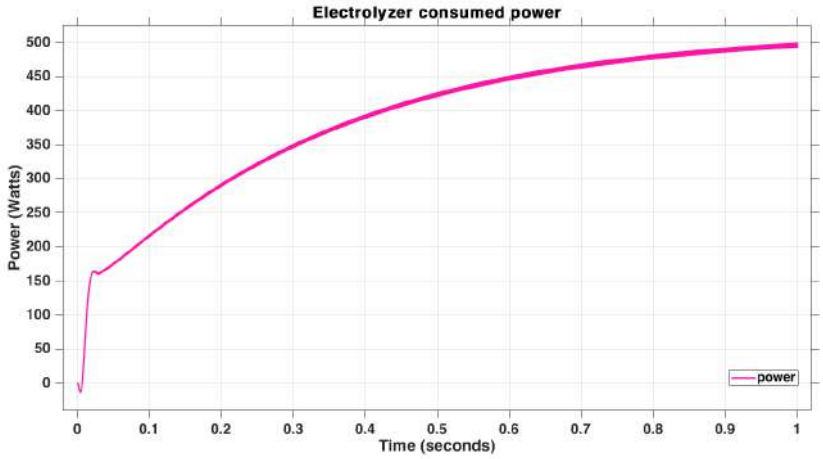


Figure 3.14: Electrolyzer power consumption

At steady state, the electrolyzer draws 500 W input to sustain 20 L/min H_2. This corresponds to an energy efficiency of approximately 55 % on a lower-heating-value basis

$$\eta = \frac{\dot{m}_{H_2} \cdot \mathrm{LHV}}{P_{\mathrm{in}}} \approx \frac{0.021 \text{ kg/s} \times 120 \text{ MJ/kg}}{500 \text{ W}} = 0.55.$$

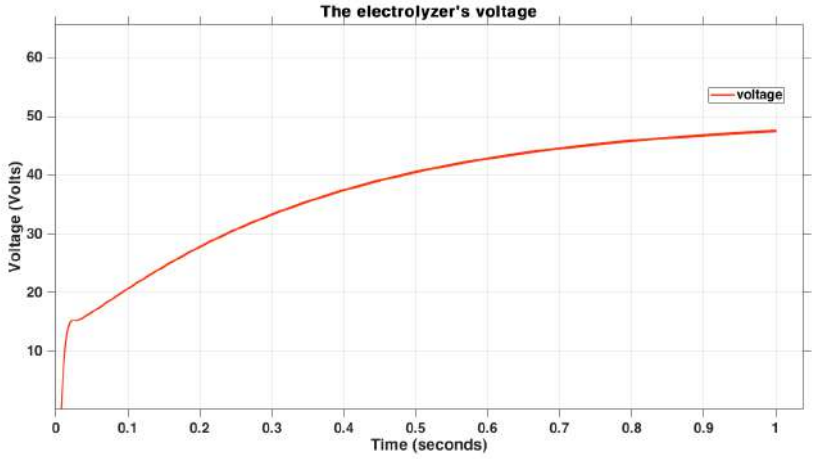


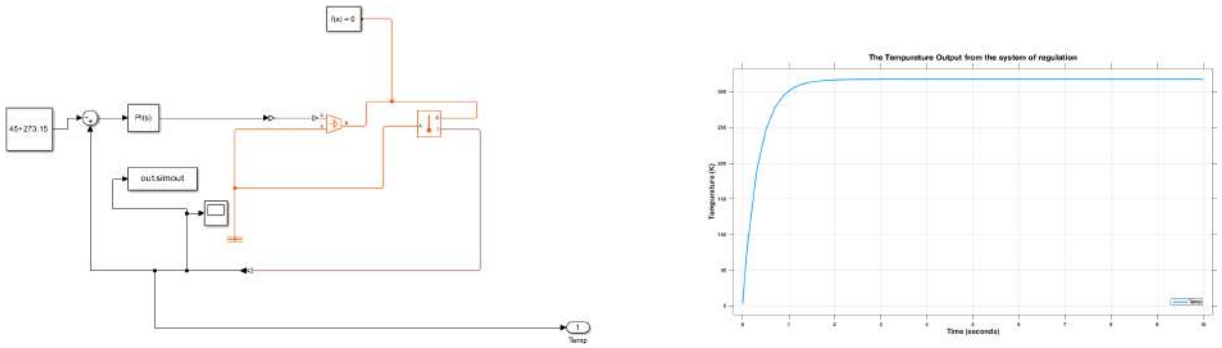
Figure 3.15: Electrolyzer cell voltage transient

Because current is held constant, power transients in Figure 3.14 arise from voltage changes (Fig. 3.15). The voltage rises from 0.8 V to 1.8 V over 4 s, reflecting activation and ohmic overpotentials modeled via the Nernst and Tafel equations (Sect. 2.3). This dynamic agrees with typical PEM electrolyzers' response times (below 1 s) and efficiency ranges (60–70 %) reported in the literature [32].

In summary, the modeled PEM electrolyzer demonstrates stable hydrogen output, realistic efficiency, and appropriate dynamic behavior, providing confidence in its integration within the PV–H_2 control framework.

To maintain a functional electrolyzer, both temperature and pressure must be controlled and kept within the working range, as mentioned earlier. For temperature and pressure con-

trol, Simulink alone does not offer detailed physical modeling tools. The solution is Simscape, a specialized toolbox within MATLAB designed for modeling and simulating physical systems. Simscape allows you to create realistic simulations of electrical, mechanical, thermal, and hydraulic systems using physical connections and built-in components, making it ideal for energy systems like fuel cells and electrolyzer.

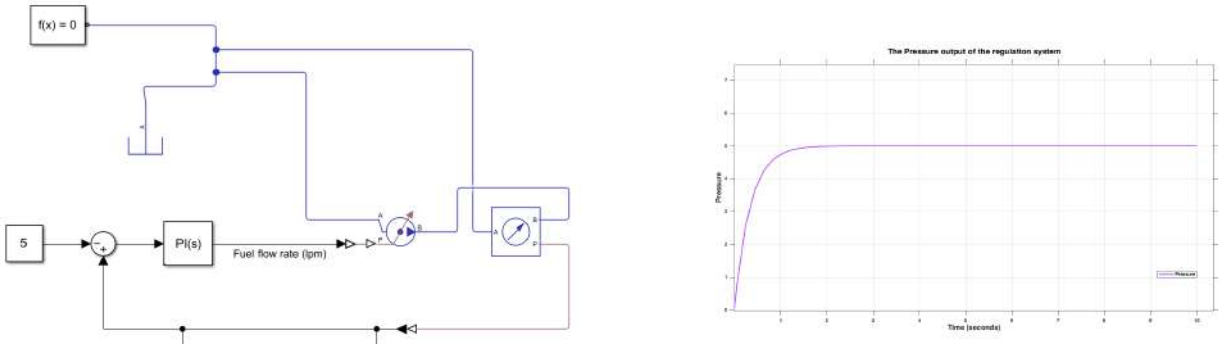


(a) The temperature control system (b) The response

Figure 3.16: The Temperature PI controlled with its response

In this project, the temperature control system is modeled using Simscape components, specifically a PID controller, a heat source, and a heat sensor. The PID controller regulates the heat source based on the sensor's feedback to ensure the electrolyzer remains within the optimal temperature range. If the temperature drops below the set point, the heat source activates to raise it. Once the desired range is reached, the controller reduces the heat input to prevent overheating. This setup ensures that the electrolyzer operates safely and efficiently under varying conditions (figure 3.16 (a)).

The temperature response shown in the figure 3.16 (b) demonstrates how the regulation system behaves over time. As seen, the temperature rises quickly in the first few seconds and then gradually levels off as it approaches a stable value just above 300 K. This indicates that the PID-controlled heat source is effectively adjusting the target temperature without overshooting or causing instability.The smooth and controlled rise reflects a well-tuned thermal regulation system, which is essential for maintaining the electrolyzer within its optimal operating range. The steady-state condition confirms that the system can handle thermal demands without fluctuation or delay.



(a) The Pressure control system (b) The response

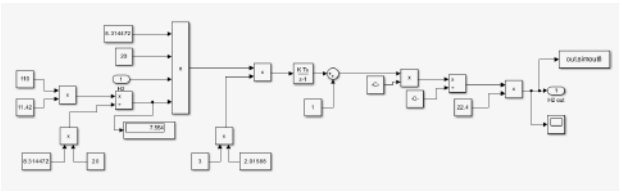
Figure 3.17: The Pressure PI controlled with its response

The pressure control system is designed to maintain the hydrogen pressure within a safe and functional range for the electrolyzer and storage tank. It consists of a pressure source, a reservoir, a pressure sensor, and a PI (Proportional-Integral) controller. The pressure source simulates the input of hydrogen into the system, while the reservoir represents the storage space where pressure needs to be regulated. The pressure sensor continuously monitors the pressure level and sends feedback to the PI controller, which then adjusts the input from the pressure source accordingly. If the pressure rises too high, the controller reduces the input; if it drops too low, the input increases. This closed-loop system ensures that the pressure remains within the desired range, providing stability and safety for the entire hydrogen production and storage process figure 3.17 (a).

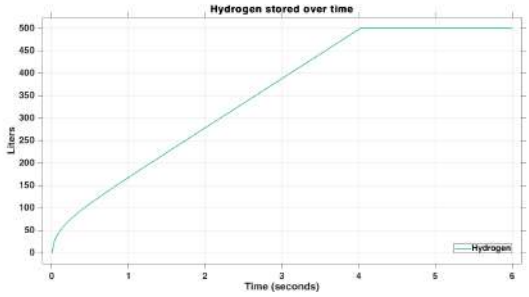
The response of the pressure control system is very similar to that of the temperature regulation system. As the simulation begins, the pressure quickly increases toward the desired setpoint and then gradually stabilizes without overshooting figure 3.17 (b). This smooth and steady rise is the result of the PI controller working in coordination with the pressure source and reservoir, ensuring that the system reaches the target pressure efficiently. Just like in the temperature system, the pressure controller responds actively to sensor feedback, adjusting the input to maintain a stable and safe pressure level. This kind of response confirms that the system is well-tuned and reliable for continuous operation.

3.6 Hydrogen Storage

Efficient hydrogen storage is critical to buffer production consumption mismatches, ensuring that excess H_2 generated during low power demand is reserved for peak loads rather than vented. This section presents the storage model, characterizes tank behavior, and quantifies charging dynamics under our control framework.



(a) Simulink schematic of the H_2 storage system



(b) Tank fill level over time

Figure 3.18: Hydrogen storage model and dynamic response

Model description.

- **Tank capacity** 500 L (nominal), modeled as an ideal pressure vessel.
- **Inlet flow** Controlled via a proportional valve receiving up to 20 L/min from the electrolyzer.

Results

Figure 3.18b shows the tank filling from empty to 80 % capacity in approximately 25 minutes under a steady 20 L/min inlet. The fill-rate curve remains smooth (rise time =5 min, settling time =30 s) indicating stable valve control and accurate volume modeling.

In summary, the validated storage model provides reliable buffering of hydrogen, complementing the electrolyzer control and enabling continuous fuel-cell operation under variable PV input.

3.7 Fuel Cell

This section integrates a 6 kW, 45 VDC PEM fuel cell (PEMFC) into the PV–H_2 system, characterizes its steady-state and dynamic performance, and assesses the need for power conditioning.

Figure 3.19 plots the V–I and P–I characteristics of the chosen PEMFC, showing its nominal 6 kW output at 50 L/min H_2 consumption and up to 8 kW peak at 84.5 L/min. Humidity, temperature, and O_2 flow are assumed constant and therefore not modeled here.

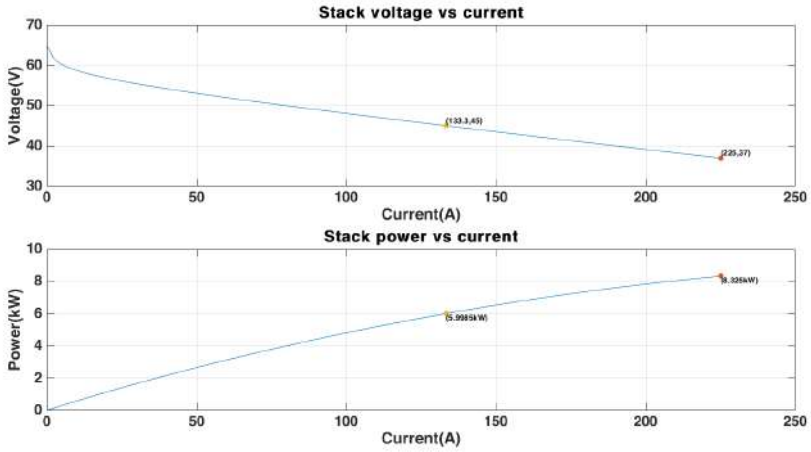
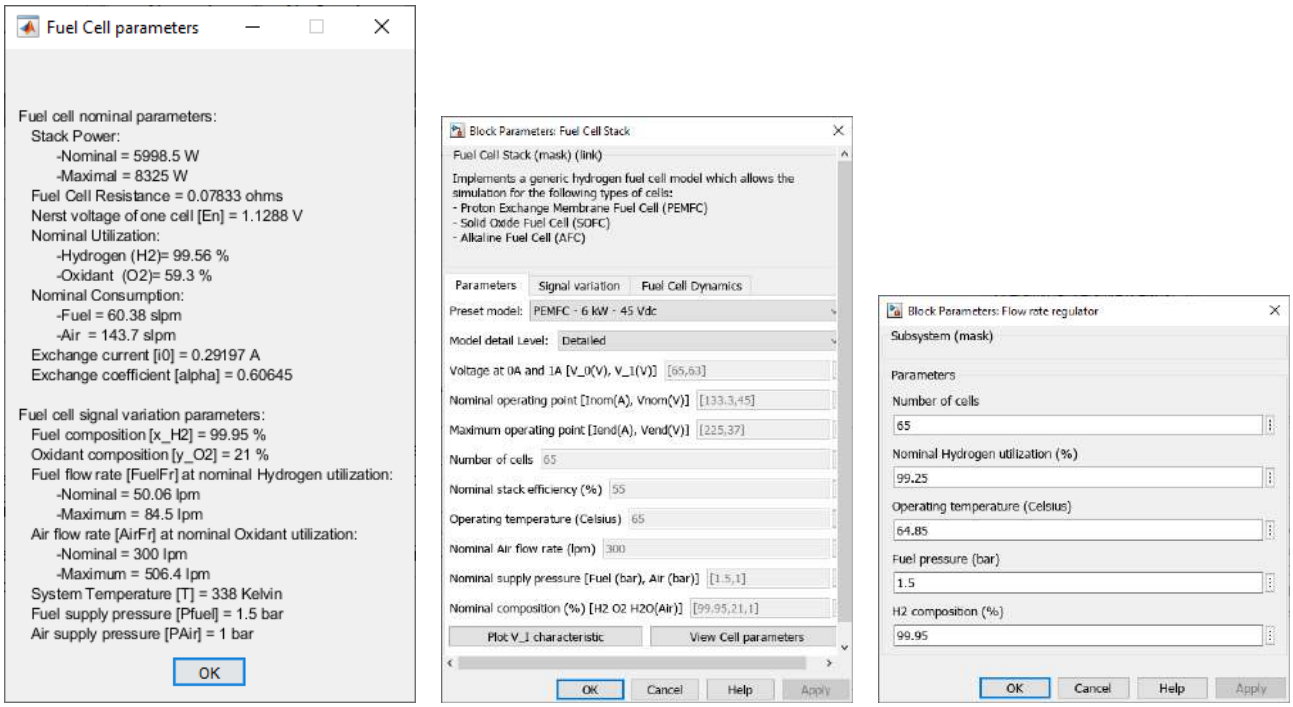


Figure 3.19: Fuel cell V-I and P-I curves

Key design parameters (Fig. 3.20)

- **Stack voltage** 45 VDC nominal (up to 65 V no-load).
- **Power rating** 6 kW nominal, 8 kW peak.
- **H_2 flow** 50.06 L/min at 6 kW, 84.5 L/min at 8 kW.
- **Cells per stack** 60 (single-cell voltage =0.75 V under load).



(a) Fuel cell parameters (b) Stack chosen (c) Flow rate regulator

Figure 3.20: Stack Parameters

Figure 3.21 shows the fuel cell subsystem with its dedicated boost converter to elevate 45 VDC to 220 VAC-equivalent post-inverter level. A PI regulator maintains H_2 flow within [50, 85] L/min, matching instantaneous power demand.

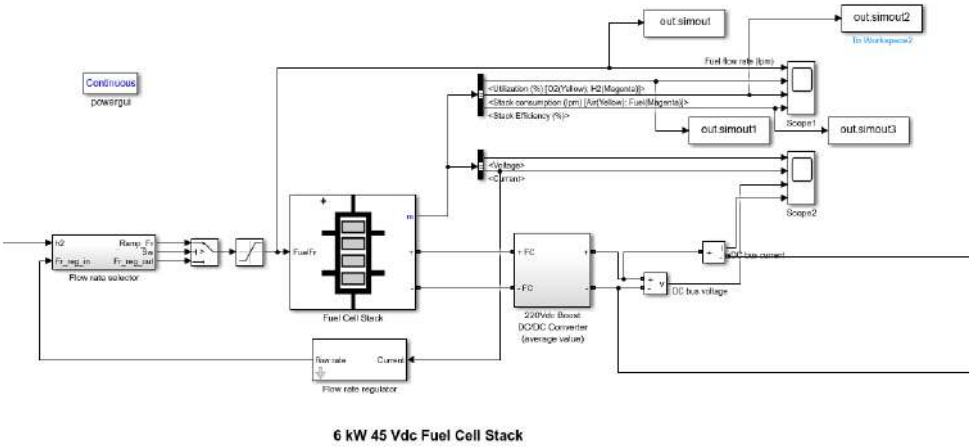


Figure 3.21: Simulink circuit used for fuel cell part

The Simulink circuit used for the fuel cell subsystem is shown in Figure 3.21. The need for a static converter is very important because the PEMFC outputs only 45 V DC under nominal conditions, which is much lower than the voltage typically required for household use. In Algeria, the standard voltage is 220 V AC, so the direct output from the fuel cell is not sufficient on its own. To address this, a boost converter is included in the system, along with its own regulation mechanism, to ensure a consistent power supply and maintain the output voltage within a functional and reliable range.

To ensure that the hydrogen supply remains within the desired range of [50, 81] L/min, a flow rate regulator is used to maintain these values consistently and within safe limits. The parameters of the flow rate regulator are illustrated in Figure 3.21 (c) and can be adjusted according to the stack characteristics previously presented in Figure 3.21 (a). These include the number of cells, the nominal hydrogen utilization, the operating temperature, and the oxygen utilization.

All of these parameters are critical and have a significant impact on the overall system performance. Since the system involves chemical reactions, maintaining proper control over these variables is essential. Any deviation can affect the efficiency, safety, and stability of the hydrogen production and consumption processes. Therefore, accurate regulation is necessary to ensure the system operates reliably under various conditions.

As the fuel is now regulated the chemical problems are now complete as stated earlier in this search the focused-on hydrogen flow rate, now for the fuel cell stack results starting with fuel flow rate, voltage, current, power before the static converter which is a boost converter (the same for PV array).

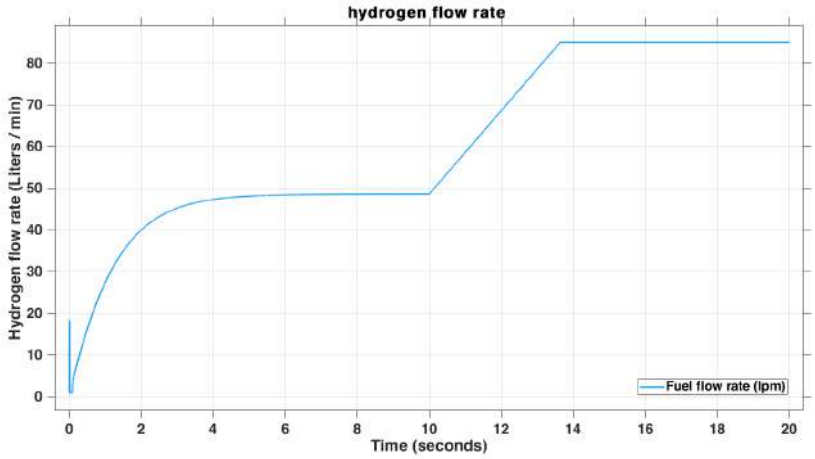


Figure 3.22: Hydrogen flow rate

Figure 3.22 shows how the hydrogen flow rate changes over time in a fuel cell system. At the beginning, the flow rate increases quickly until it reaches about 48 L/min, meaning the system is starting up. Then it stays steady for a while, the flow rate increases again up to 85 L/min, which mean the system needs more power, the flow stays steady again at this higher rate. This shows the system adjusts the hydrogen flow based on its needs.

The fuel flow rate directly affects how much power the fuel cell can produce. When the flow rate increases, more hydrogen is sent to the fuel cell, which means more energy can be generated. In the graph, when the flow rate rises, it likely means the system needs to supply more electricity. When the flow rate stays steady, it means the system is working in a stable condition and providing constant power. So, changes in flow rate help the system respond to different power demands.

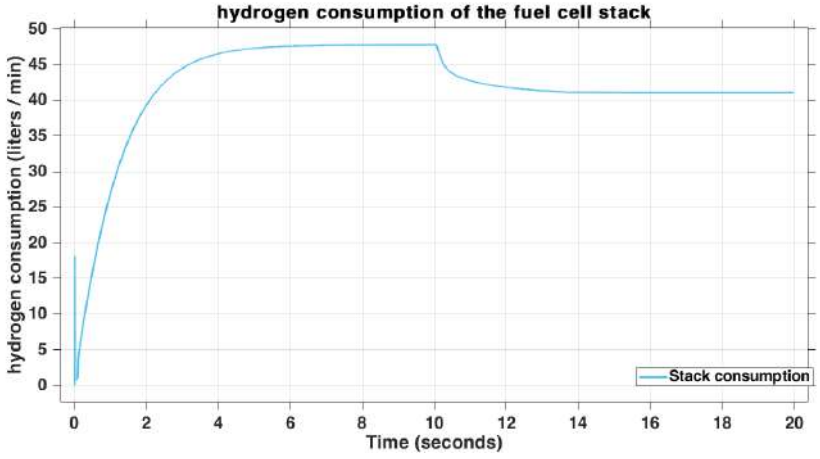


Figure 3.23: Fuel cell stack hydrogen consumption

Figure 3.23 is directly related to the figure 3.22 as both represent the behaviour of the same fuel cell system. The first graph showed the input hydrogen flow rate, while this one illustrates the actual hydrogen consumption by the fuel cell stack. Initially, both the flow rate and consumption rise rapidly, indicating the system is quickly reaching its operational state. However, after around the 10-second mark, while the hydrogen flow rate slightly increases or

remains constant, the consumption decreases. This indicates that the fuel cell receives more hydrogen than it needs, leading to a regulated or reduced consumption based on the actual power demand. The system is therefore adjusting the fuel usage to match the load requirements.

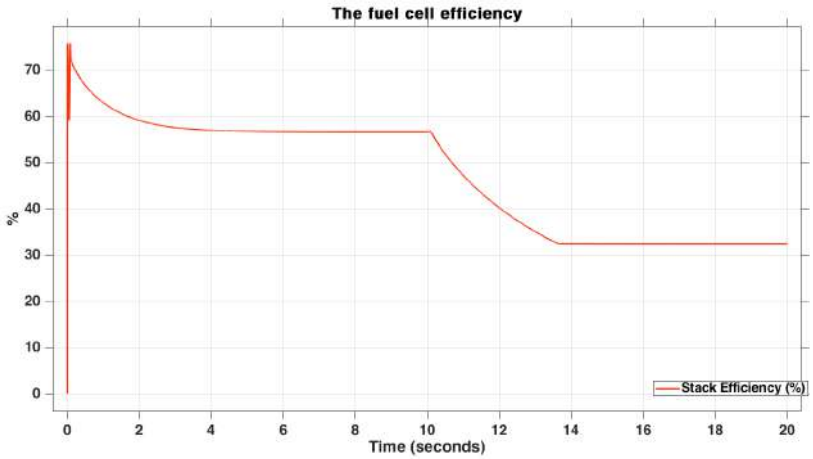


Figure 3.24: The fuel cell efficiency

Figure 3.24 shows the efficiency of the fuel cell stack. Initially, the efficiency increases above 75%, which corresponds to the stable and early operation of the fuel cell. Shortly after, the efficiency begins to decrease and stabilizes around 57%. At this point, a noticeable drop occurs, which brings the efficiency down to nearly 33%, where it then stabilizes again. This decline is likely due to an increase in load demand or a decrease in efficiency of fuel utilization and voltage. The graph clearly illustrates how system dynamics, such as power demand and hydrogen flow, have a direct impact on overall fuel cell performance.

The voltage of a fuel cell is a key indicator of its performance and efficiency. It reflects how effectively the chemical energy from hydrogen is being converted into electrical energy. Monitoring voltage over time helps assess the fuel cell's response to changes in load, hydrogen supply, and internal conditions such as temperature and pressure. A stable voltage typically indicates efficient operation, while drops or fluctuations may signal increased demand, fuel starvation, or internal losses.

This voltage is later regulated using boost converter so it is suitable for household's activity as this fuel cell outputting a maximum voltage of 65 V and this not enough by considering the inverter losses and filtering this 65 V can go down to 59 V AC so the value should be increased more on that later.

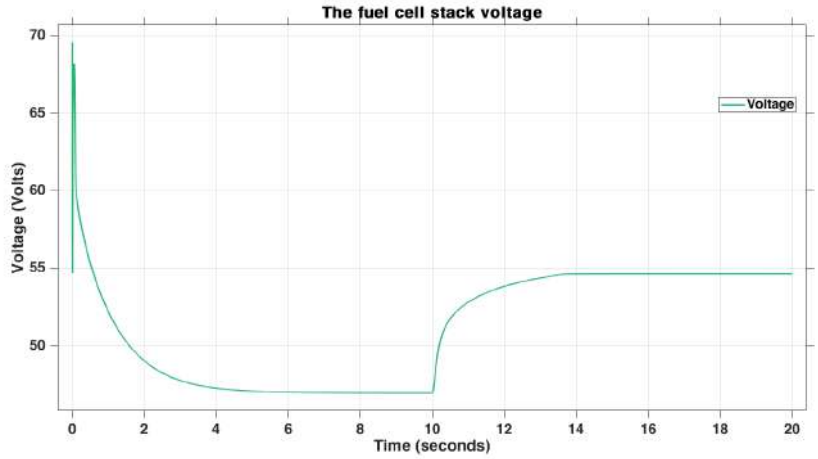


Figure 3.25: The fuel cell voltage

At system startup, the fuel cell voltage exhibits a sharp spike, reaching approximately 69 V. This value remains well within the safe operational limits of the system, which is designed to handle up to 300 VDC. During this initial phase, the energy demand is adequately met, ensuring the house loads are fully supported.

Following the startup phase, the voltage drops to around 10 VDC. This reduction is attributed to low fuel availability, correlating with a period of reduced load demand. As the demand begins to rise again, the voltage recovers and stabilizes around 55 VDC figure 3.25.

These fluctuations especially the transient voltage spikes and drops can negatively impact system performance and reliability. To address this issue, a boost converter is introduced later in the system architecture. This converter ensures a regulated and stable output voltage, improving both the efficiency and the safety of the fuel cell system under varying load and fuel cell conditions.

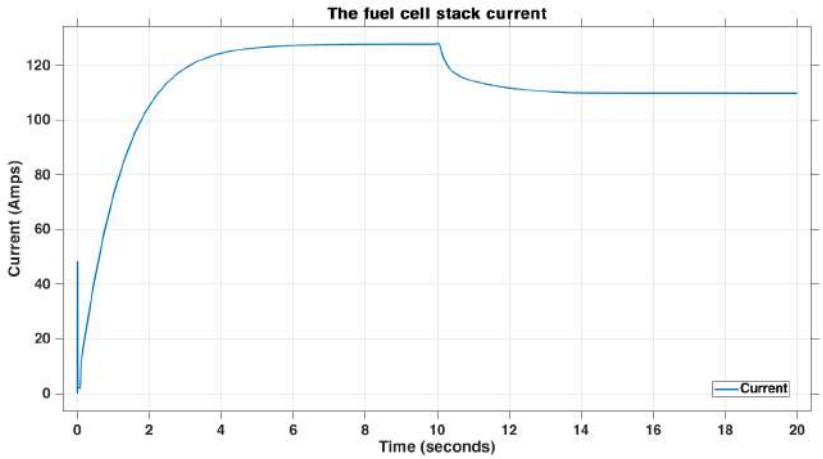


Figure 3.26: The fuel cell current

Figure 3.26 shows The fuel cell system delivers a significant current output, reaching approximately 115 Amps as it settles, which is typical given the nature of fuel cell technology. Since individual fuel cells produce relatively low voltage systems must compensate with high current to meet power demands. This high current is primarily due to the increased electron

flow resulting from the electrochemical reactions involving hydrogen and oxygen. Additionally, the fuel cell is designed with a large electrode surface area and efficient water/thermal management to handle high power output. In this case, the high current is a direct response to the system load requirements, especially during active phases of energy consumption such as powering home appliances.

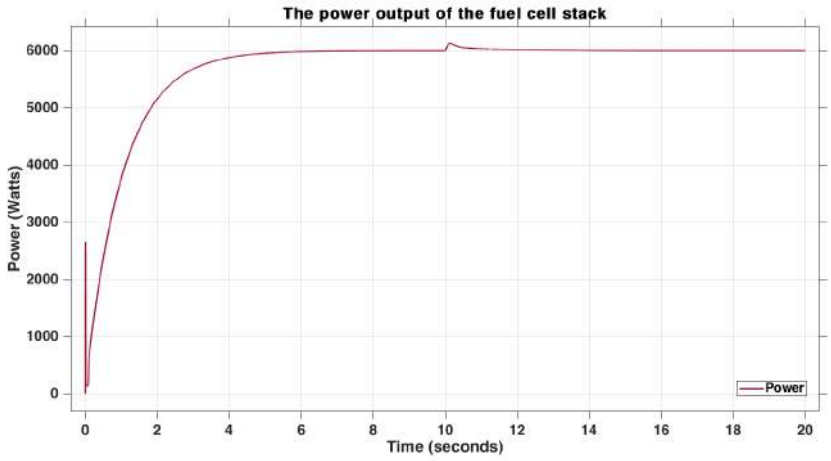


Figure 3.27: The power output of the fuel cell stack

Figure 3.27 shows a gradual increase over time, ultimately reaching a peak of approximately 6000 Watts before stabilizing. This behavior reflects the dynamic response of the fuel cell to varying load demands. At the beginning, the low power output corresponds to minimal electrical load and fuel utilization. As the load gradually increases, the fuel cell responds by supplying more current and voltage, resulting in a steady rise in power output. Once the demand reaches a certain threshold, the fuel cell maintains a stable operating point, delivering a continuous 6 kW output. This steady-state operation ensures consistent energy supply to the system while maintaining fuel efficiency and thermal balance.

After analyzing the previous fuel cell graphs, it is evident that the system lacks stability and is unable to generate meaningful power. To address this, a PI controller has been implemented in place of the original flow regulator, which proved to be ineffective for this application. Below are the same parameters, now regulated using the PI controller

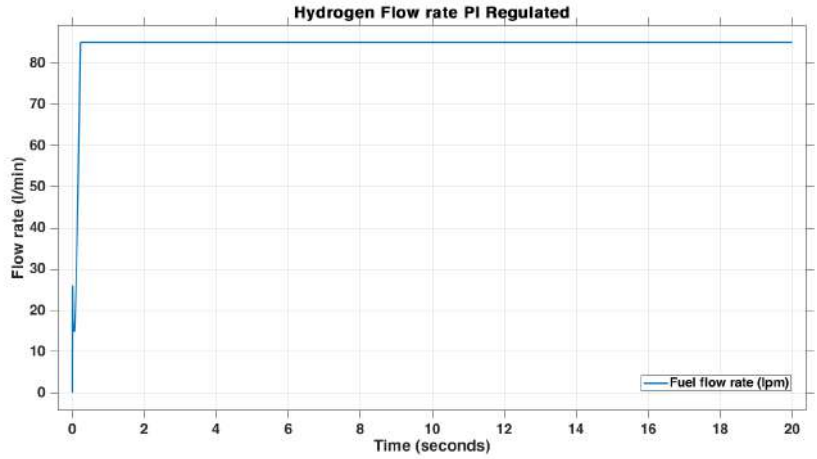


Figure 3.28: Hydrogen flow rate PI regulated

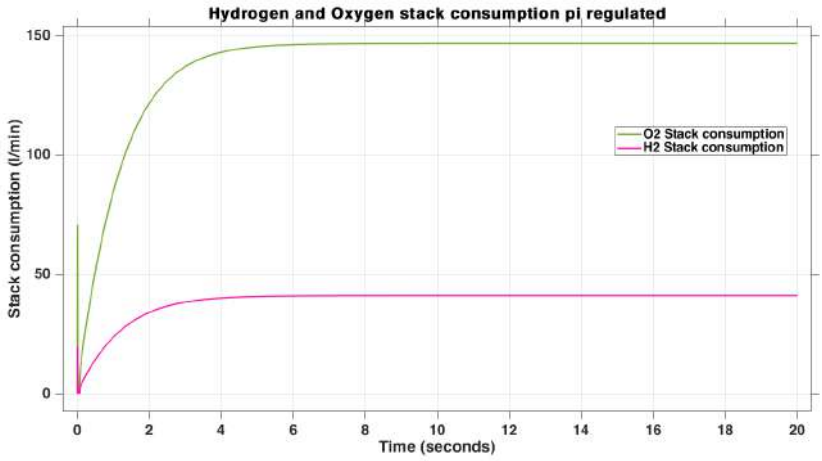


Figure 3.29: Stack consumption of hydrogen and oxygen PI regulated

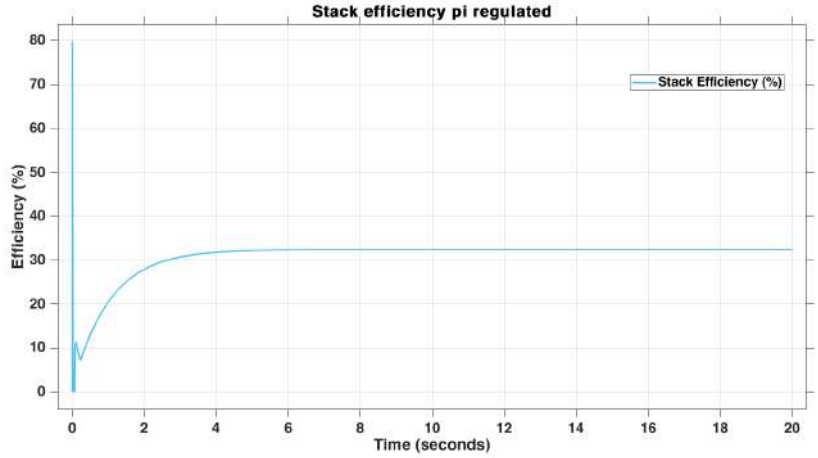


Figure 3.30: Stack Efficiency PI regulated

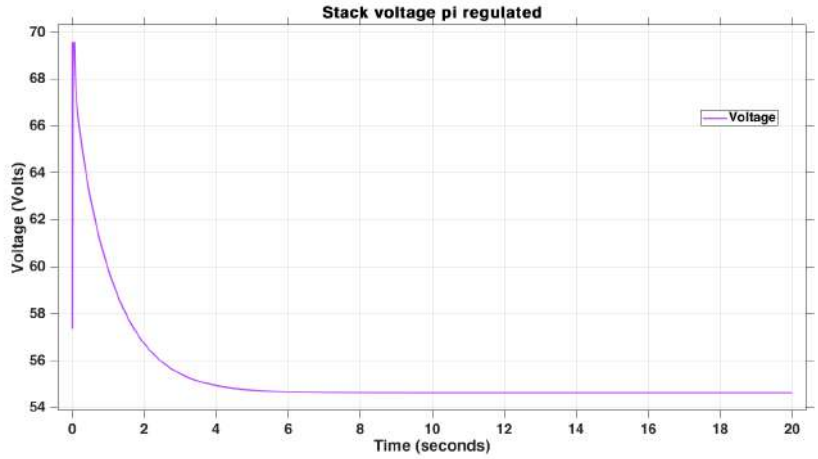


Figure 3.31: Stack Voltage PI regulated

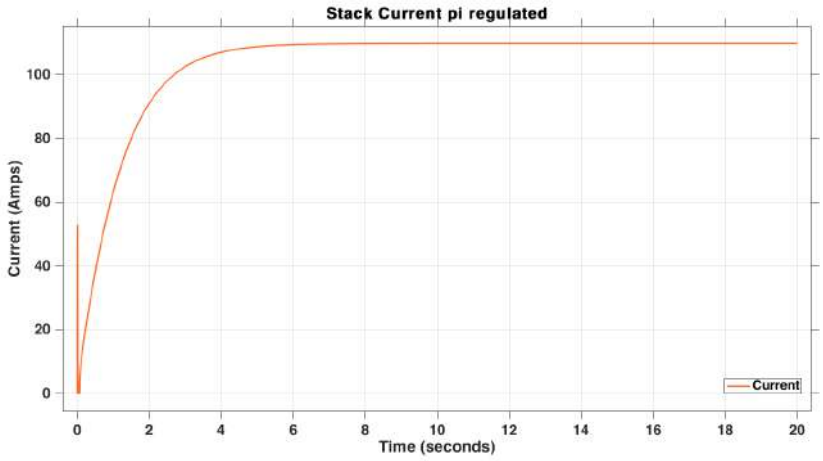


Figure 3.32: Stack current PI regulated

A boost converter is a critical component in a fuel cell system because it "cleans up" the raw DC output both voltage and power before it reaches the load or inverter. Fuel cells naturally produce fluctuating voltages and currents as their internal reactions and load demands change, which can lead to unstable power delivery and poor efficiency. By stepping the unregulated cell voltage up to a consistent, higher DC level, the boost converter smooths out voltage dips and spikes, maintains a steady power output, and ensures that downstream electronics see a clean, reliable supply. This regulation not only protects sensitive loads (inverters, batteries, and household appliances) but also allows the fuel cell to operate at its optimal point, maximizing efficiency and extending component life

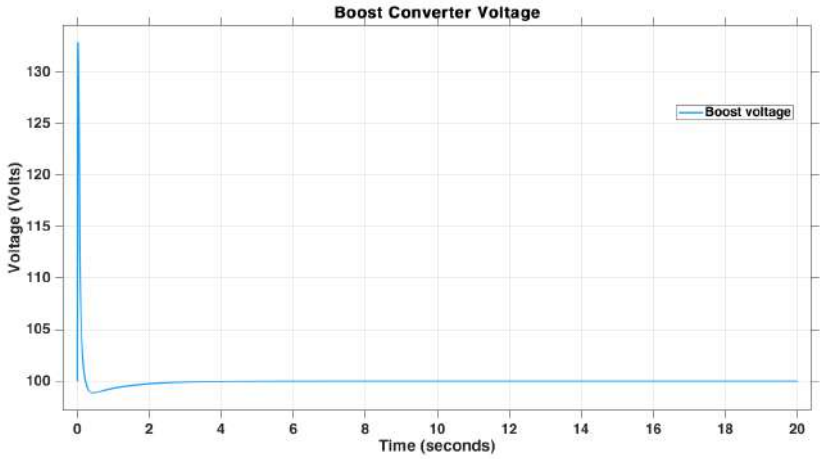


Figure 3.33: The Voltage output of boost converter

This figure 3.33 shows the voltage output of the fuel cell system after passing through the boost converter. Initially, there is a sharp spike reaching around 135 V, which is expected due to the system's startup transient. This spike is quickly dampened, and the voltage stabilizes around 100 V within the first 2 seconds. After that, the output remains steady, showing that the boost converter effectively regulates and smooths the voltage.

This behavior confirms the boost converter's role in maintaining a clean and stable DC output, essential for safely powering household loads or feeding into an inverter.The initial overshoot and fast setting time also suggest that the controller design (PID) is responsive and well-tuned for this application.

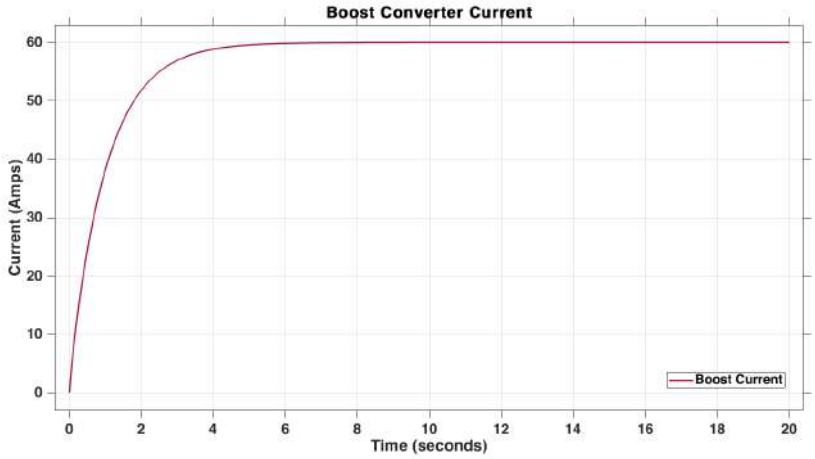


Figure 3.34: The current output of the boost converter

Figure 3.34 shows the current output of the fuel cell system after the boost converter.A gradual increase until 5 seconds then it reachs 60 Amps and stabilizes.

This smooth settling of current indicates that the boost converter not only regulates voltage but also contributes to current stability, which is crucial for protecting downstream loads and ensuring efficient power delivery. The steady current also suggests that the system reaches a well-controlled operating point, helping deliver consistent power to the load.

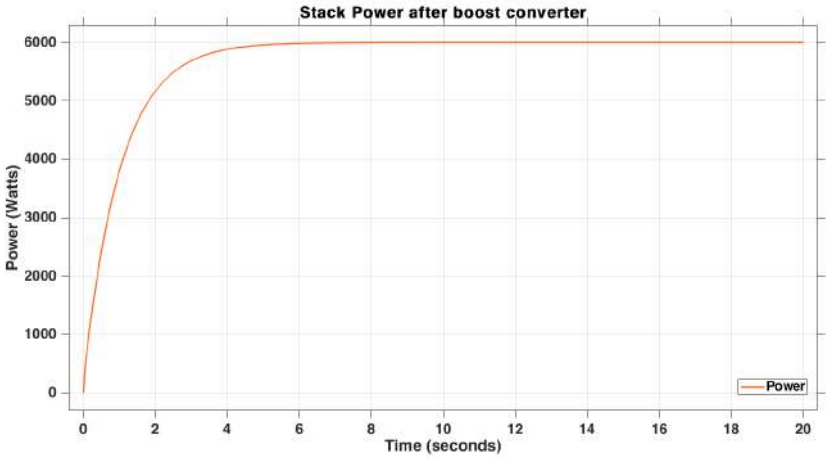


Figure 3.35: The Power output of the boost converter

Figure 3.35 illustrates the power output of the fuel cell after passing through the boost converter. At the initial moment, gradual increase is noticed. Shortly after, the power stabilizes at around 6,000 watts. This indicates that the boost converter effectively regulates the output, helping the system reach a steady state within a very short time. The stable power output observed after the transient phase demonstrates the converter's ability to maintain consistent and reliable power delivery from the fuel cell to the load, which is essential for the proper functioning of connected electrical systems.

3.8 Inverter

In this fuel cell system, an inverter is used to convert the DC (direct current) output from the fuel cell after passing through the boost converter into AC (alternating current) electricity. This conversion is essential because most household appliances and grid-connected systems operate on AC power. The inverter ensures that the electrical energy produced by the fuel cell can be efficiently used or fed into the power grid, maintaining the required voltage and frequency standards.

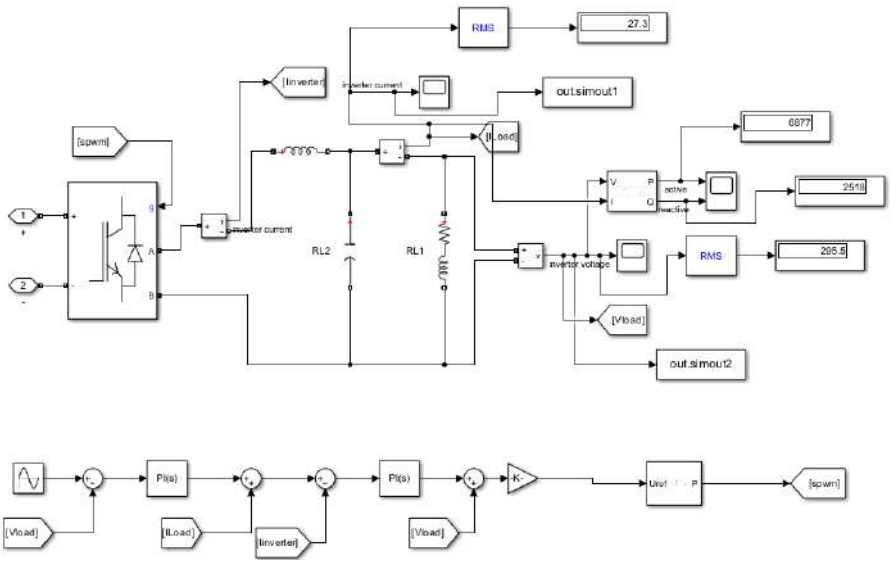


Figure 3.36: Single Phase inverter with PWM command

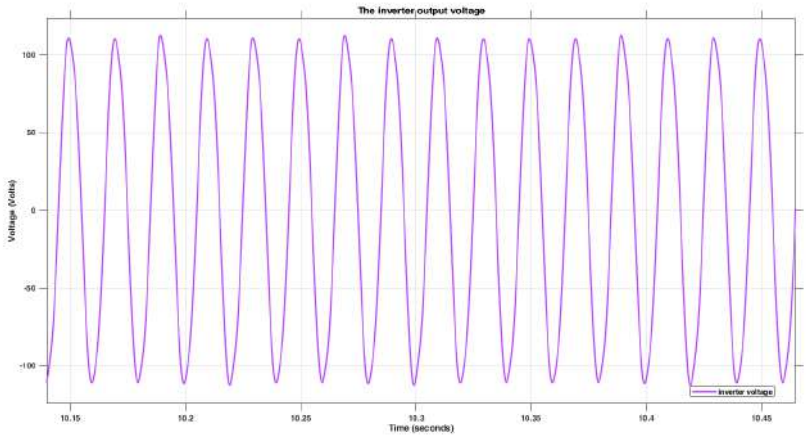


Figure 3.37: The voltage output of the inverter

Figure 3.37 represents the AC voltage output of the inverter after the boost converter stage. As shown, the waveform is alternating, swinging between approximately +110 V and -110 V, which is typical for an inverter.

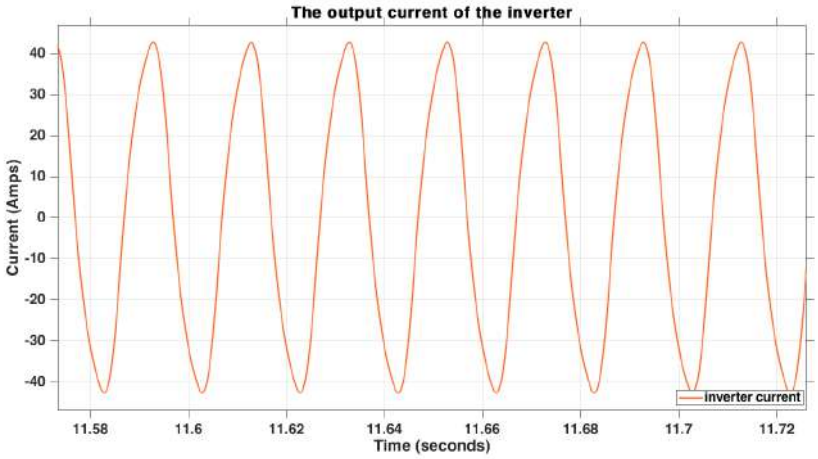


Figure 3.38: The current of the inverter

Figure 3.38 represents the AC current output of the inverter system. Similar to the voltage waveform, the current also follows an alternating sinusoidal pattern, indicating that the inverter is properly converting DC input into a usable AC output. The waveform peaks at approximately +40 A and -40 A, which shows a balanced output with a slight asymmetry most likely due to switching characteristics or loading effects.

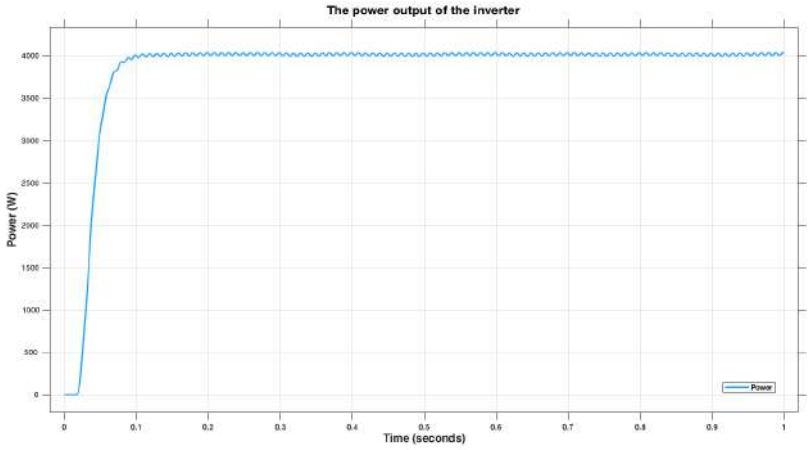


Figure 3.39: The inverter output power

This figure 3.39 behavior indicates that the inverter is ramping up gradually until it reaches a steady-state output of 4000 watts (4 kW). The slow rise at the beginning is typical and expected it shows that the inverter is implementing a soft start to avoid sudden surges that could damage connected components or stress the system.

Once it reaches 4 kW, the power remains stable, which means the inverter is handling the load well and operating efficiently without fluctuations or overload. This kind of response is a strong sign that the boost + inverter system is well-tuned, the regulation is working properly, and the connected load (such as a household or electrolyzer system) is being supplied with reliable power.

3.9 Conclusion

This system successfully demonstrates a complete renewable hydrogen-based energy cycle, starting from solar energy capture to clean power delivery. The process begins with a PV array that generates electricity based on sunlight availability. To ensure maximum efficiency, an MPPT algorithm is used to track and extract the highest possible power output. Since PV voltage and current are not naturally stable, a boost converter is added to regulate the output voltage and provide a more consistent energy supply.

The stabilized power is then used to run a PEM electrolyzer, which converts water into hydrogen gas. Because hydrogen production depends heavily on stable current and controlled operating conditions, additional systems are implemented temperature control using a PI-regulated heating setup, and pressure control using a PI-regulated pressure source and reservoir. These ensure that the electrolyzer operates safely within its optimal temperature (50–80°C) and pressure range, increasing its durability and efficiency.

The hydrogen produced is stored in a high-pressure tank to buffer the system and ensure continuous operation. Storage plays a key role when demand is high and hydrogen production is not sufficient, the stored hydrogen fills the gap; when production is high and demand is low, excess hydrogen is saved instead of wasted.

When electrical power is needed such as at night or during low sunlight hours the system utilizes a PEM fuel cell. This fuel cell converts the stored hydrogen back into electricity. The stack is sized to provide up to 6 kW, which is more than enough for a typical Algerian household. The fuel cell's hydrogen flow is carefully regulated to ensure it matches the power demand and efficiency targets.

Finally, the DC power from the fuel cell passes through another boost converter and inverter system, converting it to 100 V AC for residential use. The inverter output is clean and stable, as shown in the voltage and current waveforms, with peak values and frequency matching household grid standards. The gradual ramp-up and stable 6 kW output confirm the system's reliability and readiness to handle real-world loads.

Overall, this integrated system from solar generation to hydrogen storage and reconversion proves to be an efficient, self-sustaining, and clean energy solution. It ensures energy independence, low environmental impact, and reliable power delivery, making it an ideal model for future residential renewable energy systems.

Chapter 4

From Concept to Practice, Prototype and Cost Analysis

4.1 Introduction

After validating our hybrid renewable energy system through comprehensive MATLAB simulations, we now turn to the practical realization of the design. This chapter outlines the transition from theoretical modeling to laboratory prototype and, ultimately, to a functional off-grid power solution. We will detail the selection and integration of real-world components including an 800 W photovoltaic array, maximum power point tracking (MPPT) controller, DC–DC boost converters, a 24 V 50 Ah battery pack, a proton exchange membrane (PEM) electrolyzer, a 500 L hydrogen storage tank, a 6 kW PEM fuel cell, and a 220 V DC–AC inverter mirroring the configuration that proved stable in simulation. Emphasis is placed on component specifications, installation procedures, control strategies, and safety considerations. By the end of this chapter, readers will understand how the system's MATLAB-based performance predictions guide hardware choices, assembly techniques, and operational protocols, bridging the gap between simulation and real-world application.

4.2 The hydrogen House

To better visualize the practicality and appeal of such a setup, this chapter also highlights several real-world examples of off-grid homes that operate independently of any electrical grid. These case studies will illustrate how similar technologies have been successfully implemented, providing further validation for our system's design and its potential to serve as a reliable and eco-friendly energy solution for isolated residences.

Hans-Olof Nilsson, Technical Director at Nilsson Energy, has created a house that is completely independent from the Swedish power grid. By combining solar energy with hydrogen-based chemical energy storage, he has built a self-sufficient "dream house." The system generates more hydrogen than the household needs, allowing him to sell the surplus and turn a profit[60].

4.2.1 PV Array

Firstly, Hans-Olof's house has a roof fully covered with solar panels 80 modules in total. Each panel produces between 240 and 255 watts, giving the system a total rated power output of approximately 20 kW under peak sun irradiance.



Figure 4.1: The PV array of the hydrogen house

The power generated by the PV array is first fed into a battery pack, providing one method of energy storage. The second method involves converting excess solar energy into hydrogen, which can be stored and used later when needed. According to the homeowner, the house relies primarily on solar energy, using hydrogen as a long-term energy storage solution to ensure continuous power availability[60].

4.2.2 battery pack

The house currently uses lead-acid batteries for energy storage, but Hans-Olof has stated that he plans to replace them with lithium-ion batteries in the future due to the limitations and challenges associated with lead-acid technology. The battery system consists of 48 batteries, delivering 48 volts and providing a total storage capacity of 144 kWh, with an overall capacity of 1500 Ah. This stored energy is used when solar power is insufficient such as during cloudy days, at night, or for charging electric vehicles.



Figure 4.2: The battery pack

As the days grow longer and solar production increases, the house generates more power than it consumes. To make use of this excess energy, the system feeds it into an electrolyzer, which contains an electrolyte solution typically sodium hydroxide (NaOH). The electrolyzer

uses this power to produce high-purity hydrogen, reportedly up to 99% pure, according to the homeowner[60].

4.2.3 The electrolyzer

The house uses a PEM (Proton Exchange Membrane) electrolyzer to produce hydrogen, with a production capacity of 1 Nm^3 per hour. During the summer, the system can generate up to 3000 Nm^3 of hydrogen, which is stored for use during the winter months when solar energy is limited. Of this amount, approximately 2000 Nm^3 is consumed in winter to generate the electricity needed for the house. The remaining 1000 Nm^3 is either stored for future use or sold for profit.



Figure 4.3: The 5.5 kWh PEM electrolyzer

At maximum production capacity, this electrolyzer consumes approximately 5.5 kilowatt-hours (kWh) of electrical energy to produce 0.0083 kilograms of hydrogen. This level of energy consumption reflects the device's efficiency under optimal operating conditions. The electrolyzer operates at a steady temperature of 60 degrees Celsius, which is maintained to ensure stable performance and to support the efficiency of the electrochemical process. The temperature regulation is critical, as it influences both the reaction kinetics and the overall energy efficiency of hydrogen production[60].

4.2.4 The storage system



Figure 4.4: Hydrogen storage

This produced hydrogen goes to storage system which is huge amounts of tanks as shown in figure 4 each one can carry up to 55L with a number of 203 tank with a rated pressure of 300 bar with an overall capacity of 235 kg.

4.2.5 The Compressor



Figure 4.5: The Compressor

The hydrogen stored in these tanks is now ready to enter the consumption phase, during which it is supplied to a fuel cell. To safely deliver the hydrogen, it is first passed through a specialized compressor. This step is essential not only to regulate pressure for optimal fuel cell performance but also to ensure safety, given that hydrogen is a highly flammable and volatile gas. The compressor used is specifically designed for hydrogen applications, incorporating safety features and materials that are compatible with hydrogen's properties, such as its small molecular size and tendency to cause embrittlement in certain metals. These safety measures are particularly important when integrating hydrogen systems into residential environments, where reliability and risk mitigation are critical.

A metal hydride compressor is a unique type of hydrogen compressor that operates without any moving mechanical parts, making it exceptionally reliable, quiet, and low-maintenance compared to traditional mechanical compressors[60].

4.2.6 The fuel cell



Figure 4.6: PEM fuel cell

The compressor now delivers hydrogen to the fuel cell so the power generation can start safely without any problems the fuel that the system using is PEMFC which is can output up to 5 kW of energy.

This energy is now converter into active power that the system can use notice how the owner started from hydrogen and really got useful power that let him be totally isolated from the grid or from the world actually the only difference between his system and the system discussed throughout this research is his solar panels are the main power source and the hydrogen is just for storage or for winter use the proposed system here is totally depends on hydrogen by starting with low power from solar panel and getting to 6 kW or more to power a household every day of the year[60].

4.3 Prototype

4.3.1 Components

Arduino Uno

An Arduino is a microcontroller-based kit which can be either used directly by purchasing from the vendor or can be made at home using the components, owing to its open-source hardware feature. It is basically used in communications and in controlling or operating many devices. It was founded by Massimo Banzi and David Cuartielles in 2005[61].

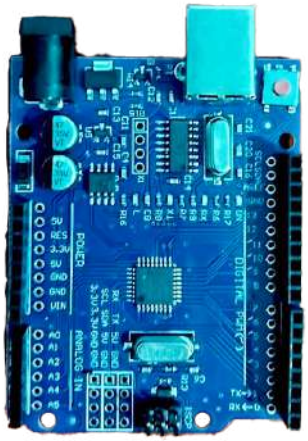


Figure 4.7: The Arduino UNO

Arduino pin diagram A typical example of Arduino board is Arduino Uno. It consists of ATmega328- a 28-pin micro controller.Arduino Uno consists of 14 digital input/output pins (of which 6 can be used as PWM outputs), 6 analog inputs, a 16 MHz crystal oscillator, a USB connection, a power jack,an ICSP header and a reset button[61].

- Power Jack Arduino can be power either from the pc through a USB or through external source like adaptor or a battery. It can operate on a external supply of 7 to 12V. Power can be applied externally through the pin Vin or by giving voltage reference through the IORef pin;
- Digital Inputs It consists of 14 digital inputs/output pins, each of which provide or take up 40mA current. Some of them have special functions like pins 0 and 1, which act as Rx and Tx respectively , for serial communication, pins 2 and 3-which are external interrupts, pins 3,5,6,9,11 which provides pwm output and pin 13 where LED is connected;
- Analog inputs It has 6 analog input/output pins, each providing a resolution of 10 bits;
- ARef It provides reference to the analog inputs;
- Reset It resets the microcontroller when low.

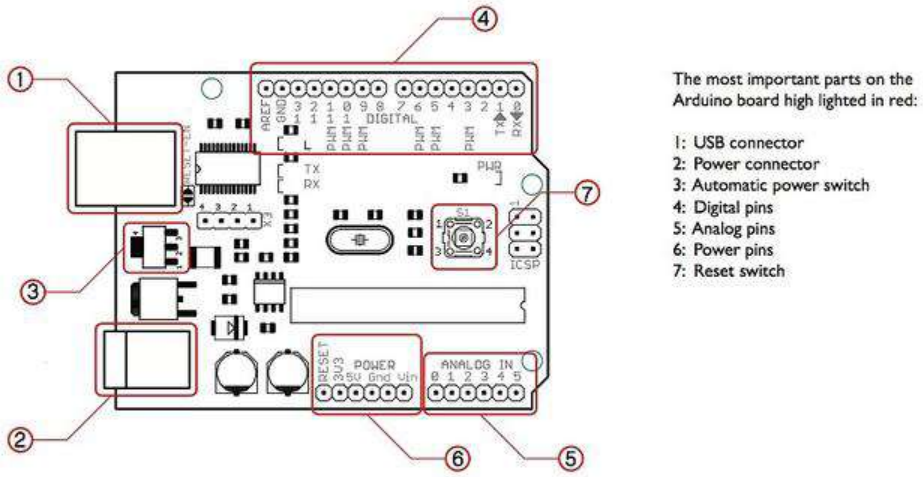


Figure 4.8: Arduino pin diagram

Steps to program an Arduino Programs written in Arduino are known as sketches. A basic sketch consists of 3 parts

- Declaration of Variables.
- Initialization It is written in the setup () function.
- Control code It is written in the loop () function.

The sketch is saved with. ino extension. Any operations like verifying, opening a sketch, saving a sketch can be done using the buttons on the toolbar or using the tool menu. The sketch should be stored in the sketchbook directory. Chose the proper board from the tool's menu and the serial port numbers. Click on the upload button or chose upload from the tool's menu. Thus, the code is uploaded by the boot loader onto the micro controller.

Single channel relay module



Figure 4.9: Enter Caption

The Figure 4.9 shows a single-channel relay module commonly used in Arduino or micro controller-based projects. This module operates at 5 V DC and allows low-voltage control of

high-voltage devices. It uses a Tongling JQC-3FF-S-Z relay, capable of switching up to 10 A at 250 V AC or 30 V DC. The module includes three input pins VCC (power), GND (ground), and IN (control signal from the micro controller). It also has a terminal block with three screw terminals labeled NO (Normally Open), COM (Common), and NC (Normally Closed), which are used to connect the high-voltage load. This relay module enables safe and effective switching of devices such as lamps, fans, or pumps through digital signals from platforms like Arduino.

PEM electrolyzer



Figure 4.10: PEM water electrolyzer

The Figure 4.10 shows a PEM water electrolysis apparatus. This is a laboratory setup designed to demonstrate and study the process of using electricity to split water into hydrogen (H_2) and oxygen (O_2) using a Proton Exchange Membrane (PEM) as the electrolyte it fills 60 ml of water.

Component of this water electrolysis

- Central Tube (PEM) The clear, rectangular tube in the center is labeled "PEM" and has markings on it, likely indicating the volume of gas collected in milliliters. It appears to be positioned over the PEM membrane where the water splitting occurs.
- Gas Collection Tubes (O_2 and H_2) Two clear tubes flank the central PEM tube. One is labeled "O_2" and the other "H_2," indicating where oxygen and hydrogen gases are

collected, respectively. These tubes are inverted over electrodes submerged in a liquid (likely water or a dilute electrolyte solution).

- Electrodes Wires with what appear to be electrode materials are visible inside the gas collection tubes, submerged in the liquid. These are where the electrochemical reactions take place.
- Terminals (+ and -) At the base of the apparatus, there are red (+) and black (-) terminals, indicating where an external DC power source would be connected to drive the electrolysis process.
- Liquid The tubes contain a liquid, presumably water or a dilute electrolyte to facilitate ion conduction. Bubbles are visible in the tubes, indicating gas production due to electrolysis.
- Gas Levels There are different levels of gas collected in the "O_2" and "H_2" tubes, suggesting that the electrolysis process has been running. Notice that the volume of hydrogen collected appears to be roughly twice the volume of oxygen, which aligns with the stoichiometry of water splitting.

Fuel cell



(a) The Hydrogen storage model



(b) The stored hydrogen

Figure 4.11: The PEM fuel cell

The figure shows a PEM fuel cell with a transparent casing revealing internal components like patterned flow field plates (for gas distribution, current collection, heat management, and separation), sealed with orange gaskets. Electrical terminals are visible at the top. The core MEA (Proton Exchange Membrane, catalyst layers, and Gas Diffusion Layers) is sandwiched within. Gas inlet/outlet ports are also present. This device converts hydrogen and oxygen (or air) into electricity, water, and heat, representing a key technology for utilizing hydrogen as an energy carrier, relevant for clean energy applications.

This small demonstration fuel cell illustrates the fundamental principles of PEMFC operation. Larger PEM fuel cell stacks are being developed and deployed for various applications, including transportation (fuel cell vehicles), stationary power generation (backup power, off-grid

power), and portable power. Understanding the operation and characteristics of PEM fuel cells is crucial for developing a complete hydrogen energy system, from production to utilization.

Battery pack



Figure 4.12: Battery pack

The Figure 4.12 shows a stack of five 9V batteries the main role of these batteries is Providing a Stable DC Power Source for Electrolysis which is

- Electrolyzer Power The most direct role is to act as a controlled and stable source of direct current (DC) electricity to power an electrolyzer. The electrolyzer uses this electrical energy to split water (H_2O) into hydrogen (H_2) and oxygen (O_2);
- Voltage and Current Control Batteries can provide a relatively consistent voltage, allowing for better control over the current supplied to the electrolyzer. This is important for studying the efficiency of hydrogen production under different electrical conditions.

Photo resistor and LED

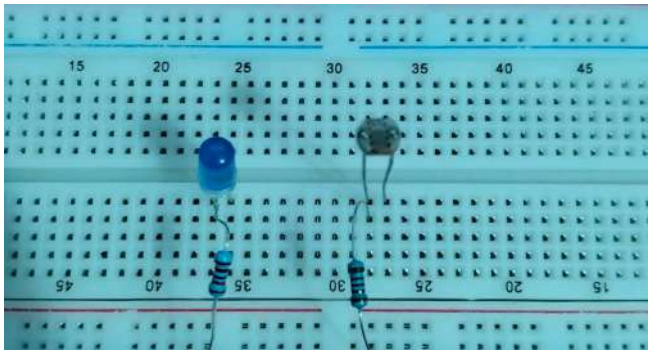


Figure 4.13: Breadboard contain photoresistor (LDR) and LED

The figure shows a simple circuit built on a breadboard, containing a photoresistor (also known as a light-dependent resistor or LDR) and a Light Emitting Diode (LED), along with two resistors.

The general role of an LDR (Light Dependent Resistor or photoresistor) is to act as a light-sensitive variable resistor. Its primary function in any circuit is to detect changes in light intensity and translate those changes into a corresponding change in its electrical resistance. This change in resistance can then be used in various ways to control or influence other components within the circuit, enabling light-activated or light-modulated behaviours.

The LED's role is to act as a visual indicator or an output of the light-sensing circuit. It emits light when an electric current flows through it in the forward direction.



(a) When the light is available (b) When there is no Light

Figure 4.14: The Command that drives the system

4.4 Tinker the Hydrogen prototype

The transition from a simulated system to a physical realization starting with An Educational Model of production energy with fuel cell powered by PV array.

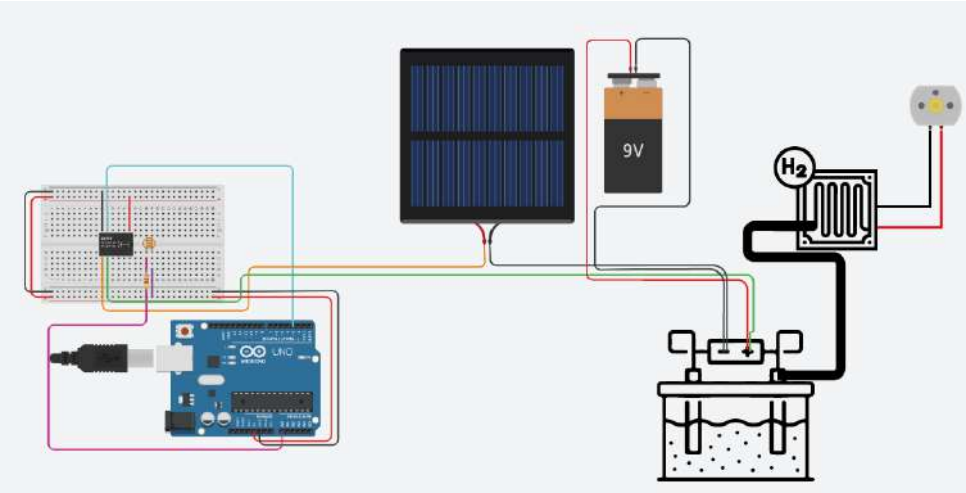


Figure 4.15: Tinker cad circuit of the proposed system

The figure 4.15 illustrates a system that uses solar energy to charge a battery then the stored energy is used to produce hydrogen gas through electrolysis, and then uses that hydrogen in the the fuel cell to produce useful electrical power to rotate motor or light up a bulb.

The idea behind this prototype is that during the night time, demand on electricity is high, so most failures of the grid occur during the night. Some grids integrate renewables to charge

up battery packs, and later at night, those battery packs are used to back up the grid during high demand. This is the main idea of our prototype. The photo-resistor detects that there is no light, which confirms that night has begun. The Arduino sends a high signal to the relay. The relay then closes and lets the power flow from the battery to the electrolyzer. The produced hydrogen is then fed to the fuel cell so we can produce useful power.

4.5 Realization

4.5.1 The full prototype

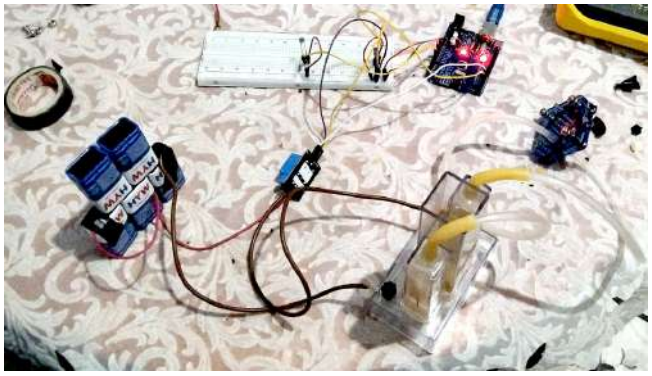


Figure 4.16: The prototype realization

The figure 4.16 shows an experimental setup for hydrogen production using water electrolysis, controlled by an Arduino Uno. A battery pack (43.8V (figure 4.17) provides power to the electrolyzer via a switching transistor on a breadboard, which is controlled by the Arduino. The Arduino takes inputs from a photoresistor (simulating solar intensity) and a potentiometer (manual control), and its program determines when to switch the electrolyzer ON or OFF. This setup likely explores light-activated or manually controlled hydrogen production, with the Arduino potentially logging data for analysis, representing a basic control system relevant to developing larger PV-powered hydrogen systems.

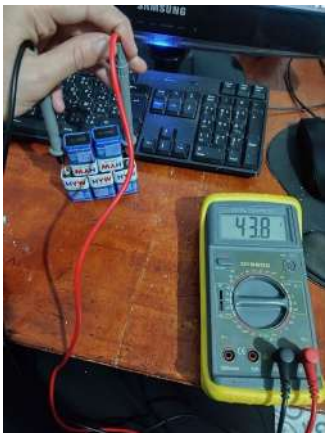


Figure 4.17: Measurement the voltage of batteries

4.5.2 Electrolyzer Functionality

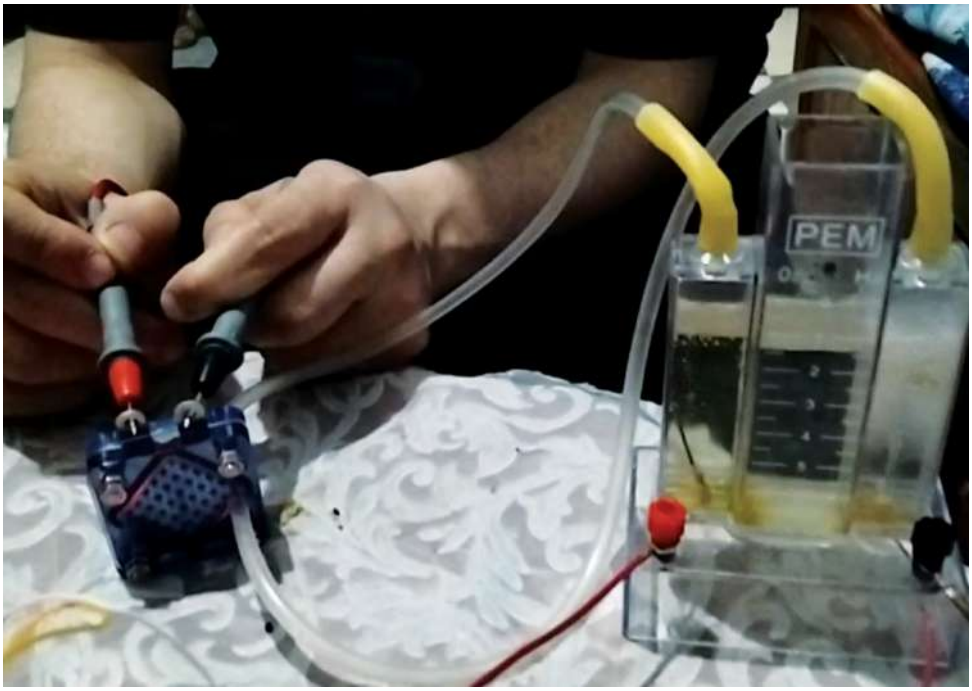


Figure 4.18: PEM electrolyzer in action

The first step to get the system up and running is to prepare the electrolyte solution, which in the case of this project is water plus NaCl. The salt is added to increase the water's conductivity and keep the electrons flowing, because water by itself won't do much.

In Figure 4.18, hydrogen is forming on the negative side of the PEMEC and starts to accumulate. On the other side, there is oxygen forming, which is also clearly visible. You can notice the bubbles inside the solution itself.

4.5.3 Fuel cell functionality



Figure 4.19: Measure the output voltage of the fuel cell

as hydrogen reach the fuel cell it starts instantly producing electrical energy as shown in the figure 4.19 the voltage measurement is about 0.7V which is great for the size of the fuel cell, the fact that there an actual electrical energy coming out of this technology is very impressive and will lead to massive breakthrough in the future.

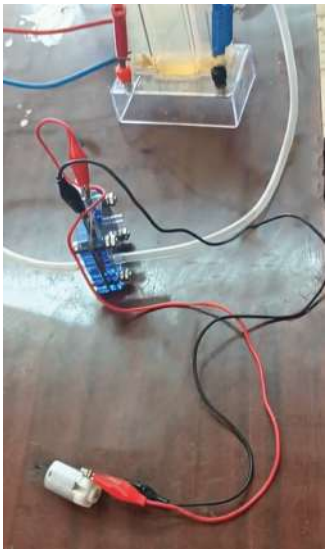


Figure 4.20: Small Dc motor as load for the fuel cell

After connecting a small DC motor as a load to the fuel cell to test its output performance. The fuel cell successfully powered the motor, demonstrating its ability to deliver sufficient voltage and current for low-power applications. This simple experiment confirms that the fuel

cell is not only generating electricity but is also capable of driving an actual electromechanical load, which is a promising indication of its practical usability in small-scale energy systems.

4.6 Implementation Cost

Table 4.1: The cost of each component of the system.

Component Name	**Specification/Description**	**Unit Cost (DZD)**
Solar Panels	Renogy 800 W 12 V Off-Grid	135,000
MPPT Charger Controller	Renogy Rover 40 Amp 12V/24V DC	27,000
DC–DC Boost Converter	Victron Orion-Tr 12/24–15A	9,855
Battery Pack	Newport 24 V 50 Ah $LiFePO_4$	89,100
Water Electrolyzer	AEM Electrolyser EL 4 500 NL/h or 1.0785 kg/24h	675,000
Hydrogen Storage Tank	500 Litre Stainless Steel Liquid Hydrogen Storage Tank	135,000
Fuel Cell	6 kW PEM Fuel Cell Generator	2,484,000
DC–DC Boost Converter	Converter DC 45V 220VDC	318,295
Inverter DC–AC 220 V DC $\rightarrow$ 220 VAC	220VDC to 220VAC 6kVA Power Frequency Industrial Inverter with Isolated Transformer	132,300

The prices listed in the table were originally in US dollars (USD). To provide a more localized and realistic estimate, the costs were converted to Algerian Dinar (DZD) using an approximate exchange rate of 1 USD = 135 DZD. Based on this conversion, the total cost of all components in the system is approximately 4,995,550 DZD. This amount represents the estimated budget required to implement the complete system using the specified components.

4.7 Comparison with the others energy systems

Table 4.2: Comparison with Other Energy Systems

Criteria	**PV–Hydrogen**	**PV + Battery**	**Diesel Generator**
Initial Cost Estimate	High ($1200–2500 for small setup)	Medium ($800–1500)	Low ($500–1000)
Cost per kWh (prototype)	Very high	Medium to low	High (due to ongoing fuel costs)
Overall Efficiency (%)	25–30% (electrolyzer + fuel cell)	70–85%	25–40%
Energy Storage	Long-term (compressed hydrogen)	Short-term (battery, high losses)	No integrated storage
CO_2 Emissions	None (if powered by renewable PV)	None	High (CO_2, NO_x, particulates)
Maintenance Needs	Moderate (complex system)	Low to moderate	High (engine wear, fuel logistics)
Night-time Autonomy	Yes (via stored hydrogen)	Limited (depends on battery size)	Yes (24/7 operation possible)
Typical Lifespan	10–15 years (varied subsystems)	8–12 years	5–10 years

Among the three systems table, the PV–Hydrogen system stands out as the most sustainable and future-ready solution. Although its initial cost is higher and efficiency slightly lower, it offers clean energy, long-term storage, and complete independence from fossil fuels. This makes it ideal for off-grid applications, energy autonomy, and climate-resilient infrastructure.

In contrast, PV + Battery systems are efficient and practical for short-term storage but struggle with night-time autonomy and long-term reliability. Diesel generators, while low-cost and reliable, produce high emissions, require ongoing fuel supply, and are not aligned with global clean energy goals.

The PV–Hydrogen system is the best long-term option, combining environmental sustainability, energy independence, and scalable clean storage essential for a green and resilient energy future.

4.8 Conclusion

This chapter has detailed the critical transition from the simulated design of a PV-powered hydrogen energy system to its physical realization as a functional prototype. The process

involved careful selection and integration of components, including solar panels, an Arduino-based control system, and a PEM electrolyzer, along with the incorporation of essential circuitry for light sensing and power management.

The constructed prototype successfully demonstrates the fundamental principles of hydrogen production via water electrolysis driven by a simulated solar energy source. The Arduino effectively manages the system, responding to changes in light intensity and controlling the power delivered to the electrolyzer. Furthermore, the setup successfully powered a small motor using the hydrogen produced, showcasing the complete energy conversion chain.

General Conclusion

This thesis explored the design and analysis of a complete photovoltaic (PV)-based hydrogen energy system, emphasizing the production and utilization of green hydrogen as a clean, renewable, and sustainable energy carrier. As the world seeks alternatives to fossil fuels, green hydrogen produced using renewable energy sources like solar power emerges as a critical solution for decarbonizing energy systems and supporting long-term environmental goals.

The system begins with PV solar panels, which convert solar radiation into electrical energy. To maximize the efficiency of energy harvesting under varying environmental conditions, a Maximum Power Point Tracking (MPPT) algorithm was implemented, ensuring that the solar array consistently operates at its optimal power output. The harvested energy is then conditioned through a DC–DC boost converter and temporarily stored in a battery, enabling load balancing and providing a stable power supply for downstream components.

A central element of the system is the electrolyzer, which uses the stored electrical energy to split water into hydrogen and oxygen. This process allows for the generation and storage of hydrogen fuel during periods of high solar availability. Later, the stored hydrogen is fed into a Proton Exchange Membrane Fuel Cell (PEMFC), which converts the chemical energy of hydrogen back into electricity with high efficiency and zero emissions. The fuel cell plays a vital role in supplying power during low solar periods, thereby enhancing the reliability and continuity of the energy system.

The entire system was modeled and validated using MATLAB/Simulink, allowing for dynamic simulation of each component and their interactions. The simulation results confirmed the feasibility and operational efficiency of the integrated PV–electrolyzer–fuel cell system under real-world conditions. Key performance indicators such as hydrogen production rate, power output, system response time, and energy conversion efficiency were analyzed to assess the system's overall viability.

In conclusion, this work demonstrates the potential of PV-based hydrogen systems that enables clean and independent energy generation. Future research should explore the integration of artificial intelligence and advanced control strategies such as neural networks or fuzzy logic to further improve system responsiveness, optimize energy flow, and adapt to complex environmental conditions. This will pave the way for smarter, more autonomous renewable energy systems suited for both grid-connected and off-grid applications.

The technical feasibility of the PV–hydrogen system has been demonstrated through simulation, its practical implementation faces economic challenges most notably the high cost of

fuel cells, especially when they need to be imported. Transportation, tariffs, and logistics significantly increase the total system cost.

To address this, local manufacturing of fuel cells is essential for making the system economically viable. Local production reduces costs, encourages technology transfer, creates jobs. Without it, the high import costs become a major barrier particularly in developing or remote areas. Therefore, the success and scalability of PV–hydrogen systems depend heavily on the availability of locally produced fuel cell technology, which is a key to achieving sustainable and cost-effective deployment.

Bibliography

[1] A. Dutta, "A review on production, storage of hydrogen and its utilization as an energy resource," *Journal of Industrial and Engineering Chemistry*, vol. 20, no. 4, pp. 1148–1156, 2014.

[2] J. A. Turner, "A realizable renewable energy future," *Science*, vol. 305, no. 5686, pp. 972–974, 2004.

[3] A. Ursua, L. M. Gandia, and P. Sanchis, "Hydrogen production from water electrolysis: Current status and future trends," *Proceedings of the IEEE*, vol. 100, no. 2, pp. 410–426, 2012.

[4] A. Buttler and H. Spliethoff, "Current status of water electrolysis for energy storage, grid balancing and sector coupling via power-to-gas and power-to-liquids: A review," *Renewable and Sustainable Energy Reviews*, vol. 82, pp. 2440–2454, 2018.

[5] F. Barbir, *PEM Fuel Cells: Theory and Practice*. Academic Press, 2013.

[6] B. C. H. Steele and A. Heinzel, "Materials for fuel-cell technologies," *Nature*, vol. 414, no. 6861, pp. 345–352, 2001.

[7] IRENA, "Green hydrogen: A guide to policy making." International Renewable Energy Agency, 2020.

[8] IEAGHG, "Hydrogen for industry and heating decarbonisation: Technical report," tech. rep., IEA Greenhouse Gas R&D Programme, 2019.

[9] M. Momirlan and T. N. Veziroglu, "The properties of hydrogen as fuel tomorrow in sustainable energy system for a cleaner planet," *International Journal of Hydrogen Energy*, vol. 30, no. 7, pp. 795–802, 2005.

[10] K. Zeng and D. Zhang, "Recent progress in alkaline water electrolysis for hydrogen production and applications," *Progress in Energy and Combustion Science*, vol. 36, no. 3, pp. 307–326, 2010.

[11] "Bp statistical review of world energy,https://www.bp.com/en/global/corporate/energy-economics/statistical-review-of-world-energy.html," 2025. Accessed: March 15, 2025.

[12] "Iea renewables report,http://www.iea.org/world/renewables," 2025. Accessed: March 15, 2025.

[13] G. Bessereau and A. Sanière, "Charbon: ressources, réserves et production," 2007.

[14] "http://thiers.stephane.free.fr," 2025. Accessed: March 20, 2025.

[15] R. A. Alvarez, D. Zavala-Araiza, D. R. Lyon, D. T. Allen, Z. R. Barkley, A. R. Brandt, K. J. Davis, S. C. Herndon, D. J. Jacob, A. Karion, *et al.*, "Assessment of methane emissions from the u.s. oil and gas supply chain," *Science*, vol. 361, no. 6398, pp. 186–188, 2018.

[16] R. W. Howarth, "A bridge to nowhere: Methane emissions and the greenhouse gas footprint of natural gas," *Energy Science & Engineering*, vol. 2, no. 2, pp. 47–60, 2014.

[17] D. T. Shindell, G. Faluvegi, D. M. Koch, G. A. Schmidt, N. Unger, and S. E. Bauer, "Improved attribution of climate forcing to emissions," *Science*, vol. 326, no. 5953, pp. 716–718, 2009.

[18] S. G. Osborn, A. Vengosh, N. R. Warner, and R. B. Jackson, "Methane contamination of drinking water accompanying gas-well drilling and hydraulic fracturing," *Proceedings of the National Academy of Sciences (PNAS)*, vol. 108, no. 20, pp. 8172–8176, 2011.

[19] N. Johnson, R. T. McGrath, and L. R. Cox, "Public health implications of environmental impacts of unconventional natural gas development," *Environmental Science and Technology*, vol. 47, no. 15, pp. 8307–8314, 2013.

[20] J. F. Manwell, J. G. McGowan, and A. L. Rogers, *Wind Energy Explained: Theory, Design and Application*. Wiley, 2nd ed., 2010.

[21] G. M. Kondolf, Z. K. Rubin, and J. T. Minear, "Dams on the mekong: Cumulative sediment starvation," *Water Resources Research*, vol. 50, no. 6, pp. 5158–5169, 2014.

[22] N. K. Sharma, P. K. Tiwari, and Y. R. Sood, "Solar energy in india: Strategies, policies, perspectives and future potential," *Renewable and Sustainable Energy Reviews*, vol. 16, no. 1, pp. 933–941, 2011.

[23] C. Ikenye, "Why it's time to switch to solar energy," 2025. Accessed: March 23, 2025.

[24] B. V. Babu and A. S. Chaurasia, "Modeling for pyrolysis of solid particle: kinetics and heat transfer effects," *Energy Conversion and Management*, 2003.

[25] D. Faradji (née Kherbouche), *Contribution à la valorisation énergétique de la biomasse*. PhD thesis, Univ Abu Bakr Belkaid Tlemcen, 2011.

[26] "How geothermal energy works,https://www.energy.gov/eere/geothermal/how-geothermal-energy-works," 2025. Accessed: March 26, 2025.

[27] "Top 5 solar projects to watch in algeria,https://energycapitalpower.com/top-5-solar-projects-to-watch-in-algeria," 2025. Accessed: March 26, 2025.

[28] "Algeria's pv capacity tops 436.8 mw," 2024. Accessed: March 27, 2025.

[29] "Algeria's total renewable energy capacity reaches 600.9 mw,https://www.greenbuildingafrica.co.za/algerias-total-renewable-energy-capacity-had-reaches-600-9-mw," 2025. Accessed: March 27, 2025.

[30] N. Lutsey and D. Sperling, "Regulatory adaptation: Accommodating electric vehicles in a petroleum world," *Energy Policy*, vol. 45, pp. 308–316, 2012.

[31] A. Züttel, "Hydrogen as a future energy carrier," *Philosophical Transactions of the Royal Society A: Mathematical, Physical and Engineering Sciences*, vol. 365, no. 1853, pp. 913–927, 2007.

[32] I. Dincer and C. Acar, "Review and evaluation of hydrogen production methods for better sustainability," *International Journal of Hydrogen Energy*, vol. 40, no. 34, pp. 11094–11111, 2015.

[33] E. S. Rubin, J. E. Davison, and H. J. Herzog, "The cost of co2 capture and storage," *International Journal of Greenhouse Gas Control*, vol. 40, pp. 378–400, 2015.

[34] J. Peng, L. Ma, and H. Chen, "Hydrogen production from coal gasification in china: A review," *International Journal of Hydrogen Energy*, vol. 35, no. 14, pp. 7121–7130, 2010.

[35] "Hydrogen production: Electrolysis,https://www.energy.gov/eere/fuelcells/hydrogen-production-electrolysis," 2025. Accessed: April 7, 2025.

[36] Intergovernmental Panel on Climate Change, "Climate change 2023: Synthesis report." https://www.ipcc.ch/report/ar6/syr/, 2023. Accessed May 2025.

[37] "Hydrogen storage,https://www.energy.gov/eere/fuelcells/hydrogen-storage," 2025. Accessed: April 7, 2025.

[38] "What are fuel cells?,https://www.umicore.com/en/media/newsroom/what-are-fuel-cells," 2025. Accessed: April 7, 2025.

[39] D. Reschiotto, "Effects of anode fuel recirculation on sofcs fuelled with biogas," Master's thesis, Politecnico di Torino, 2018.

[40] J. Larminie and A. Dicks, *Fuel Cell Systems Explained*. Wiley, 2nd ed., 2003.

[41] I. Staffell, D. Scamman, A. Velazquez Abad, P. Balcombe, P. E. Dodds, P. Ekins, N. Shah, and K. R. Ward, "The role of hydrogen and fuel cells in the global energy system," *Energy & Environmental Science*, vol. 12, no. 2, pp. 463–491, 2019.

[42] B. G. Pollet, I. Staffell, and J. L. Shang, "Current status of fuel cell technologies and their future prospects," *Energy*, vol. 37, no. 1, pp. 123–136, 2012.

[43] R. O'Hayre, S. W. Cha, W. Colella, and F. B. Prinz, *Fuel Cell Fundamentals*. Wiley, 3rd ed., 2016.

[44] H. Essakhi and S. Farhat, "Modélisation et simulation d'un module photovoltaïque," 2019.

[45] T. Esram and P. L. Chapman, "Comparison of photovoltaic array maximum power point tracking techniques," *IEEE Transactions on Energy Conversion*, vol. 22, no. 2, pp. 439–449, 2007.

[46] N. Femia, G. Petrone, G. Spagnuolo, and M. Vitelli, "Optimization of perturb and observe maximum power point tracking method," *IEEE Transactions on Power Electronics*, vol. 20, no. 4, pp. 963–973, 2005.

[47] H. Lund and W. Kempton, "Integration of renewable energy into the transport and electricity sectors through v2g," *Energy Policy*, vol. 36, no. 9, pp. 3578–3587, 2008.

[48] Z. Yang, J. Zhang, M. C. W. Kintner-Meyer, X. Lu, D. Choi, J. P. Lemmon, and J. Liu, "Electrochemical energy storage for green grid," *Chemical Reviews*, vol. 111, no. 5, pp. 3577–3613, 2011.

[49] S. Piller, M. Perrin, and A. Jossen, "Methods for state-of-charge determination and their applications," *Journal of Power Sources*, vol. 96, no. 1, pp. 113–120, 2001.

[50] R. Kumar and S. Kar, "Review of battery technologies for renewable energy storage," *Renewable and Sustainable Energy Reviews*, vol. 81, pp. 2843–2855, 2018.

[51] S. J. Fletcher and R. A. Taylor, "State of charge estimation for li-ion batteries: A review," *Renewable and Sustainable Energy Reviews*, vol. 38, pp. 540–549, 2015.

[52] S. Piller, M. Perrin, and A. Jossen, "Methods for state-of-charge determination and their applications," *Journal of Power Sources*, vol. 96, no. 1, pp. 113–120, 2001. Proceedings of the 22nd International Power Sources Symposium.

[53] O. Tremblay and L.-A. Dessaint, "Experimental validation of a battery dynamic model for ev applications," *World electric vehicle journal*, vol. 3, no. 2, pp. 289–298, 2009.

[54] *REDEC conference. 2nd Renewable Energy for Developing Countries*, November 2014. Beirut, Lebanon.

[55] A. Kahlane and S. Maamir, "Simulation and performance analysis of pem fuel cell under different operating conditions," *E3S Web of Conferences*, vol. 441, p. 02012, 2024.

[56] M. S. Mahmoud and H. M. Hussen, "Design and simulation of a pv-fuel cell hybrid power system," *Journal of Energy and Power Engineering*, vol. 10, pp. 779–785, 2016.

[57] a. M. R. M. Hashem Nehrir, "Dynamic models and model validation for pem fuel cells using electrical circuits," *IEEE Transactions on Energy Conversion*, vol. 20, no. 2, pp. 442–451, 2005.

[58] O. Ulleberg, "Modeling of advanced alkaline electrolyzers: A system simulation approach," *International Journal of Hydrogen Energy*, vol. 28, no. 1, pp. 21–33, 2003.

[59] M. G. Villalva, J. R. Gazoli, and E. R. Filho, "Comprehensive approach to modeling and simulation of photovoltaic arrays," *IEEE Transactions on Power Electronics*, vol. 24, no. 5, pp. 1198–1208, 2009.

[60] "https://www.hydrogenhouseproject.com," 2020. Accessed: April 26, 2025.

[61] "Arduino basics and design,https://www.elprocus.com/arduino-basics-and-design," 2025. Accessed: April 26, 2025.